EVALUATING THE PERFORMANCE OF GEORGIA'S CRCPs USING GROUND PENETRATION RADAR (GPR)

by

NAZİK ÇITIR

(Under the Direction of Stephan Durham)

ABSTRACT

In an effort to provide reliable decisions regarding highway pavements, condition assessment is often conducted to evaluate pavement performance. For Continuously Reinforced Concrete Pavements (CRCP) evaluated in this study, pavement distress is classified as having transverse and longitudinal cracks and/or punchouts. This thesis evaluated the influence of reinforcement placement and concrete cover on distresses through the use of non-destructive testing methods that included Ground Penetrating Radar (GPR) and eddy current technology. In addition, this research evaluated whether an eddy current technology could be used in the absence of a cored sample for the calibration process of GPR in the field. Ultimately, six site investigations on major interstates in Georgia were performed by collecting data including a documentation of pavement distress type and severity, reinforcement location, and cover depth. This study confirmed that the location and depth of reinforcements affect the performance of CRCPs in terms of cluster cracking and punchouts.

INDEX WORDS: Continuously Reinforced Concrete Pavement, Ground Penetration Radar, Eddy Current Technique, Condition Assessment

# EVALUATING THE PERFORMANCE OF GEORGIA'S CRCPs USING GROUND PENETRATION RADAR (GPR)

by

NAZİK ÇITIR

B.S. in Civil Engineering, Ege University, Turkey, 2013

A Thesis Submitted to the Graduate Faculty of The University of Georgia in Partial Fulfillment of the Requirements for the Degree

MASTER OF SCIENCE

ATHENS, GEORGIA

2017

# EVALUATING THE PERFORMANCE OF GEORGIA'S CRCPs USING GROUND PENETRATION RADAR (GPR)

by

NAZİK ÇITIR

| | |
|---|---|
| Major Professor: | Stephan A. Durham |
| Committee: | Mi Geum Chorzepa |
| | Sung-Hee "Sonny" Kim |

Electronic Version Approved:

Suzanne Barbour
Dean of the Graduate School
The University of Georgia
December 2017

## ACKNOWLEDGEMENTS

Behind any significant research project there are countless others who support wholeheartedly and give their support, expertise and time.

First and foremost, the author would like to express her sincerest gratitude to her advisor, Dr. Stephan Durham. Without his continuous support, guidance, knowledge and mentoring, this work would not have been possible. He spent countless hours and effort in coordinating this project and assisting the author on this thesis.

In addition, many thanks go to the members of the advisory committee, Dr. Mi Geum Chorzepa and Dr. Sung-Hee "Sonny" Kim for their valuable time, assistance and suggestions, as well as guidance throughout this project.

The work conducted in this report was sponsored by the Office of Research in the Georgia Department of Transportation (GDOT Research Project 16-39). The author would like to thank the support provided by its employees, Mr. David Jared, Mr. Binh Bui, Mr. Peter Wu, Mr. Gary Wood, Mr. Ian Rish, Mr. JT Rabun, and Ms. Supriya Kamatkar for their research support and valuable inputs. A special thanks to Mr. Brennan Roney who advised the research team to successfully perform the study.

Additionally, the author would like to thank Dennis Kehres from Proceq Inc. for his assistance with training for the eddy current technology device.

A special word of thanks goes to the author's family from overseas and friends for their unfailing support and continuous encouragement during this study.

TABLE OF CONTENTS

Page

LIST OF TABLES

Page

LIST OF FIGURES

Page

# CHAPTER 1

# INTRODUCTION

## 1.1. Introduction

Forensic investigations of pavement failures are needed to investigate and diagnose the major causal effect resulting in pavement distress. The primary concern in the operation and maintenance of pavement is the cracking because of structural and functional failures. Cracks form because of some inadequacies of the pavement properties or from the design and construction of pavement.

Although the specifications, equipment, and construction processes have improved in recent years, variables still exist that may impact the long-term durability of constructed pavements. These variables result from "the low bid process, lack of experienced inspectors and project managers, poor selection of construction materials, lack of knowledge of the existing pavement conditions, unfamiliar construction methods and procedure and other issues unforeseen during design and construction phases." (Chen and Scullion 2008).

This thesis examines the existing and potential distresses in Continuously Reinforced Concrete Pavement (CRCP) sections of Georgia. The causes of distress include, but are not limited to, poor construction practices involving concrete placement, traffic loading, environment or climate influences, and materials. Additionally, inconsistency in longitudinal reinforcement placement in CRCP sections evaluated in the study is diagnosed. Specifically, this study investigates the variation in longitudinal and transverse reinforcement placement height by mobilizing a Ground Penetrating Radar (GPR) unit over areas of severe punchout and patching

to identify the cause of serious and repeated distress. Finally, a recommended GDT non-destructive test method-GPR for CRCPs will be developed as a result of this study.

### 1.2. Objectives

The objective of this thesis is to evaluate CRCPs throughout the state of Georgia to identify common characteristics between CRCPs having good performance with long history and those with repetitive significant distresses such as punchouts, excessive transvers and longitudinal cracking. Specifically, the following are the primary tasks that were accomplished through the completion of this study:

1. Determine the influence of reinforcement placement and concrete cover has on the punchout of CRCPs.
2. Identify and discuss the factors that affect the location and extent of distresses and punchouts.
3. Investigate the estimated depth of the sub-layer and the effect pavement profile has on the CRCP performance (if any).
4. Evaluate whether eddy current technology could be used in the absence of a cored sample for the calibration process of GPR in the field.
5. Create a standard procedure for the evaluation of pavements utilizing GPR technology.

The non-destructive test methods (NDTs), GPR and eddy current technique (Profometer 600) were selected for this study in order to investigate the existing condition of distressed and patched CRCP areas and determine reinforcement location at distress and punchout locations of Georgia.

### 1.3. Scope

A review of previous research involving the forensic investigation of CRCP in Georgia is included in Chapter 2. Furthermore, a literature summary of work related to CRCPs, the utilization of GPR and Profometer as the non-destructive testing methods for pavement investigations is provided in Chapter 3. The literature review includes discussion on the design, construction, and performance of CRCPs as well as common distresses found in the pavement type. In addition, the development and utilization of GPR technology is provided. Chapter 4 states the significance and benefit of this study in addition to the overall goals for the project. Chapter 5 details the experimental work plan for this research study. Chapter 6 presents the experimental results obtained from the site investigations and post-processing. Chapter 7 provides the conclusions of the research together with the recommendations for future studies.

# CHAPTER 2

# BACKGROUND

## 2.1. CRCP History in Georgia

Built in 1967, Interstate 75 (I-75) consisted of 13 miles (21 km) of State Route 42 (SR-42) between Forsyth and Macon to become the southbound lanes of I-75. In 1971, the first CRCP overlay in Georgia was designed and built on top of the existing State Route 42 (SR-42) jointed concrete pavement. The thickness of this CRCP overlay was 8 in (203 mm) throughout 10 miles (16.1 km) and 7 in (178 mm) throughout the remainder miles of the project. For 8 in (203 mm) and 7 in (178 mm)-thick sections, #5 reinforcing bars spaced 6 in (152 mm) were used on center with 0.6 and 0.7 percent steel, respectively. In 1989, GDOT built new four lanes in each direction, two northbound and southbound lanes, on I-75 to reinforce it against heavy traffic load. The new two southbound lanes were designed with 8 in (203 mm) -thick full-depth CRCP, with #6 longitudinal and #4 transverse reinforcing bars spaced 6 in (152 mm) on-center. Between 1990 and 2002, the vehicular load increased by 64% from traffic on Forsyth. After 2001, GDOT stated that the three lanes of I-75 needed the rehabilitation and the outside lane of I-75 needed to be replaced since it showed transverse cracking (CRSI 2003).

Gulden (1980) evaluated the conditions of the six CRCP sections on I-95. The I-95-1 (32) section is 12.6 miles (20.3 km)-length from US-17 in Bryan County to I-16 in Chatham County. The pavement structure has 8.5 in (216 mm) of CRC with a 6 in (152 mm) soil-cement base. The majority of the project was in good condition, and included some cluster cracking and wide cracks with spalling. The northbound lane (NBL) between MP 94.85 and 95.35 had three

punchouts due to poor base or subgrade support. These locations had been patched. Another distressed area located at the MP 91.2 southbound lane (SBL) had a longitudinal crack about 40 ft. (1219 cm) in length, which was located approximately 3 ft. (91 cm) from the centerline. This distress indicated that the pavement subsided in this area. The average crack spacing was determined as a range from 6.3 ft. (192 cm) to 9.8 ft. (299 cm) with a great number of cluster cracking and Y cracking.

One project, I-95-1 (27), was conducted on the 10.45 mile (16.8 km)-length section located from the end of the asphalt section north of SR-38 south to US-17. The pavement structure has 9 in (229 mm) of CRC with a 6 in (152 mm) base including 1 in (25.4 mm) of asphaltic-concrete and 5 in (127 mm) of soil-cement. The project was in excellent condition with a few tight cracks. The average crack spacing ranged from 2.8 ft. (85 cm) to 6.1 ft. (186 cm) in the NBL and from 4.2 ft. (128 cm) to 9.2 ft. (280 cm) in the SBL.

The I-95-1 (36) section runs between US-17 at South Newport River and SR-99 near Eulonia with a 9.1 mile (146 km)-length. The pavement structure has 8.5 in (216 mm) of CRC with a 6 in (152 mm) soil-cement base. The project was in good condition. Since this section is located in a marsh area, most problems were a result from settlement and poor concrete quality. Longitudinal cracking, which can lead to significant problems in the future, was detected at MP 58.2 and MP 58.7 in the NBL. In addition, two punchouts were noticed in the inside wheel path of the outside lane at MP 58.15 SBL. The average crack spacing ranged from 4.4 ft. (134 cm) to 7.1 ft. (216 cm) in the NBL and from 4.8 ft. (146 cm) to 8.6 ft. (262 cm) in the SBL.

Another project, I-95-1 (41) Glynn-McIntosh section, is located from SR-251 near Darien to US-25 near Brunswick with the distance of 13.3 miles. The pavement structure has 9 in

(229 mm) of CRC and a 6 in (152 mm) soil-cement base with a 3 in (76 mm) asphaltic-concrete drainage layer under shoulder at the base pavement interface. The project was in good condition with the major problems being longitudinal cracking. The average crack spacing ranged from 3.8 ft. (116 cm) to 6.1 ft. (186 cm) except for one section with 8.2 ft. (250 cm) crack spacing.

I-95-1 (29) Camden, limits from SR-40 near Kingsland to the Satilla River Bridge near Woodbine with 10.6 miles (17.1 km)-length. The project had a tine texture, which was in excellent condition. The average crack spacing ranged from 5.3 ft. (162 cm) to 8.9 ft. (271 cm) The last project, I-95-1 (38) Camden, is 4.1 miles (104 mm) from SR-40 near Kingsland to the Florida-Georgia State Line. The project was in excellent condition with a few cluster cracks. The average crack spacing ranged from 7.2 ft. (219 cm) to 10.1 ft. (308 cm).

Based on the recommendations in Gulden's study, the existing cracks should not be used as the face for the patch when patching punchouts. The boundaries of the patch should be determined by considering the location of distress caused by a loss of support such as an edge punchout. Generally, the poor support extends beyond the boundaries of punchout. Thus, NCHRP Report 60 "Failure and Repair of Continuous Reinforced Concrete Pavement" includes the suggested practices for the repair of CRCP (Gulden 1980).

In 2006 and with CRCP a major pavement type, State Route 6 was reconstructed with CRCP. The rebuilt section has two lanes each way of 12 in (305 mm) thick CRCP throughout 6.2- mile (10 km). In 2007, other projects included three sections of I-20; four sections of I-75; four sections of I-85; and at least two projects on I-95 (CMC 2007).

Based on a book publishing an overview of Georgia's pavement history, information on the original construction of each of the Interstates in Georgia (GGfGA Engineering 2016), CRCP

placed in 1974 on I-75 Cobb County was presented in Figure 2.1 by a photo in the 1990s. In addition, CRC pavement was placed on I-95 in Georgia; however, the settlement from hydraulic fills on the coast were observed. Therefore, the pavers simultaneously had to feed the steel reinforcements, which caused a shorter than normal service life for some of CRCP sections during testing.

**Figure 2.1 - I-75 Cobb County (CRCP) in 1974 (GGfGA Engineering 2016)**

Around 2000, GDOT began to carry out maintenance on PCC for both concrete pavement rehabilitation (CPR) of the inside lane and full lane replacement of the outside lane. Approximately 100 lane miles of full lane were replaced on I-20, I-75, and I-85. Along with the use of CRCP again, the pavements on I-75 in Cook, Tift, Crisp, and Dooly Counties below Macon were replaced with JPCP. In order to provide a proper method for maintenance of traffic, the traffic was first diverted to one side of the interstate. After the construction of the pavement, the traffic was switched to be able to construct the new pavement. Georgia preferred to use 13 ft. (396 cm) outside lanes instead of 14 ft. (427 cm) since the pavements with 14 ft. (427 cm) lanes in other states had longitudinal cracks.

A computer program, the 1972 AASHTO Pavement Design Guide, is currently used to design pavements (GGfGA Engineering 2016). GDOT is currently in the implementation stage of the most recent pavement software, AASHTO Pavement ME. This software required local calibration because there was a concern that the asphalt pavement was too conservative in the estimation of depth. One of the problems with the existing software is that it provides consistent PCC thicknesses that are unrealistic for interstates. For this reason, GDOT has been limiting PCC thicknesses of up to 12 in (305 mm) since 2000. Therefore, current typical GDOT Interstate pavement design for rigid pavements has 11 in (279 mm) or 12 in (305 mm)-thickness of PCC or CRCP, 3 in (76 mm) hot-mix asphalt (HMA) interlayer used as a separator between Graded Aggregate Base (GAB) and PCC/CRCP.

Based on the original typical sections for the 15 Interstate sections in Georgia, some information about pavements were obtained from various sources and projects in the 1990s. The typical CRCP sections and their locations were listed as the following (GGfGA Engineering 2016);

1. I-20-1(21)24 710140
    - 1975 in Douglas County
    - 9 in (229 mm) CRCP, 1 in (25.4 mm) HMA, 5 in GABCS, 6 in Aggregate Stabilized Soil
    - From MP 23.7 to MP 34.3

2. I-75 -3(35)280 710003
    - 1974 in Cobb County
    - 9 in (229 mm) CRCP, 1 in (25.4 mm) ‘H’ mix, 6 in (152 mm) GABCS, 5 in (127 mm) crushed aggregate ends at MP 269.6
    - From MP 265.6 to MP 269.6

3. I-95-1(38)00 H007219 and I-95-1(29)04 H007252
    - 1973 in Camden County
    - 8.5 in (216 mm) CRCP, 6 in (152 mm) premixed soil cement stabilized sub-base course
    - From MP 0 to MP 4 and from MP 4 to MP 14.8
4. I-95-1(41)36 H007221
    - 1973 in Glynn/McIntosh Counties
    - 9 in (229 mm) CRCP, 6 in (152 mm) premixed soil cement stabilized sub-base course
    - From MP 35.3 to MP 48.5
5. I-95-1(36)59 H007217
    - 1973 in McIntosh/Liberty Counties
    - 8.5 in (216 mm) CRCP, 6 in (152 mm) premixed soil cement stabilized sub-base course
    - From MP 58.1 to MP 67.3
6. I-95-1(27)36 510017-
    - 1975 in Liberty Counties
    - 9 in (229 mm) CRCP, 1 in (25.4 mm) 'H', 5 in (127 mm) premixed soil cement
    - From MP 67.3 to MP 77.6
7. I-95-1(32)84 H007257
    - 1971 in Bryan/Chatham Counties
    - 8.5 in (216 mm) CRCP, 6 in (152 mm) premixed soil cement sub-base
    - From MP 86.3 to MP 99

### 2.2. Overview of the Related Research Project

A research conducted by Johnson at University of Georgia evaluated three pavement types, Jointed Plain Concrete (JPC), Continuously Reinforced Concrete (CRC), and Hot Mix Asphalt

(HMA), to present the recommendation for forensic investigations for Georgia Department of Transportation (GDOT). The National Cooperative Highway Research Program (NCHRP) Report 747 was used as a guide in this study. In addition, this report was recommended for conducting forensic investigations of highway pavements for use in Georgia. Based on the recommendations of the guide, Johnson's thesis included destructive and on-site field testing and non-destructive testing using a Ground Penetration Radar (GPR) and Falling Weight Deflectometer (FWD).

In Johnson's study, the selected CRCP site including two pavement sections was on Interstate (I) 85 through Coweta County, Georgia. I-85 was composed of three lanes in one direction. The pavement at distance of 10 miles apart was in fair performance; the other pavement was in poor performance. A forensic site investigation was conducted with non-destructive, destructive, and laboratory testing.

The first site showed fair performance was from MPs 45 to 44, called as MP 45 in this study. MP 45 consisted of 11.5 in (292 mm) of PCC, 3.5 in (89 mm) of Asphalt-Concrete (AC), and 12 in (305 mm) of GAB. The second pavement in poor performance was located between MPs 55-54, called as MP 55. MP 55 consisted of 12 in (305 mm) of PCC, 3 in (76 mm) of AC, and 12 in (305 mm) of GAB.

The transverse cracks varied from 8 in (203 mm) to 36 in (914 mm) in length were observed throughout all three lanes in both sites. According to the Federal Highway Administration (FHWA 2012), crack spacing shall be between 24 in (610 mm) to 96 in (2439 mm). Another source notes that the recommended crack spacing is between 21 in (534 mm) and 84 in (2134 mm) between cracks (Caltrans, 2007). In MP 45, the depth and width of cracks were

measured as about 3.5 in (89 mm) and 0.02 to 0.04 in (0.5 to 1 mm), respectively. In addition, this site had the 3 ft. (92 cm) rebar spacing and 2 -3 longitudinal cracks. In MP 55, in the case of MP 45, the distance between cracks varied from 3.5 in (89 mm) to 13 in (330 mm).

### 2.2.1. Non-Destructive Testing Methods

In this study, non-destructive testing was performed on CRC pavements by using GPR and FWD. The GPR testing results showed the level pavement layers. When the GPR unit scans reinforcement steel, some distorted area appeared in the GPR images as it is seen in Figure 2.2. Therefore, transverse rebar spacing was detected as 3 ft. (92 cm) on center. Other design parameters were presented in Table 2.1.

**Table 2.1 - CRCP Non-Destructive Testing Results and Design Parameters (Johnson 2016)**

| | Parameters | I-85 MP 45-44 (Fair) | | I-85 MP 55-54 (Fair/ Poor) | |
|---|---|---|---|---|---|
| | | Outside | Inside | Outside | Inside |
| | Average ISM (kip/in) | 9400 | 3800 | 3600 | 4100 |
| | Back-calculated subgrade reaction (pci) | 460 | 221 | -- | -- |
| CRC Design Parameters | Surface Texture | Transverse Tining | | Transverse Tining | |
| | Epoxy Coated Rebar | No | No | No | No |
| | Longitudinal Rebar Depth (Clear Cover) (in.) | 3.75 | 3.75 | 3.25 | 4.5 |
| | Longitudinal Rebar Diameter (No.) | 0.75" (#6) | 0.75" (#6) | 0.75" (#6) | 0.75" (#6) |
| | Transverse Rebar Depth (Clear Cover) (in.) | 4.25 | 4.25 | 4 | 5.75 |
| | Transverse Rebar Diameter (No.) | 0.5" (#4) | 0.5" (#4) | 0.5" (#4) | 0.5" (#4) |
| | Longitudinal Rebar Spacing (ft.) | 0.45 to 0.5 | 0.45 to 0.5 | 0.42 to 0.46 | 0.42 to 0.46 |
| | Transverse Rebar Spacing (ft.) | 3 | 3 | 3 | 3 |

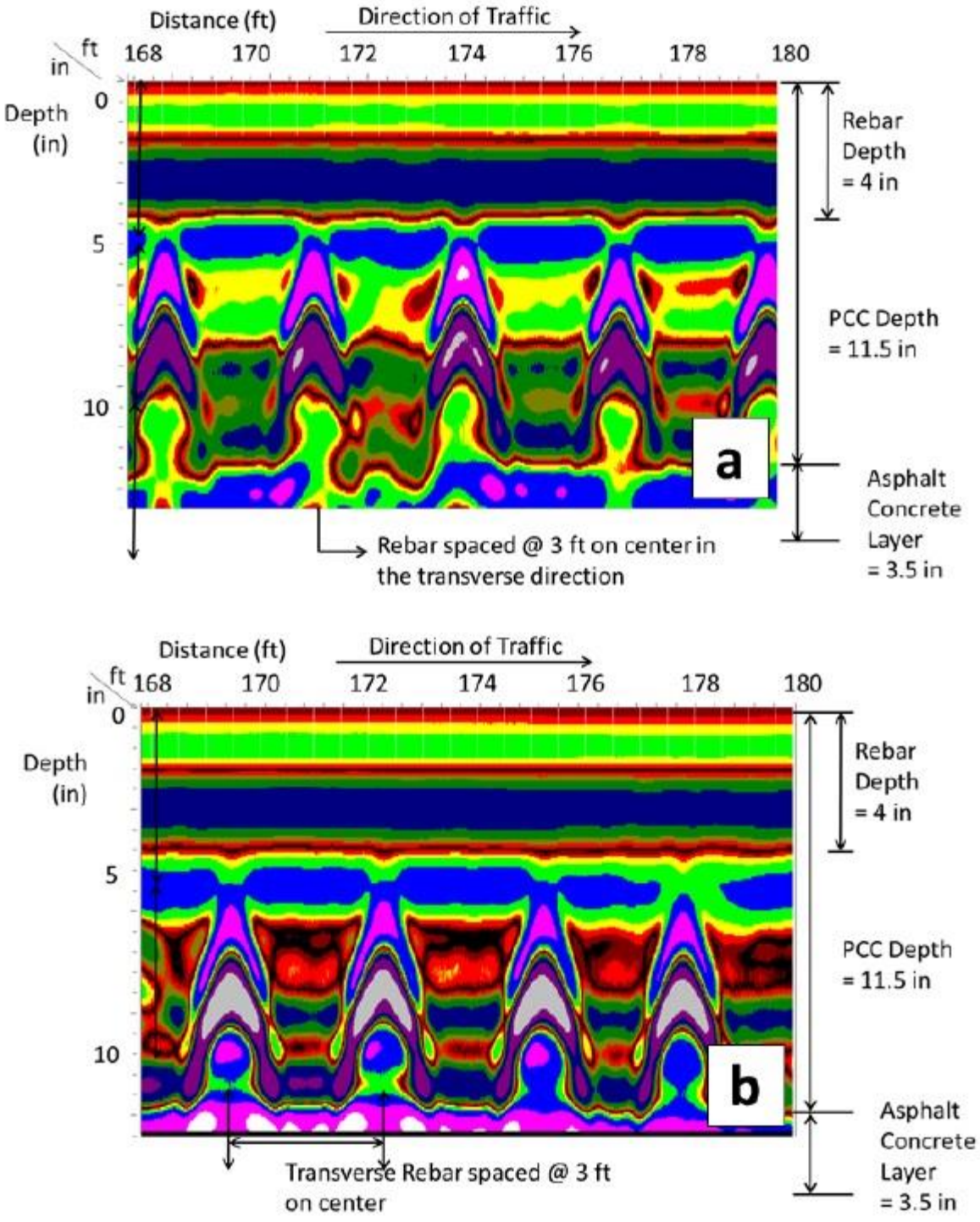


**(a) I-85 MP 55 (inside lane); (b) I-85 MP 45 (inside lane)**

**Figure 2.2 - GPR scans in the traffic direction (Johnson 2016)**

### 2.2.2. Destructive Testing Methods

#### 2.2.2.1. Coring and Field Testing

For the coring test done on the I-85 sections, a 4 in (102 mm) core drill was used for the laboratory test. In order to detect the pavement thickness and reinforcement size and location, a 6 in (152 mm) core bit was performed. For the carbonation and ASR test, one core (C8M-TR) was taken from MP 45 and two cores were extracted from MP 55 outside and inside lanes. Both test results showed a negative reaction for both sections.

The core sample taken from MP 45 outside lane indicated the constant longitudinal reinforcement depth, although this depth varied by as much as 0.75 in (19 mm) in the inside lane since the pavement surface was levelled. Many transverse cracks were observed on MP 55 section. It was noted that both longitudinal and transverse reinforcements were not epoxy coated for MP 45 and MP 55.

#### 2.2.2.2. Laboratory Testing

The laboratory tests including CTE, RCP, and MOE were conducted for the core specimens in accordance with the AASHTO T 336 (2011), ASTM C1202-12, and ASTM C469, respectively. Results from these tests are presented in Table 2.2. The CTE values of MP 45 and MP 55 were measured as 4.73 and 4.6, respectively. These values are acceptable values because the range for the CTE of PCC is between 4.4 to 5.5 microstrains/°F. The RCP values seen in Table 2.4 were evaluated as reasonable. For the MOE tests, the average MOE for MP 45 (3550 ksi) showed higher value in comparison of MP 55 (2790 ksi).

#### 2.2.2.3. Petrographic Analysis

Two cores (C3W-LR and C8M-LR from I-85 from MP 55) were selected for petrographic analysis. The outside lane of MP 55 had a similar concrete mixture to MP 45, therefore no cores from MP 45 were taken. Based on the analysis results, the MP 55 outside lane included a nominal maximum aggregate size (NMAS) of ¾ in (19 mm) crushed granite for coarse aggregate and natural quartzite and gray quartz for fine aggregate. See Table 2.2. The selected section with Class C fly ash had the water-to-cement ratio ranged from 0.40 and 0.45 and an entrained air content of 5%-7%. The concrete did not include slag. According to the requirements from GDOT, the material properties of MP 55 outside lane may meet the acceptance criteria (GDOT 430.3.06, 2013).

The sample analyzed from MP 55 inside lane showed that the crushed granite and amphibolite with NMAS of 3/8 in (9.5 mm). and the natural quartz were used as coarse and fine aggregate, respectively. The selected section without Class C fly ash was identified as fair quality with a water-to-cement ratio of 0.4 and 0.45 and an air content of 3%. Taking into account of GDOT acceptance criteria, the water-to-cement ratio is acceptable, although the air content is not in the required range (4.0 to 5.5). Therefore, the material properties of MP 55 inside lane do not meet the design requirements (GDOT 430.3.06, 2013).

**Table 2.2 - CRCP Destructive Testing Results and Design Parameters (Johnson 2016)**

| | Parameters | I-85 MP 45-44 (Fair) | | I-85 MP 55-54 (Poor) | |
|---|---|---|---|---|---|
| | | Outside | Inside | Outside | Inside |
| Condition | Good/Fair/ Poor | Fair | Fair | Fair | Poor |
| On-site Field Testing | ASR | No | No | No | No |
| | Carbonation | No | No | No | No |
| Laboratory Testing | MOE (ksi) | 3687 | 3417 | 3125 | 2450 |
| | f'c (psi) | 7,400 | 7,300 | 7,700 | 7,900 |
| | RCP (Coulomb) | 2085 | 3058 | 3382 | 3909 |
| | CTE ( in/in/°F) | 4.73 | 4.6 | 5.25 | 5.34 |
| Petrographic Analysis | Coarse Aggregate | See I-85 MP 55-54 Inside Lane | | Crushed Granite and Amphibolite | Crushed Granite |
| | Maximum Aggregate Size | | | 3/8" | 3/4"; Segregation at the surface |
| | Fine Aggregate | | | Natural quarts; The max sand particle size s 3mm. | Natural quartzite and gray quartz; The maximum sand particle size is 1/5". |
| | W/C ratio | | | 0.4-0.45 | 0.4-0.45 |
| | Fly ash | | | Class C fly ash and no slag in the cement. | Class C fly ash and no slag in the cement. |
| | Paste | | | The paste is of fair quality. | The paste is of fair quality. The paste is somewhat soft as it is scratched by a Mohs 3 hardness point. |
| | Air entrained | | | No | Yes |
| | Air content | | | Approximately 3% air consisting of mostly entrapped voids.; The air is not evenly distributed as there is more air in the middle of the core. | Approximately 5-7%. Mostly air entrained air voids. There is frequent ettringite in the voids. |
| | Cracks | | | Rare microcracks in the paste. | There are occasionally internal cracks in the aggregate. These cracks could present durability issues but do not appear to be presently detrimental. |
| | Other distresses to note | | | No corrosion is present at the periphery of the rebar. It has 3and3/4 inches of top surface concrete cover. | |

# CHAPTER 3

# LITERATIVE REVIEW

## 3.1. Portland Cement Concrete Pavement

Portland Cement Concrete (PCC) is exposed to volumetric changes as a result of moisture loss and temperature variations. In PCC pavement, those volume changes are controlled by concrete self-weight, reinforcement, and friction between concrete and sub-base. Concrete stresses within the pavement increase during traffic flow because of wheel loading. Together with this physical loading and volume change, cracks might occur if the total applied stress exceeds the maximum allowable stress capacity of the PCC pavement. Therefore, PCC pavement is separated into two types based on the effects of cracking potential on the durableness of those pavement types: Jointed Plain Concrete Pavement (JCP) and Continuously Reinforced Concrete Pavement (CRCP) (Ha et al. 2012). This study will focus entirely on CRCPs.

### 3.1.1. Continuously Reinforced Concrete Pavement (CRCP)

In this study, only selected CRCP sections in Georgia will be investigated to determine the vertical location of the reinforcement within the pavement section at selected punchout locations.

In 1921, the Bureau of Public Roads built the first experimental use of CRCPs on Columbia Pike in Arlington, Virginia. In 1938, the State of Indiana constructed the first notable length of CRCP (Highway Research Board 1973). CRCP was first used for the construction of the Interstate Highway System in the United States between the 1960s and 1970s (American Iron and Steel Institute 2014). Folliard and Prozzi (2005) reported that utilization of CRCP increased throughout the U.S. during the construction of the Interstate Highway System in the 1960s,

1970s, and 1980s. Historically, Texas and Illinois have used CRCPs more often than other states regardless of weather and environmental conditions.

Based on GDOT design practice for full-depth (12 in [305 mm]) or overlay (11 in [280 mm]) CRCP, the cover depth is required to range between 3.5 to 4.25 in (89 to 108 mm). However, the previous work conducted by Johnson (2016) indicated that the thickness of CRCP in some section of I-85 is greater than 12 in (305 mm) and longitudinal rebar depth varies in I-85 CRCP sections.

#### 3.1.1.1. CRCP Design

CRCP contains continuous longitudinal reinforcement and does not employ the use of transverse contraction joints at intermediate locations. The pavement is allowed to crack at random locations with the cracks held tightly together by the longitudinal reinforcing steel.

Transverse cracks are allowed to free concrete stresses in the transverse direction, which typically form at intervals of 1.5 to 6.0 ft. (46 to 183 cm.). In addition, the cracks are held together with continuous longitudinal reinforcing steel as shown in Figure 3.1. The percentage of reinforcing steel for CRCPs is commonly 0.6 to 0.7 percent of the pavement cross-sectional area (ACPA CRCP 2016). The 0.6% is recommended as a minimum percentage of steel content to keep the crack spacing between 3.5 ft. (107 cm) and 8 ft. (244 cm). The minimum (3.5 ft.) and maximum (8 ft.) criteria are recommended by FHWA to be able to control the formation of punchouts and spalling, respectively (Tsai and Wang 2014). If the crack spacing is greater than 8 ft. (244 cm), it causes the joint opening made concrete vulnerable against to spalling. In addition, the large crack spacing causes wider crack width, which creates the loss of LTE across transverse

cracks and end up with punchouts and faulting (ARA, Inc. 2004). The MEPDG recommends 3-6 ft. (91-183 cm) for the mean crack spacing range (Tsai and Wang 2014).

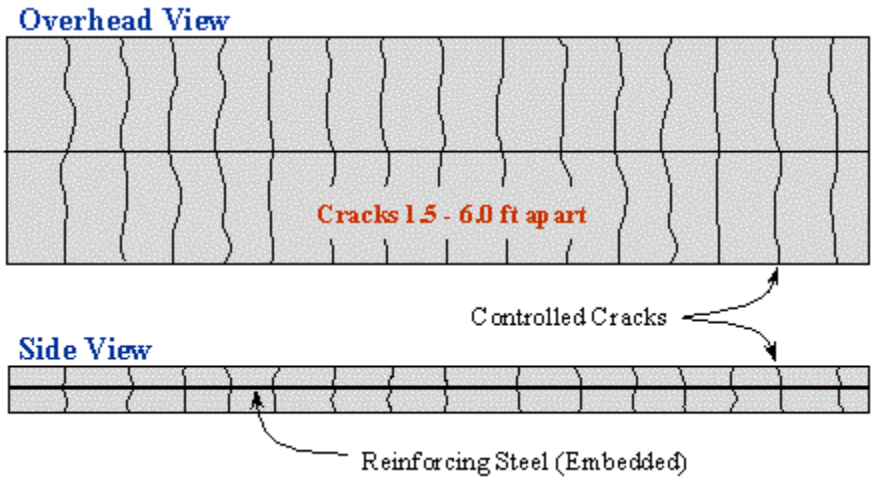


**Figure 3.1 - Overhead and Side Views of CRCP (ACPA CRCP 2016)**

The crack width of CRCPs is virtually always smaller than 0.04 in (1.02 mm) and typically less than 0.02 in (0.508 mm) (Kohler and Roesler 2005). It was suggested that a maximum crack width at the pavement surface was 0.04 in (1 mm) to prevent water infiltration (AASHTO 1986,1993). If the crack width was 0.025 in (0.635 mm) or less, it reduced water penetration for temperatures below freezing, resulting in reducing the corrosion of the steel and sustaining high load transfer efficiency (Ren 2015). The essential difference between JPCP and CRCP is that while the behavior of cracks is accepted as a distress in JPCPs, it is not considered a distress in CRCP (Ha et al. 2012). Distresses including punchouts, crack spalling, and steel rupture, might occur from traffic and environmental loadings. Engineers working on CRCP design manage the cracking that develops so as to reduce this distress. Therefore, CRCP can be constructed for many miles without joints (FHWA 2012). According to the performance factors mentioned in Topic 622 in the guide of the California Department of Transportation, CRCP

design is made to have at most 10 punchouts/ mile at the end of its design life under worst case conditions (Caltrans 2015).

Kohler and Roesler (2006) analyzed crack width (CW) and crack spacing (CS) data from full-scale CRCP sections. The authors utilized CRCP CW and CS models with the new Mechanistic-Empirical Pavement Design Guide (MEPDG) to compare measured CS data, and CW data was collected under different temperature conditions by selecting five test sections. Based on their results, the CW model was calibrated to standardize the measurements. Instead of using MEPDG software, CS and CW were calculated with MEPDG formulas. In Figure 3.2, the predicted CS is compared with the measured CS for 4-sections located at the center of the CRCP test strip. According to Figure 3.2, the CS prediction model based on MEPDG closely matched the actual mean.

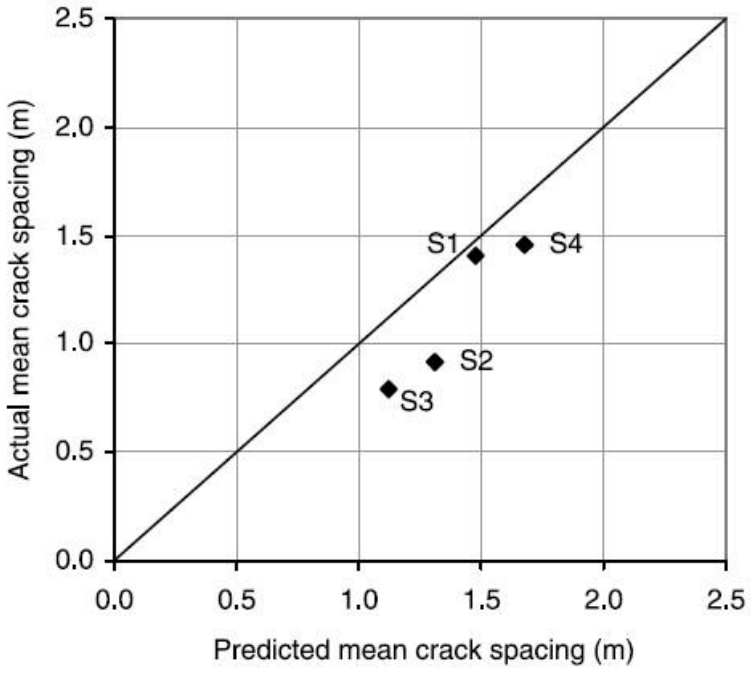


**Figure 3.2 - Predicted and Measured Crack Spacing (Kohler and Roesler 2006)**

The authors defend that CW acts a key role affecting the performance of CRCP. CW manages the aggregate interlock and, later, shear load transfer capabilities between adjacent concrete sections. In the presented research, CW predicted model was calibrated by using a defined factor to be able to represent the model correctly and to obtain a reasonable prediction of actual CW. According to the results, using of high amount of steel content reduced the average CW on the selected sections.

Figure 3.3 shows a typical CRCP section typically specified by GDOT. The CRCP slab thickness is between 11 to 12 in (280 to 305 mm) above a 3 in (76 mm) asphalt cement concrete (ACC) layer with a 12 in (305 mm) graded aggregate base (GAB) below that is no less than 8 in (203 mm). Longitudinal reinforcement typically utilized for CRCPs is a #6 steel bar. The reinforcing bar used in the transverse direction to support the longitudinal steel is a #4. Steel reinforcement is placed no less than 3.5 in (89 mm) or no more than 4.25 in (108 mm) below the top surface of the slab (Tsai and Wang 2014). This distance provides adequate concrete cover while positioning the steel reinforcement such that it prevents cracks from widening.

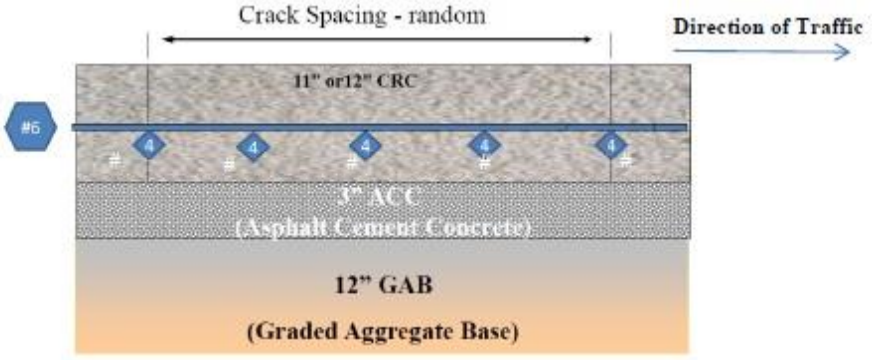


**Figure 3.3 - CRCP Section in GDOT (Tsai and Wang 2014)**

#### 3.1.1.2. CRCP Performance

CRCP pavements perform well in the U.S. and other countries when appropriately designed and constructed. According to Topic 612 in the guide of the California Department of Transportation (Caltrans 2015), pavement design life is defined as the optimum number of years that CRCP properly provides its service without any major recovery or restoration. CRCP performance is contingent upon materials, design, construction, and environmental factors as follow (Folliard and Prozzi 2005);

- PCC properties that include elastic modulus, tensile strength, coefficient of thermal expansion and drying shrinkage,
- Steel properties that include steel bar diameter and location, percent reinforcement,
- Slab and sub-base resistance,
- Size and geometry of pavement (ie. thickness)
- Environmental loads that include ambient air temperature, wind speed and humidity,
- Traffic loads that include static wheel load and mobile dynamic load

#### 3.1.1.3. Distress Type of CRCP

Distress types of CRCP are categorized in two main groups defined as structural distress and functional distress. Yoder et al. made a distinction between two different types of failure. The first type including a collapse of the pavement structure or pavement components is defined as structural failure. The second type occurs when the pavement will not perform its intended function without causing discomfort to passengers or high stress in the vehicle crossing over it, due to its roughness, and is a functional failure. Thus, the differences between both type failures must be analyzed properly since they need different maintenance. Functional failure requires minimal and regular maintenance such as resurfacing to bring back smooth-riding qualities to the

pavement; however; structural failure might require a complete removal and replacement of the pavement section (Yoder and Witczak 1975).

There are many contributing factors affecting structural and functional distresses as seen in Table 3.1. The table shows the possible causes and the primary, contributing and negligible factors for the types of distresses in detail (Rada et.al 2013).

FHWA (2013) indicated that punchouts, wide transverse cracks, and longitudinal cracks are the most detrimental structural distresses. Other type distresses occurred in concrete are spalling, patch deterioration, faulting, and blowup. Table 3.2, provided as support for given information by Rada et.al (2013), shows severity of distress types caused by traffic loading, and climate & materials.

#### 3.1.1.3.1. Cracking

Cracks in the transverse direction in CRCP are allowed to remain tight. Therefore, this type of cracking is not considered distress. However, wide transverse cracks and longitudinal cracks might need rehabilitation (FHWA 2013).

##### 3.1.1.3.1.1. Wide Transverse Cracks

Wide transverse cracks are perpendicular to the pavement centerline and occur due to inadequate and defective structural design and loss of support. In addition, large crack spacing formed from low levels of reinforcement can make the transverse cracks widen. Therefore, it increases tensile stress in the reinforcement. When the reinforcement ruptures, the transverse cracks will not transfer loads of weight. When medium and high severity cracks occur (ranging between 0.12 in to 0.24 in (3 to 6 mm), they must be rehabilitated extremely fast (FHWA 2013).

**Table 3.1 - Types of distress and possible causes (Rada et.al 2013)**

| Structural Distress | Contributing Factors[1] | | | | | |
|---|---|---|---|---|---|---|
| | Pavement Design | Load | Water | Temp. | Pavement Materials | Construct. |
| **Structural Distress** | | | | | | |
| **Cracking[2]** | | | | | | |
| Transverse | P | P | N | C | C | P |
| Longitudinal | P | P | N | C | C | P |
| Corner | C | P | C | C | N | N |
| Intersecting | C | P | C | N | C | N |
| Possible causes of cracking: Fatigue, joint spacing too long, shallow or late joint sawing, base or edge restraint, loss of support, freeze-thaw and moisture-related settlement/heave, dowel bar lock-up, curling, and warping. | | | | | | |
| **Joint/Crack Deterioration** | | | | | | |
| Spalling | C | C | N | C | P | C |
| Pumping[2] | C | P | P | N | C | N |
| Blowups | C | N | N | P | C | N |
| Joint Seal Damage[2] | C | C | C | C | P | C |
| Possible causes of joint/crack deterioration: Incompressibles in joint/crack, material durability problems, subbase pumping, dowel socketing or corrosion, keyway failure, metal or plastic inserts, rupture and corrosion of steel in JRCP, high reinforcing steel. | | | | | | |
| **Punchouts[2]** | P | P | C | N | C | N |
| Possible causes of punchouts: Loss of support, low steel content, inadequate concrete slab thickness, poor construction procedures. | | | | | | |
| **Durability** | | | | | | |
| D-cracking | N | N | P | C | P | N |
| Alkali-Silica Reactivity (ASR) | N | N | P | C | P | N |
| Freeze-thaw damage | N | N | P | P | P | C |
| Possible causes of durability distresses: Poor aggregate quality, poor concentrate mixture quality, water in the pavement structure. | | | | | | |
| **Functional Distress** | | | | | | |
| **Roughness** | | | | | | |
| Faulting[2] | P | P | P | C | C | N |
| Heave/swell[2] | C | N | P | P | C | N |
| Settlement[2] | C | C | C | N | N | C |
| Patch deterioration | C | C | C | C | C | C |
| Possible causes of roughness: Poor load transfer, loss of support, subbase pumping, backfill settlement, freeze-thaw, and moisture-related settlement/heave, curling and warping, and poor construction practices. | | | | | | |
| **Surface Polishing** | N | C | N | N | P | N |
| Possible causes of surface polishing: High volumes of traffic, poor surface texture, wide uniform tine spacing, wide joint reservoirs, and wheel path abrasion because of studded tires or chains. | | | | | | |
| **Noise** | P | C | N | N | C | P |
| Possible causes of noise: High volumes of traffic, poor surface texture, wide uniform tine spacing, wide joint reservoirs, and wheel path abrasion because of studded tires or chains. | | | | | | |
| **Surface Defects** | | | | | | |
| Scaling | N | N | C | C | P | P |
| Popouts | N | N | C | C | P | C |
| Crazing | N | N | N | C | C | P |
| Plastic shrinkage cracks | N | N | N | C | C | P |
| Possible causes of surface defects: Over-finishing the surface, poor concrete mixture, reactive aggregates, and poor curing practices. | | | | | | |

[1] P= Primary Factor C= Contributing Factor N= Negligible Factor

[2] Loss of support is an intermediary phase between the contributing factors and these distresses. Loss of support is affected by load, water, and design factors.

**Table 3.2 - Common distress types and their severities formed by causes (FHWA 2013)**

| Distress Type | Caused by Traffic Loading | Caused by Climate / Materials |
|---|---|---|
| Punchout | X | |
| Cracking | | |
| Wide transverse cracks | X (M,H) | X (L) |
| Longitudinal cracks | | X |
| Spalling | X | X |
| Faulting | | |
| Longitudinal joint faulting | X | X |
| Lane/Shoulder dropoff or heave | | X |
| Erodibility | | |
| Pumping and water bleeding | X (M,H) | X (L) |
| Joint distress | | |
| Construction joint distress | X | X |
| Lane/shoulder joint separation | | X |
| Materials-related distresses | | |
| D-cracking | | X |
| Alkali–silica reactivity | | X |
| Popouts | | X |
| Scaling, map cracking, and crazing | | X |
| Corrosión | | X |
| Swell | | X |
| Depression | | X |
| Localized distress | | X |
| Blowup | | X |
| Patch deterioration | | |
| Asphalt patch deterioration | X | |
| Concrete patch deterioration | X (M,H) | X (L) |
| Adjacent slab deterioration | X | X |

Note: L = low severity, M = medium severity, and H = high severity.

The severity levels of the transverse cracks are separated into three groups; low, moderate, and high levels (FHWA 2003). In low severity, the cracks are not spalled or with spalling, formed less than 10 percent of the crack length. In moderate severity, the cracks have spalling formed between 10 and 50 percent of the crack length. There is spalling developed more than 50 percent of the crack length at high severity as seen in Figure 3.4.

**a. Low severity** **b. Moderate Severity** **c. High Severity**

**Figure 3.4 - The examples of severity levels of transverse cracks (FHWA 2003)**

**3.1.1.3.1.2. Longitudinal Cracks**

Longitudinal cracks occur due to the poor construction techniques or settlement and are parallel to the pavement centerline. As long as repeated loadings exist on the pavement, these cracks typically expand and allow water to get into the structure (FHWA 2013). According to FHWA (2012), in Georgia, the longitudinal rebar shall be placed no less than 3.5 in (89 mm) or no more than 4.25 in (108 mm) beneath the top of slab.

Roesler et.al (2005) conducted research that showed a failure investigation on longitudinal cracking distress on CRCPs in Illinois. The aim of his study was to determine the distress mechanisms causing premature longitudinal cracking on CRCP. The longitudinal

cracking occurred over the driving and passing lanes embedded with reinforcement steel. The results showed that this cracking was not triggered by steel corrosion, damaging reactions in the concrete materials, or insufficient constructional design. Instead of those parameters, cracking was linked to settlement of reinforcing steel in the concrete. Settlement cracking typically occurs in the concrete slabs with high slump and small concrete cover depth. However, the team found that the longitudinal reinforcing steel in CRCP settled within the concrete due to the large cover depth, low slump concrete, and the technique (tube-feeding) of placing the steel bars in the fresh concrete. Then, longitudinal cracks occurred.

Longitudinal cracks have three different severity levels (low, moderate, and high) (FHWA 2003). These cracks at low severity have no spalling or faulting and crack widths are less than 0.12 in (3 mm). At moderate severity level, the cracks ranged from 0.12 in (3 mm) to 0.52 in (13 mm) in width have spalling or faulting, which are less than 3 in (75 mm) and 0.52 in (13 mm), respectively. The cracks at the high severity are more than 0.5 in (13 mm) in width; with spalling formed more than 2.95 in (75 mm) or with faulting formed more than 0.5 in (13 mm) as is seen from Figure 3.5.

a. **Low severity** **b. High Severity**

**Figure 3.5- The examples of severity levels of longitudinal cracks (FHWA 2003)**

#### 3.1.1.3.2. Spalling

FHWA (2013) reported that spalling defined as the cracking, breaking, chipping or fraying of the slab edges develops up to 2.4 in (60 mm) of a crack or joint. The spalling of CRCP might be related to weak surface concrete, corrosion of reinforcing steel, inadequate concrete cover, poor structural design, misaligned reinforcement and extensive pressures. Figure 3.6 shows the spalling formed at transverse cracks and joint.

**a. Form at transverse cracks** **b. Form at transverse joint**

**Figure 3.6 - The examples of spalling at cracks and joint (FHWA 2013; NCHRP 2001)**

#### 3.1.1.3.3. Punchouts

Punchouts and longitudinal cracking are considered major structural distresses in CRCPs (NCHRP 2001). A study by McCullough et al. found that punchout is a major structural failure in which a small segment of pavement is broken loose from the main body and dislocated downward under traffic. The punchout usually is bounded by two closely spaced transverse cracks, a longitudinal crack, and the pavement edge (Sub and McCullough 1992). Punchouts are defined as a form of cracking that develops between two closely spaced transverse cracks in CRCP (ARA, Inc. 2003). Punchout occurs when a short longitudinal crack links together two closely spaced transverse cracks. The longitudinal crack develops as a result of the large

deflections and high stresses under traffic wheel loads across the pavement area between the transverse cracks.

Punchouts affect the long-term performance of CRCP resulting in pavement failure and negatively impacting ride quality and safety. In order to estimate pavement life, the severity levels must be determined. Severity levels are categorized in three phases: low, moderate, and high levels as they are shown in Figure 3.7. In low severity, the transverse and longitudinal cracks are tight and might have spalling less than 2.95 in (75 mm) or faulting less than 0.24 in (6 mm) without losing material. There are no 'Y' cracks in this level. In moderate severity, spalling might be more than 2.95 in (75 mm) or faulting might be between 0.24-0.51 in (6-13 mm). In high severity, spalling might be more than 5.91 in (150 mm). In addition, the concrete in punchouts might be pushed down by 0.51 in (13 mm), moved by traffic flow, and/or broken into pieces. Figure 3.8 illustrates pavement examples in each of these three severity cases. The number of punchouts are recorded at each severity levels (FHWA 2003).

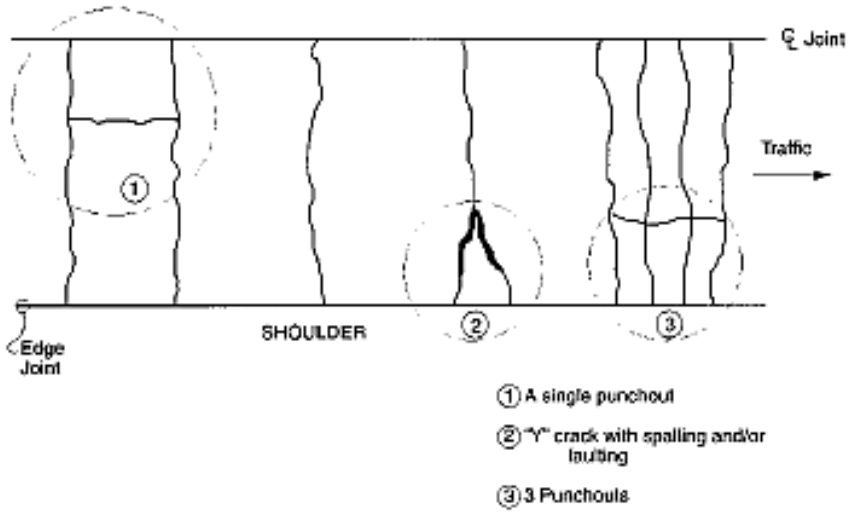


**Figure 3.7 - Severity levels of punchouts (FHWA 2003)**

**a. Low severity** **b. Moderate Severity** **c. High Severity**

**Figure 3.8 - The examples of severity levels of punchouts (FHWA 2003)**

Kohler and Roesler (2004) investigated the crack spacing and crack width by conducting experiments on CRCP sections. The authors found that punchouts and spalling distresses, which are unwanted crack patterns on the pavement, had formed in the presence of small crack spacing, cluster cracks, divided cracks, and Y-cracks (Figure 3.9). Based on a study referenced by the authors, cluster cracking was described as the moving average of five cracks which are spaced less than 2 ft. (61 cm). Another research mentioned in this researcher's study proved that if the depth of reinforcement increased, Y-cracking decreased. However, this increase in depth developed more cluster cracking. Likewise, the increase in cluster cracking together with concrete shrinkage decreased Y-cracking (Kohler and Roesler 2004).

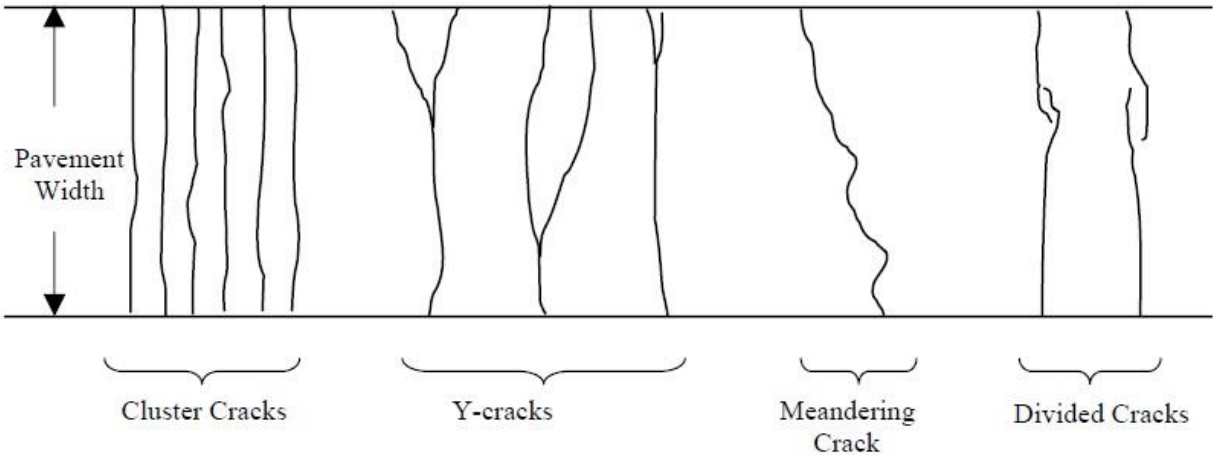


**Figure 3.9 – Crack Shapes and Patterns (Kohler and Roesler 2004)**

The research showed that the cluster of transverse cracks was defined as the group of three or more transverse cracks having a spacing of 2 ft. (61 cm) or less. It was accepted that if two consecutive transverse cracks were spaced at more than 3 ft. (91 cm), the cluster cracking ended and the next cluster cracking (or single transverse crack) began at the next transverse crack (McGhee 1998).

In a study referenced by Kohler and Roesler (2004), the average crack spacing in CRCP was in the range of 1-6 ft. (30-183 cm) based on the data obtained approximately 80 sections. They noted that the ideal spacing between cracks was accepted as the range of 3-5 ft. (91 -152 cm). In addition, they stated that more variability on the crack spacing increases the likelihood of punchout growth (Kohler and Roesler 2004). The punchouts are often formed between two transverse cracks spaced at 2 ft. (61 cm) or less (ARA, Inc. 2003).

According to previous AASHTO pavement design guides, the two most important factors causing punchouts were crack spacing and width, although punchouts were not taken into account during design calculations. In addition, these guides indicated that when the space of cracks is at intervals of 3.5 ft. – 8 ft. (107 cm-244 cm), it is considered ideal. Otherwise, the narrowly spaced cracks are undesired (AASHTO 1986, 1993). Based on prior research, another structural casual factor is weak support of a concrete slab. Due to sub-base erosion, the failure of cracks might occur because of poor support (ARA, Inc. 2004). The National Cooperative Highway Research Program (NCRHP) states that the number and magnitude of applied wheel loads, slab thickness and stiffness, base stiffness, steel reinforcement, drainage conditions, and erosion of slab support are factors affecting the punchout development (NCHRP 2001).

In a study examining the effect of reinforcement cover on punchouts, the lower the reinforcement was placed in the pavement section, the more punchouts occurred over time as illustrated in Figure 3.10. Ultimately, as reinforcement is placed closer to the pavement surface, crack openings will remain relatively small as the reinforcing steel holds the crack together. Therefore, the number of cracks will be reduced (ARA, Inc. 2003).

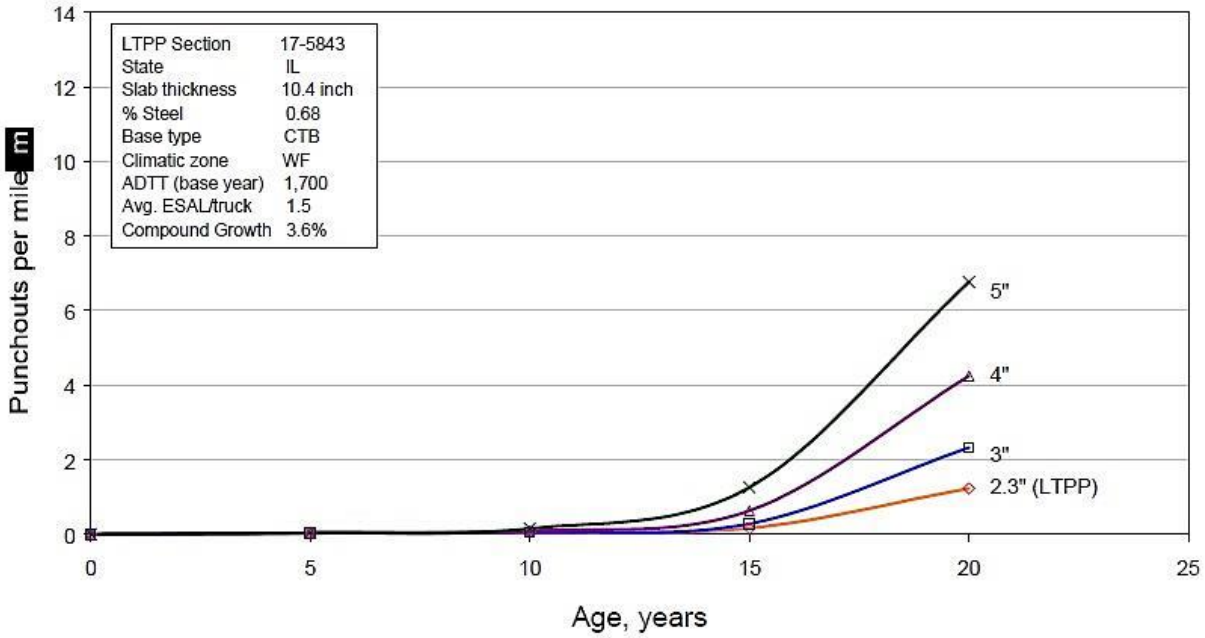


**Figure 3.10 - Effect of cover depth on punchouts over time (ARA, Inc. 2003)**

An experimental project, which supports the above mentioned theory regarding the relationship between cover depth and punchouts, was conducted in 1963 in Illinois (Gharaibeh et al. 1999). Reinforcing steel was placed in varying depths from 2 to 4 in (51 to 102 mm) from the top of an 8 in (203 mm) thick slab. As the results in Table 3.3 indicate, the closer that steel is placed to the slab surface, the tighter the transverse cracks remain, and fewer punchouts occur over the life of the pavement. Conclusions from the study showed that proper depth of steel reinforcement should be at least 3 in. (76 mm). With consideration of factors that include

construction and steel reinforcing protection from chlorides, steel reinforcement is placed at a depth of about 3.5 in (89 mm) within a 10 to 12 in (254 to 305 mm) CRCP in Illinois State.

**Table 3.3 - Effect of reinforcement depth on CRCP performance (Gharaibeh et al. 1999)**

| Reinforcement Depth, mm (in) | Crack Width in Winter, mm (in) (pavement age = 9 years) | Patching, $ft^2/1000\ ft^2$ ($m^2/1000\ m^2$) (pavement age = 14 years) |
|---|---|---|
| **51 (2)** | 0.475 (0.0187) | 7.0 (7.0) |
| **76 (3)** | 0.7925 (0.0312) | 12.7 (12.7) |
| **102 (4)** | 0.8306 (0.0327) | 30.9 (30.9) |

A report prepared for NCRHP referenced investigations that show the causes and factors of punchouts in CRCPs (ARA, Inc. 2003). Studies by LaCourserie et al. (1978) and Darter et al. (1979) explain the mechanism of edge punchout based on the field investigations of punchout distress in CRCP in Illinois. The development of high tensile stresses occurred at the top of the slab approximately 3.28 to 6.56ft. (100 to 200 cm) from the longitudinal edge of the slab was investigated. The results showed poor load transfer across the transverse cracks. In addition, crack spacing was defined as a significant factor impacting the magnitude of the critical tensile lateral stresses on the slab top. Selezneva (2001 and 2002) affirmed these conclusions by observing Long-Term Pavement Performance (LTPP) sections located in 22 states. Approximately 90 percent of all punchouts observed were on CRCP sections surrounded by two transverse cracks spaced at 2 ft. (61 cm) or less. Findings of these studies identify the following factors as affecting the development of punchouts (ARA, Inc. 2003);

- The narrow transverse crack spacing (0.6 m or less) (2 foot or less) existing in the crack spacing distribution,
- Loss of load transfer efficiency (LTE) along the transverse cracks due to aggregate intertwined from heavy crack opening and repetitive loads,

- Base erosion due to the support lose along the sidewalk,
- An increase in bending stresses due to the negative temperature above the slab thickness and shrinkage at the slab drying,
- The repeated cycles of heavy tensile bending stresses formed from the heavy axles, causing the longitudinal fatigue cracking defined as punchout.

The computation of the total number of failures per 1 mile (1.61 km) consists of the sum of punchouts, existing repairs, transverse cracks, and sectional failures. In this case, some factors affect the failures such as a percentage of steel and slab thickness, steel placement method, and base type. It is clearly seen that, an increase in slab thickness or percentage of steel (or both) reduce the number of failures. In addition, the steel placement methods affect the CRCP performance, which are done by placing steel on chair or placing it by using tubes. When comparing both methods, use of chairs provides a slightly better performance than tubes at high traffic loading levels.

In order to evaluate the effect of base type on punchout, CRCP pavement with a slab thickness of 8 in (203 mm) , 0.62 steel reinforcement percentage and reinforcement placed on chairs was constructed and evaluated utilizing different base types. These base types were no base, cement-aggregate mixture (CAM), granular mixture (GRAN), and bituminous-aggregate mixture (BAM). The results showed that BAM, GRAN, CAM, and no base types are ranked from well to poor performing, respectively (Gharaibeh et al. 1999).

Tsai and Wang (2014) reported solutions to reduce or control the development of punchouts as being (ARA, Inc. 2004);

-Increased longitudinal steel reinforcement content
-Increased load transfer efficiency (LTE)
-Increased slab thickness,

-Increased PCC strength,

-Decreased PCC coefficient of thermal expansion (CTE) to lower the thermal causing tensile stresses,

-Decreased bending after placement;

-The placement of reinforcing steel above the midsection of slab thickness which satisfies the minimum cover,

-The use of a stabilized base,

-The use of a connected PCC shoulder to prevent the movement of the CRCP slab

### 3.2. Ground Penetration Radar (GPR)

The most common types of Non-Destructive Testing (NDT) equipment for evaluating pavement performance are GPR, Falling Weight Deflectometer (FWD), friction testers and profilometers. FWD equipment measures the deflection responses by applying impulsive load to a pavement surface to evaluate structural issues. The impact load, loading duration, and area are set to correspond to the actual loading by a standard truck carried on a service load (Sharma and Das 2008).

Friction testers determine the frictional resistance by using a two-wheeled trailer and water. The trailer spray a measured amount of water on the pavement. After spraying, the trailer is locked by braking. Friction is then generated between the tire and the pavement surface when the tire slides over the wet surface. As a result, a torque develops on the trailer axle and is then measured, and friction numbers (FN) showing the frictional properties of pavement are calculated (IDOT 2005).

Another method, profile-measuring equipment, evaluates ride quality issues. Lasers in customized vehicles are used to measure profiles by collecting data including longitudinal and transverse profile, crack pattern, and micro and macro textures. GPR effectively assesses the

layer thickness of the slab and identifies certain problem areas in the pavement "such as debonding, presence of moisture, voids under concrete slabs, and other issues that are typically assessed through coring" (Rada et.al 2013). This thesis focuses on the utilization of GPR to investigate causes of punchouts in Georgia's CRCPs.

Recently, GPR has gained widespread acceptance as a geophysical technique. The GPR method has been particularly practical form imaging certain sediments and soils that are located approximately from 8 in (203 mm) to 16.4 ft. (500 cm) below the ground surface (Conyers 1995).

In 1929, the first attempt at a non-destructive testing system, precursor to the modern GPR, was used to determine the depth of ice in a glacier in Austria (Conyers 1998). Individuals working with electromagnetic energy transmitting within a medium other than air pioneered this technique. In 1930, the U.S. military realized that an airplane flying overhead interrupted radio communication. Then, the military initiated a work to detect objects using radio waves. In 1934, the word "RADAR", an acronym for Radio Detection and Ranging, was coined. The use of radar to determine ice, underground water table and subsoil properties was began during this time (Lohonyai 2015). In 1972, The National Aeronautics and Space Administration (NASA) built a prototype GPR system and sent it on Apollo 17 to the moon for investigating the electrical and geological properties of the lunar subsurface (Conyers 1998). GPR has been successfully used in a number of areas for non-destructive, underground measuring applications, "including detecting buried explosives, locating possible archaeological dig sites, buried pipes, and embedded reinforcing steel, inspecting pavements, mapping soil strata, contaminant plumes, groundwater levels, and ice thicknesses" (Lohonyai 2015).

A GPR system comprises three main components; an antenna, control unit and a power supply shown in Figure 3.11. The control unit includes electronics stimulating a pulse of energy waves that are sent into the ground by the antenna. The system also contains a computer and hard disk to store data for analysis once testing has been completed (GSSI 2016). GPR uses the antenna placed on the ground surface to penetrate high-frequency electromagnetic (EM) waves through pavement, structures or other media and identify the various layers beneath the subsurface. Data is typically received via the antenna (ASTM-D6432 2011).

To penetrate radio waves for the desired depth of the structure, the selection of the antenna frequency is one of the most significant factors when using the GPR system. The frequency of GPR antennas commonly range from approximately 10 to 1,200 megahertz (MHz) (Conyers 1998). When the frequency of the antenna is higher, the penetration into the ground will be superficial (GSSI 2016).

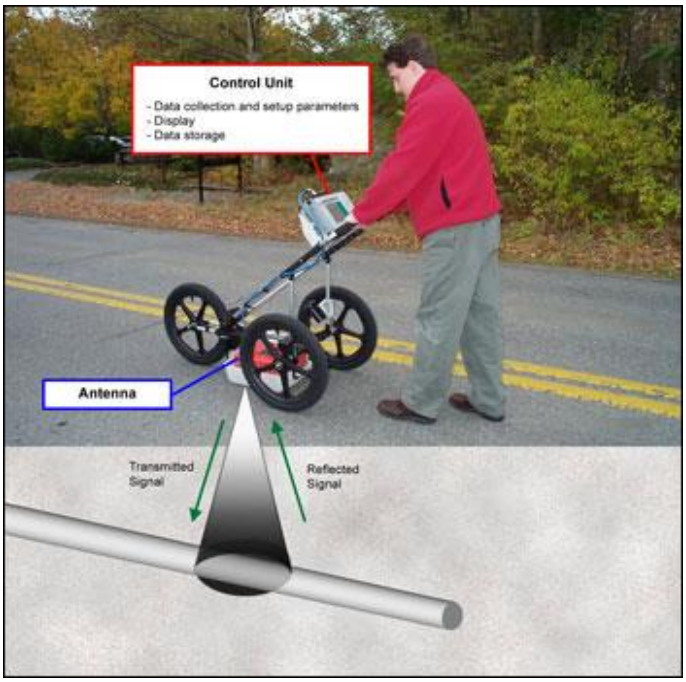


**Figure 3.11 - GPR units (GSSI 2016)**

In a forensic investigation performed by Chen and Scullion (2008), GPR was used for pavement evaluation with a 1.0 GHz antenna through approximately the top 24 in (610 mm) of the pavement. The team notes that GPR has become a practical test method to explore cracks through asphalt layers and has been found to provide comprehensive results of underground conditions. Due to having a large number of GPR traces for each GPR test, a color coding scheme was used to convert the variations of dielectric signals from these traces to subsurface images. An example of the color coding for a hot-mix asphalt pavements is presented in Figure 3.12 and Figure 3.13. Figure 3.12 represents the reflections of well-compacted pavement without defects. GPR reflection indicates that the two reflections in the color-map are a red line at the top of the figure that is the pavement surface and a yellow area located between 16 and 17 in (400 mm and 425 mm) depth that is the top of the base layer. The right and bottom axes show the depth and distance scales, respectively. When the pavement section has a weak structure, a GPR unit registers strong reflections (blue and red signs) as shown in Figure 3.13. The primary aim of a study conducted by Chen and Scullion (2008) was to evaluate the rehabilitation for pavements with stripping. One of the sections investigated was approximately 18 miles (29 km) of US281. This site has 6 in (150 mm) of AC and 12 in (300 mm) of granular caliche base. Many locations were determined to have stripping problems at various depths by using GPR. In addition, FWD test results showed that the structure of the pavement was inadequate. Based on both test results, the bases were found to be wet and very weak. The other objective conducted by the team was to determine causes of distress. The selected area was US69. A porous layer causing debonding was detected at 2-4 in (50-100 mm) by GPR, FWD, and coring. The results showed that the presence of the porous layer caused the surface distress.

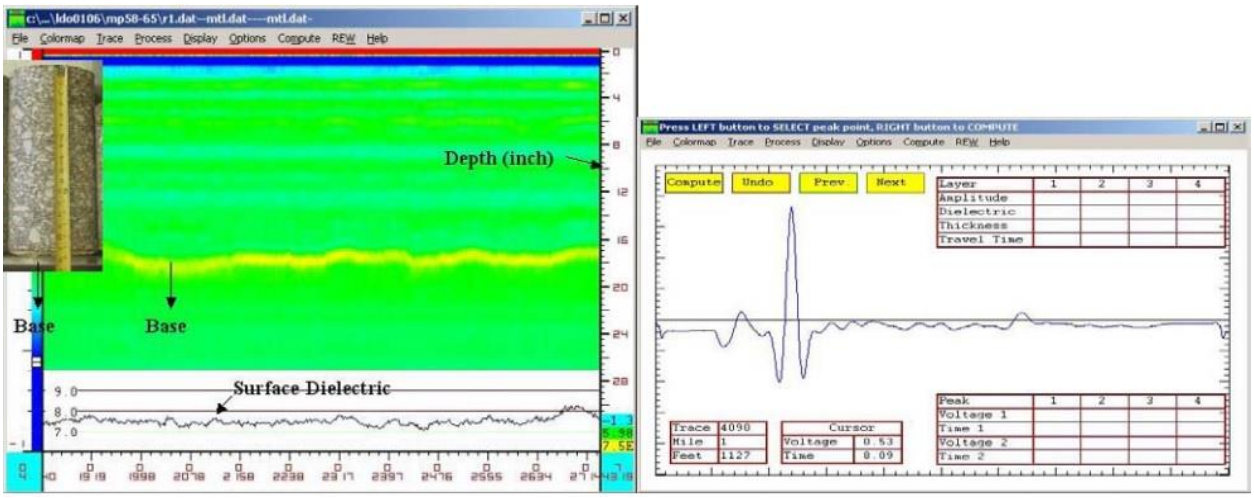


**Figure 3.12 – 18 inches (450 mm) depth pavement with no defects in thick asphalt pavements (Chen and Scullion 2008)**

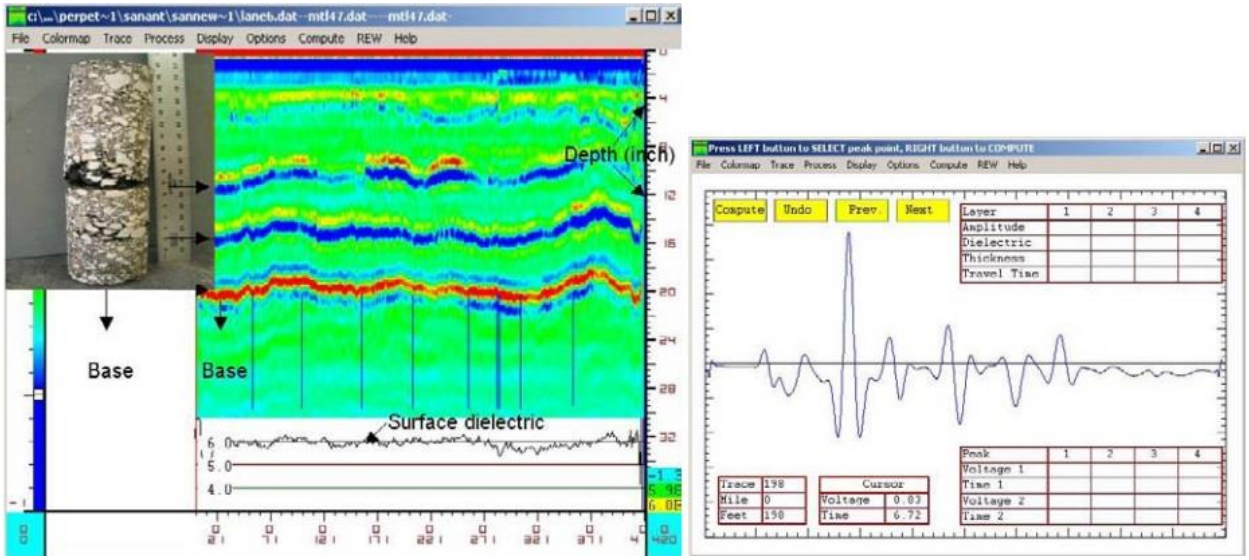


**Figure 3.13 – 20 inches (500 mm) depth pavement with defects in thick asphalt pavements (Chen and Scullion 2008)**

A survey conducted by Annan (2004) was applied to the floor of a one-story slab by using GPR system with 1200 MHz antennas. The results represent the location of rebar at a depth of 3.2 to 6 in (81 to 152 mm) and the condition of rebar as bent during construction.

Diamanti and Redman explored on two different topics related to GPR and concrete pavements. First, they observed reflective cracking in the asphalt layer located over contraction joints in the PCC layer below. The results indicated that the strongest reflection in GPR energy results develops at the intersection area between the bottom of crack and the asphalt pavement because of the presence of a granular layer. The other conclusion reached by Diamanti and Redman was that by using the GPR system with different antenna frequencies; 250 and 1000 MHz, GPR could be effectively used to investigate asphalt pavements over a granular layer. The results indicated that the 250 MHz GPR was more efficient than the 1000 MHz GPR at detecting cracks due to the roughness of crack and waveguide issues (Diamanti and Redman 2012).

Several studies have demonstrated the various functions of GPR. In some investigations, GPR test results have been verified with coring tests. This has demonstrated the reliability of the GPR test. GPR is used to determine the locations of the punchouts and the structural properties of the material being tested. The resulting images of the GPR test provide accurate results to interpret the layers of a pavement.

### 3.3. Eddy Current Technology (Profometer 600)

Detection of the rebar location for reinforced structures is the main activity for a site investigation. A common need is to find the location of rebar when drilling, cutting coring as well as a requirement for most other non-destructive investigations. The principle of eddy current pulse induction is to provide an image, that is not affected by moisture and concrete composition, which results in high accuracy for the concrete cover under all circumstances (Proceq 2017).

Szymanik et. al (2016) studied the detection of steel bars in reinforced concrete structures using two different methods: active infrared thermography with microwave excitation

and eddy current sensors. The authors noted that the multi-frequency eddy current technique may be used for both the detection of the location of reinforcements and the diagnosis of some properties of the structures. It was found that the massive multi-frequency method can be used as a complementary technique to the standard single-frequency eddy current method.

The Profometer, one of the eddy current techniques, is known as a rebar locator (Figure 3.14). The working principle of this instrument is on detection of the change in the electromagnetic field in the reinforced concrete. The device is easy and handy to use. To be able to get accurate data, this unit shall be calibrated before beginning the applications. The accuracy of the calibration is checked by using a test block including reinforcement. The location and size of reinforcement in the test block is measured at different sections on the block. Then, it is scanned by Profometer. The results should overlap (Lokesh et. al 2014).


**Figure 3.14 – The Covermeter - Profometer 600 (Impact Test Equipment 2017)**

The reinforcement bar diameter can be detected by Pachometer or Profometer, which are two different commercial brand name of eddy current techniques. The most recent generation

of Pachometer is Profometer and both techniques work with the pulse induction measuring method. The Profometer provides more accuracy due to being sensitive to external influence such as adjacent, parallel bars (Mihai et. al 2010). A research team used a Profometer 4 to focus on identifying the limitations and capabilities of utilizing it in high strength concrete (Sivasubramanian et. al 2013). The team stated that spacing between reinforcement bars is significant in order to obtain more accurate data by using the Profometer. When this spacing is small, the measurement of bar diameter is affected from external influences such as the adjacent bars. In addition, the smaller probe showed more accurate results if the clear concrete covers were less than 2.75 in (70 mm) as claimed by the manufacturer. It meant that as the concrete cover depth was deeper, the accuracy of the Profometer decreased.

Barnes and Zheng (2008) conducted research on detecting the factors affecting the accuracy of concrete cover measurement. The authors found that British Standard 1881 Part 204, titled as 'Recommendations on the use of electromagnetic covermeters', states that the concrete cover detected by a calibrated covermeter shall be accurate to ±5% or ±2 mm (0.08 in), (whichever is the greater) in the operating range given by the manufacturer. In addition, they noted that this specification mentions that when the size of reinforcement is known, the concrete cover can be measured to an approximate accuracy obtained in the laboratory. The accuracy of measurement for reinforcements having less than 100 mm (3.94 in) concrete cover depth is within (the greater of) 15% or 5 mm (0.2 in). Based on these findings, the cover measurement was affected by many factors, such as bar diameter settings, existence of neighboring bars under and parallel to the bar being measured, probe settings for concrete cover depending on being shallow or deep.

# CHAPTER 4

# PROBLEM STATEMENT

The primary goal of this project is to evaluate CRCPs throughout the state of Georgia to identify common characteristics between CRCPs having good performance with long history and those repetitive significant distresses such as punchouts.

In order to achieve this primary goal, the overall objectives of this thesis is twofold. First analyze the correlation between the depth of longitudinal reinforcement, concrete cover depth, and the formation of distresses at evaluating the severity and crack density on the pavement surface. Second, this study examines the usability of eddy current technology in the calibration process of the GPR unit in the field without taking any core specimen from the sites.

Some CRCPs result in significant structural distress such as punchout while some CRCPs perform exceptionally well. Based on previous work, it is suspected that the location of the longitudinal reinforcing steel is associated with the distresses such as cluster cracking and punchout. Therefore, the evaluation of the reinforcement placement height at the location of distresses provides a definitive answer to this hypothesis and may identify the cause for punchout distress being experienced on this section of interstate.

Six sites on major interstates and highway in Georgia were selected for the investigations. A preliminary site investigation revealed that each consisted of different structural conditions in terms of the density and severity of cluster crackings, the existence of punchouts and patched areas, and material problems when relatively compared to one another.

This project provides supportive information on distressed problems. According to the previous study (Johnson 2016), it was determined that the CRCP on the I-85 had different reinforcement depths. Therefore, the purpose of this study is to investigate the effect of reinforcing steel placed at different depths on transverse cracks and punchouts. In order to determine the causes of this repetitive and severe distress, severe clusters of single transverse cracks, punchouts and patching areas were identified. The selected sections in Georgia were investigated using a GPR unit and Profometer over the damaged area and non-damaged area.

As a result of this study, a GDT-GPR standard has been developed based on the outcomes obtained from these site investigations. This standard procedure may aid future investigations in detecting other factors affecting punchouts and, typically, evaluating the performance of pavements utilizing GPR technology. The GPR method provides significant benefits for the long-term monitoring plan of Georgia CRCP.

# CHAPTER 5

# EXPERIMENTAL PLAN

In order to successfully accomplish the objectives of this thesis, the proposed research program is categorized in the following specific steps:

## 5.1. Calibration of Ground Penetration Radar (GPR) unit

Ground Penetration Radar (GPR) is a common non-destructive testing system for evaluating pavement performance and subsurface features. To secure the accurate data with the results obtained from GPR unit, the equipment, comprising principal components and the frequencies for appropriate pavement type and depth, must be calibrated as discussed in Chapter 3. In this chapter, a few related terms will be defined below before discussing how to calibrate a GPR unit to determine pavement type and profile.

All material is governed by two physical properties: electrical conductivity and dielectric constant. Since GPR uses electromagnetic (EM) energy, the depth of scan is measured by the electrical conductivity of the material scanned. When a material has low conductivity such as dry sand, dry concrete or ice, the radar will penetrate deeper. Because the lower the water content of a material, the less conductivity, which results in deeper ground penetration. The other physical property, dielectric constant, illustrates how fast GPR energy travels over a material by means of descriptive numbers. These numbers range from 1 for air which radar energy propagates easily, to 81 for water which radar energy does not propagate continuously. Wet material will slow the radar signal due to an increase in the dielectric of the material. In other

words, the higher the dielectric constant number, the slower at GPR energy travels through the medium (GSSI 2006).

Amplitude, frequency, and velocity are terms used to describe a reflected GPR wave. Amplitude is defined as the maximum extent of a vibration or oscillation as is seen in Figure 5.1. Larger amplitudes generate brighter images on a GPR screen. The greater the difference between the dielectrics of different materials, the larger the amplitude of the reflections. Frequency is described as the total number of oscillations per a given amount of time, shown in Figure 5.1. Velocity is typically determined by the dielectric constant and used to detect the depth of the material. Lower velocity indicates higher dielectric number and vice versa (Penhall 2017).

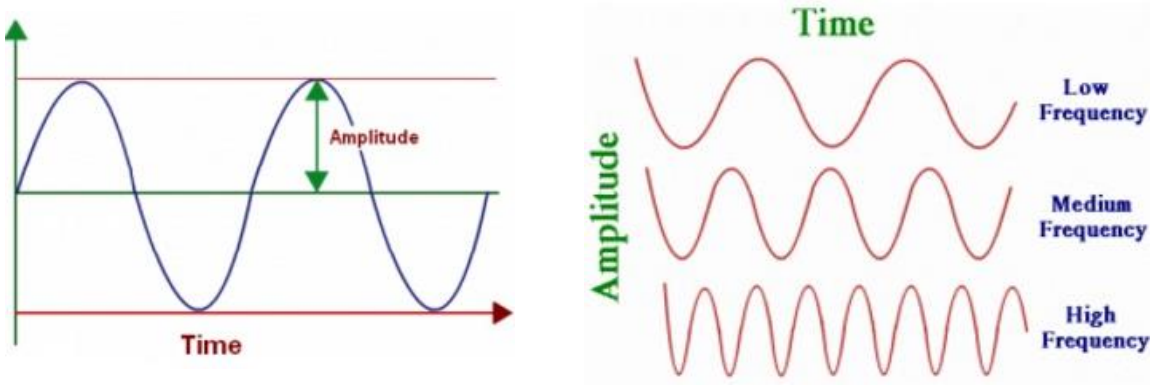


**a. Amplitude** **b. Frequency**

**Figure 5.1 – Terms describing a reflected GPR wave (Penhall 2017)**

This research was conducted by using a GSSI TerraSIRch SIR System-3000 referred to as SIR-3000. The SIR-3000 is preferred for a wide variety of applications due to it being a lightweight, portable and single channel ground penetrating radar system (GSSI 2003). It consists of six modes: TerraSIRch, Concrete, Structure, Utility, Geology Scans and Quick 3D.

TerraSIRch mode was used to detect shallow structural features and locations in concrete. GSSI TerraSIRch system includes four subsections; Collect Playback, Output, and System as shown in Figure 5.2.

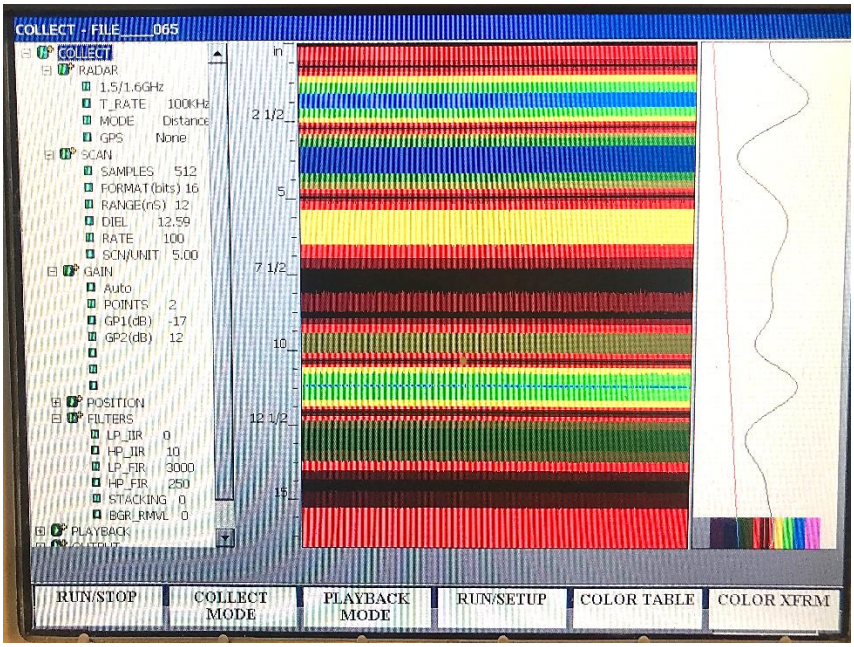


**Figure 5.2 – GSSI ConcreteScan System Submenus (GSSI 2003)**

The Collect mode consists of Radar, Scan, Gain, Position and Filters.

### 5.1.1. Radar

#### 5.1.1.1. Antenna Choice

The frequency under the Radar submenu authorizes the SIR-3000 to carry out the auto-surface operation (GSSI 2003). The lower frequencies penetrate the subsurface deeper than higher frequencies. The frequency of the antenna determines the maximum theoretical distance which the GPR unit can penetrate (Penhall 2017). This depth depends on the properties of the applications seen in Table 5.1. The frequency was selected as 1.5/1.6 GHz antenna in this research because the material is CRC pavement as shown in Table 5.1. When the 1.5/1.6 GHz

antenna is selected, the scanned depth was 1.5 ft. (0.5 m) which was enough depth for the selected sites.

**Table 5.1 - Antennas by Applications (GSSI 2003)**

| Frequency | Sample Applications | Typical Max Depth Feet (meters) | Typical Range (ns) |
|---|---|---|---|
| 1.5 GHz | Structural Concrete, Roadways, Bridge Decks | 1.5 (0.5) | 10-15 |
| 900 MHz | Concrete, Shallow Soils, Archaeology | 3 (1) | 10-20 |
| 400 MHz | Shallow Geology, Utility, Environmental, Archaeology | 12 (4) | 20-100 |
| 200 MHz | Geology, Environmental | 25 (8) | 70-300 |
| 100 MHz | Geology, Environmental | 60 (20) | 300-500 |

#### 5.1.1.2. T_RATE

The T_RATE is set for the antenna transmit rate in KHz. The maximum rate is 100 KHz. The GPR unit with higher transmit rate collects data faster (GSSI 2003). In this survey, the T_RATE was set as 100 KHz.

#### 5.1.1.3. Mode

The Mode provides three different options to collect data. These options are point, time, and distance-based. *Point data collection* is usually used for very deep investigations. Once the mark is pressed, the system will record one scan every time. Then, when the antenna is moved to the next location, the next scan will be recorded. *Time based data collection* records a certain number of scans per second. The survey speed plays a key role in terms of the data density over

ground. *Distance based data collection* is carried out with a survey wheel. A certain number of scans are recorded per unit of distance. This mode is recommended because it gives the most accurate data (GSSI 2003). In this study, distance based data collection was selected for more accurate results.

When the distance based data collection is selected, the survey wheel shall be calibrated to local conditions at every different site. For difficult terrain, the calibration can be made manually. A measured line shall be prepared on the survey surface. The longer the measured line, the more accurate the survey wheel calibration. Then, the calibration distance, taken from the measured line, is entered and the position of the antenna is set for the beginning of the line as front, center, or rear of the antenna. After that, the antenna is moved the survey distance. If this process is done several times and the average of the results is taken, the calibration will be more accurate. In this way, the GPR unit is calibrated for the survey wheel (GSSI 2003).

#### 5.1.1.4. GPS

The GPS selection provides an option to connect the GPS during collecting data. The GPS capability can be set as ‘on’ or ‘off’ (GSSI 2003). In this project, this selection was selected as ‘off (none)’ because the GPS was not used.

### 5.1.2. Scan

#### 5.1.2.1. Samples

Each scan curve is formed by data points. A set number of each data points is called as samples. The more samples that are collected, a better vertical resolution and a smoother scan curve are obtained. When the number of samples increases, the file size increases. This selection

presents six options: 256,512,1024,2048,4096, and 8192. GSSI recommends using 512 or 1024 samples per scan (GSSI 2003). In addition, the option of 512 samples per scan is recommended within the use of 1.5 GHz frequency. Therefore, in this study, the 512 sample per scan was chosen.

#### 5.1.2.2. Format (bits)

This selection is set for the resolution of the outputs. There are two options as 8-bit and 16- bit format. 16- bit data format, which was used in this project, is recommended because its dynamic range is greater than 8-bit. As the format size increases, the data profiles occupy more place in the computer storage (GSSI 2003).

#### 5.1.2.3. Range (nS)

The Range selection is to set time in nanoseconds (nS) for the recording of reflections from a single pulse. It depends on the depth. In other words, the longer range, the deeper ground penetration and, therefore, the GPR unit gives reflections from deeper sections in the ground (GSSI 2003). The 12-nS range was selected in this survey.

#### 5.1.2.4. Dielectric Constant (Diel)

This selection indicates the dielectric constant value of material and, relatedly, the velocity that the radar can move through a material. The higher dielectric value, the slower survey speed. The dielectric values are presented in Table 5.2 for common materials. If this value is known, it can be entered directly under this submenu (GSSI 2003). If the dielectric value of material is not known exactly, it can be determined by the calibration in the field. This part of the survey plays a key role for the site investigations.

The calibration process of the GPR unit in this study began by considering a dielectric value between 5 and 8 for concrete material (Table 5.2.). At the beginning of the site investigation, a short scan was done in the longitudinal direction, the direction of traffic, through the GPR unit to be able to see where the transverse reinforcements were placed. After designating the locations of transverse reinforcements, one of them was selected. On the selected transverse reinforcement, both GPR and Profometer units were used to scan the pavement in the transverse direction, from shoulder to the inner lane. Thus, the locations of the longitudinal reinforcements were determined. For the confirmation of the depth and size of reinforcements and layer thicknesses, a core, 6 in (152 mm) diameter, was taken from each site. The core location was marked on the ground by selecting one of the longitudinal reinforcement (Figure 5.3).

**Table 5.2 - Dielectric values for common materials (GSSI 2003)**

| Material | Dielectric | Velocity (mm/ns) |
|---|---|---|
| Air | 1 | 300 |
| Water (fresh) | 81 | 33 |
| Water (sea) | 81 | 33 |
| Polar snow | 1.4 – 3 | 194 - 252 |
| Polar ice | 3 - 3.15 | 168 |
| Temperate ice | 3.2 | 167 |
| Pure ice | 3.2 | 167 |
| Freshwater lake ice | 4 | 150 |
| Sea ice | 2.5 – 8 | 78 – 157 |
| Permafrost | 1 – 8 | 106 – 300 |
| Coastal sand (dry) | 10 | 95 |
| Sand (dry) | 3 – 6 | 120 - 170 |
| Sand (wet) | 25 – 30 | 55 – 60 |
| Silt (wet) | 10 | 95 |
| Clay (wet) | 8 – 15 | 86 – 110 |
| Clay soil (dry) | 3 | 173 |
| Marsh | 12 | 86 |
| Agricultural land | 15 | 77 |
| Pastoral land | 13 | 83 |
| "Average soil" | 16 | 75 |
| Granite | 5 – 8 | 106 – 120 |
| Limestone | 7 – 9 | 100 – 113 |
| Dolomite | 6.8 – 8 | 106 – 115 |
| Basalt (wet) | 8 | 106 |
| Shale (wet) | 7 | 113 |
| Sandstone (wet) | 6 | 112 |
| Coal | 4 – 5 | 134 – 150 |
| Quartz | 4.3 | 145 |
| Concrete | 5 – 8 | 55 – 120 |
| Asphalt | 3 – 5 | 134 – 173 |
| PVC | 3 | 173 |

After taking a core, information for the reinforcements and layers was confirmed. For instance, if the concrete cover, the depth of longitudinal reinforcement, was measured as 3.70 in (94 mm) from the core and the GPR image produced a differing cover value, then the concrete cover shown on the GPR screen was corrected as 3.70 in (94 mm). This calibration process was used at each site. Calibrating the depth in GPR unit affects the dielectric constant values. Thus, the last step of the calibration process should be saved in the system to be able to use the same dielectric value along the same site.

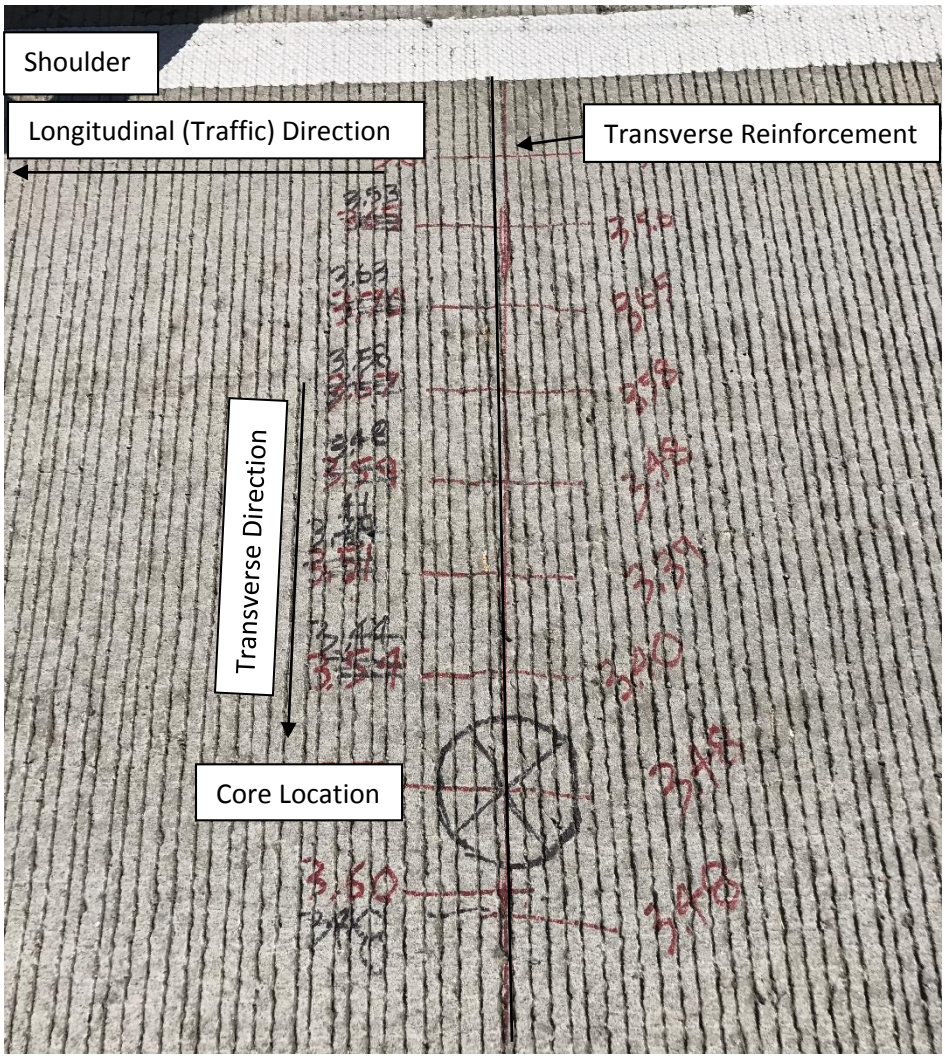


**Figure 5.3 – The Designation of the Core Location at the site (Tift County)**

### 5.1.2.5. Rate

This selection indicates the scans per second. If the distance based data collection mode is selected, this number shall be set very high because the system holds the number of scans in its memory per second. If the number of scans are not enough to collect data for the defined distance per second, the data collection will not be successful. It is recommended that if the transmit rate is set to 100 KHz, the scan rate should be set to 100 scans per second (GSSI 2003), which was used in this project.

### 5.1.2.6. Scan/Unit

The scans per unit of horizontal distance detects how detailed the survey will be along lines. In other words, the more scans per unit, the slower the survey speed. Figure 5.4 shows the effects of scans per unit, including 5/in (2/cm), 7.5/in (3/cm), and 10/in (5/cm) (GSSI 2006). In addition, the smaller the scan spacing, the higher the resolution in data, which results in a larger file size. The unit is set to English feet as a default property. Thus, it is considered as the scans per foot or inch. It is recommended that 60 scans/ foot or 5 scans/inch, the densest scan spacing, should be set for shallow structures, in the case of using the 1.5 GHz antenna (GSSI 2003). In this study, this recommended value, 60 scans/foot or 5 scans/inch, was set for the scan/unit selection.

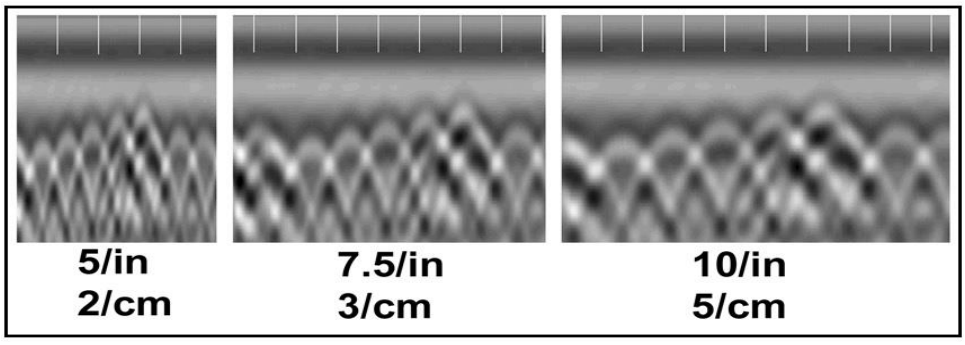


**Figure 5.4 - Scan per unit and its effects (GSSI 2006)**

### 5.1.3. Gain

The gain selection allows to neutralize effects of attenuation. While a radar scan unit travels on the ground, some of the scans are reflected and the rest of them are absorbed. In addition, the deeper scan causes weaker reflections. At this point, the gain selection provides the artificial addition of signal to make the subtle sections more visible (GSSI 2003). The 2 gain points were added to the system in these site investigations.

### 5.1.4. Filters

Filters allow the user to remove noise in the ground. This selection includes six subsections: LP_IIR, HP_IIR, LP_FIR, HP_FIR, Stacking, and BGR_Removal. LP stands for low-pass, which allows the system to pass any frequency which is lower than one entered in this section. HP stands for high-pass, which has the opposite meaning of LP. The first four subsections, vertical filters, are the frequency filters and their values are in MHz. Stacking technique reduces the noise. BGR_Removal, standing for background removal filter, is a horizontal high pass, which removes low frequency noise. In this study, HP_IIR, LP_FIR, and HP_FIR filters were set 10 MHz, 3000 MHz, and 250 MHz, respectively.

Based on the preloaded setups for the SIR-3000 (GSSI 2003), the system's data collection parameters and filters, mentioned above, are listed in Table 5.3. These parameters are recommended for 1.5 GHz antenna to view approximately 18 in (457 mm) depth in concrete (GSSI 2003).

**Table 5.3 - Data Collection Parameters and Filters (GSSI 2003)**

| **Frequency** | **1.5 GHz (Model 5100)** |
|---|---|
| **Transmit Rate (T_RATE)** | 100 KHz |
| **Samples per Scan** | 512 |
| **Format (Resolution, bits)** | 16 bits |
| **Range (nS)** | 12 nS |
| **Scan per Unit** | 5/inch |
| **Number of Gain Points** | 2 |
| **Vertical IIR High Pass (HP_IIR)** | 10 MHz |
| **Vertical Low Pass Filter (LP_FIR)** | 3000 MHz |
| **Vertical High Pass Filter (HP_FIR)** | 250 MHz |

## 5.2. Calibration of Cover Meter (Profometer 600)

A project objective was to confirm the results regarding the location and position of the reinforcements placed into the concrete reinforced pavement, which were obtained from GPR technology, by employing Profometer, one of the eddy current techniques. This concept, specifically for this instrument, is rare in the literature. It served to determine the locations of cores fast and accurately for this project. Then, it contributed to the calibration process of the GPR unit during the field investigations.

The Profometer 600 detects rebar locations by using electromagnetic pulse induction. A magnetic field is produced through coils charged by current pulses in the probe (Figure 5.5). Then, eddy currents are generated on the surface of any conductive material in the magnetic field and induces this magnetic field in the opposite direction. At the end of this action, the voltage undergoes change, which is used for the measurement of concrete covers (Proceq 2017).

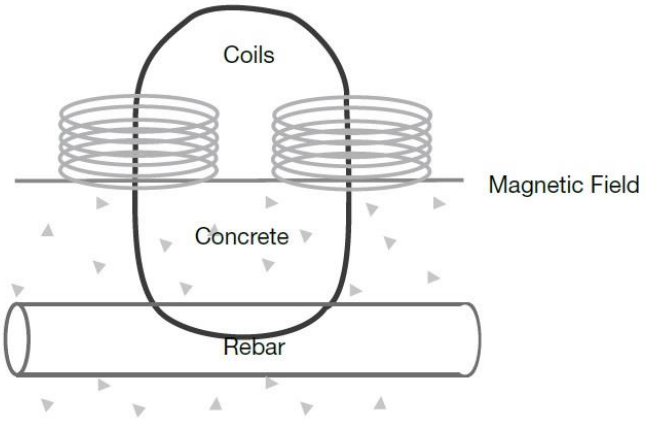


**Figure 5.5- The Measuring Principle of Profometer (Proceq 2017)**

The Profometer 600 has only 'Locating Mode', which can measure the concrete cover. The measuring range setting has four different selections capable of measuring the full range of concrete covers: standard, large, auto and spot probe range. The standard range, default, setting provides the most accurate data. The large range setting shall be selected if the concrete cover is deeper and could not be detected with standard range setting. The spot range setting shall be selected if the measured area is small such as between the close reinforcements. In addition, the auto range setting provides the automatic switch option between standard and large range settings. Figure 5.6 indicates that the expected accuracy of the concrete cover measurement depends on the reinforcement size (Proceq 2017). In this project, the auto range setting was used to measure sites accurately for any case.

There are minimum limits for the spacing between reinforcements such that the Profometer can detect reinforcement location accurately. These minimum limits of rebar spacing depend on the rebar diameter and cover depth. If the limits (curves indicated in Figure 5.7) are exceeded, the reinforcements cannot be detected (Proceq 2017).

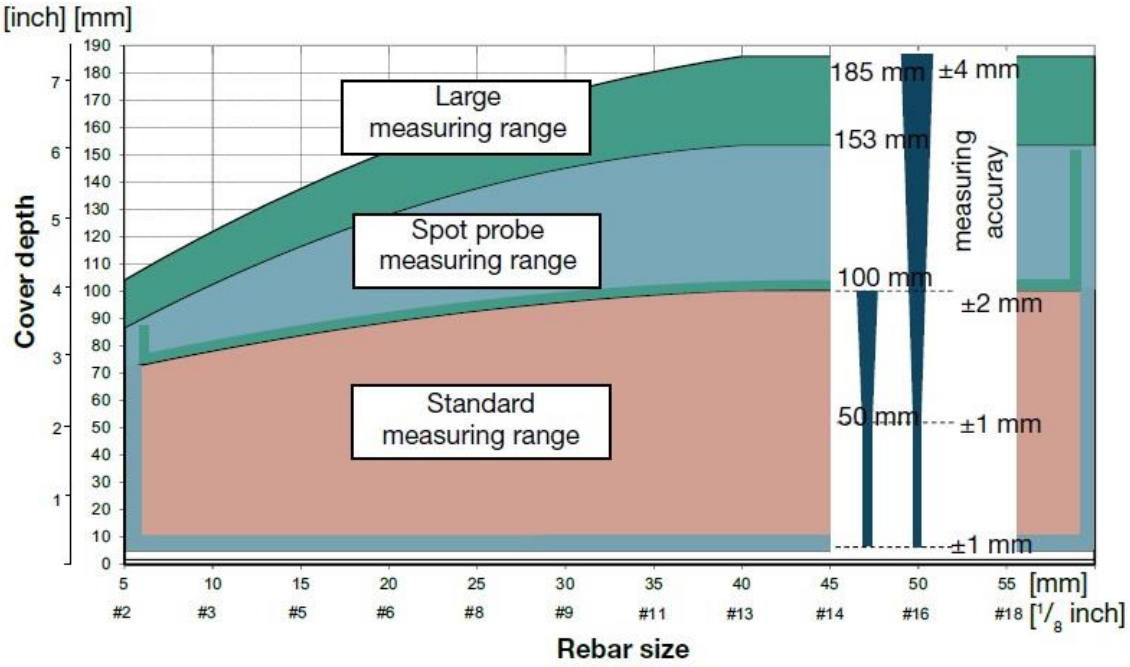


**Figure 5.6- The Measuring Range and Accuracy of Cover Depth (Proceq 2017)**

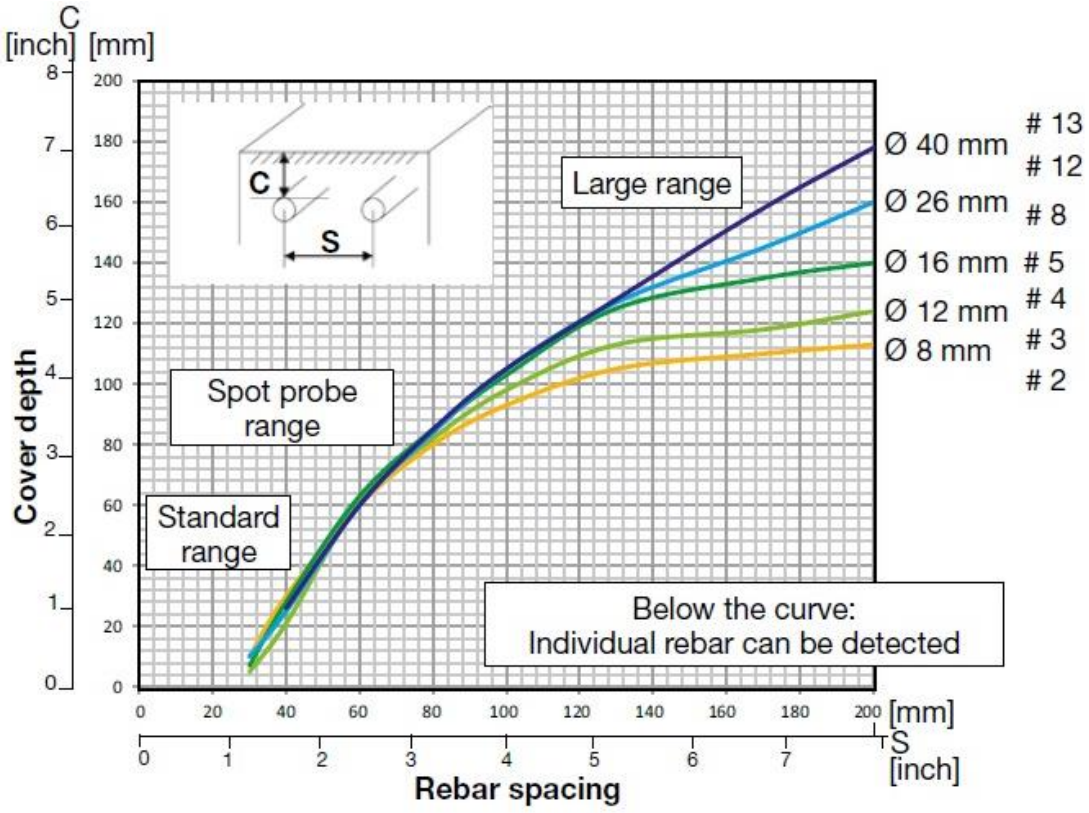


**Figure 5.7 The Minimum Limits for Spacing of Reinforcements (Proceq 2017)**

Overall, the calibration process of GPR requires several preparations and settings prior to operation. The flow chart in Figure 5.8 indicates the summary on how to calibrate GPR in the field.

Based on the process explained in Section 5.1 and 5.2, GPR shall first be prepared for the site investigation by adjusting its settings in compliance with the specifics of the pavement section. Then, the location of longitudinal and transverse reinforcements shall be determined by GPR together with Profometer. In the next step, a core shall be taken to confirm the concrete cover depth value and layer thicknesses. In the final step of the calibration process, the GPR unit shall be corrected using the measured data from the core or the predicted data from Profometer.

In a site investigation, there is no requirement to simultaneously perform the Profometer along with the operation of taking a core to calibrate GPR. Only for this project, both techniques were used to be able to evaluate the results predicted by Profometer. In the general process, either a Profometer or a core might be utilized to calibrate the GPR unit. In the flow chart (Figure 5.8), all steps to calibrate GPR were indicated in the case that both Profometer and a core would be used. However, in this chart, each method used for this aim was stated as optional.

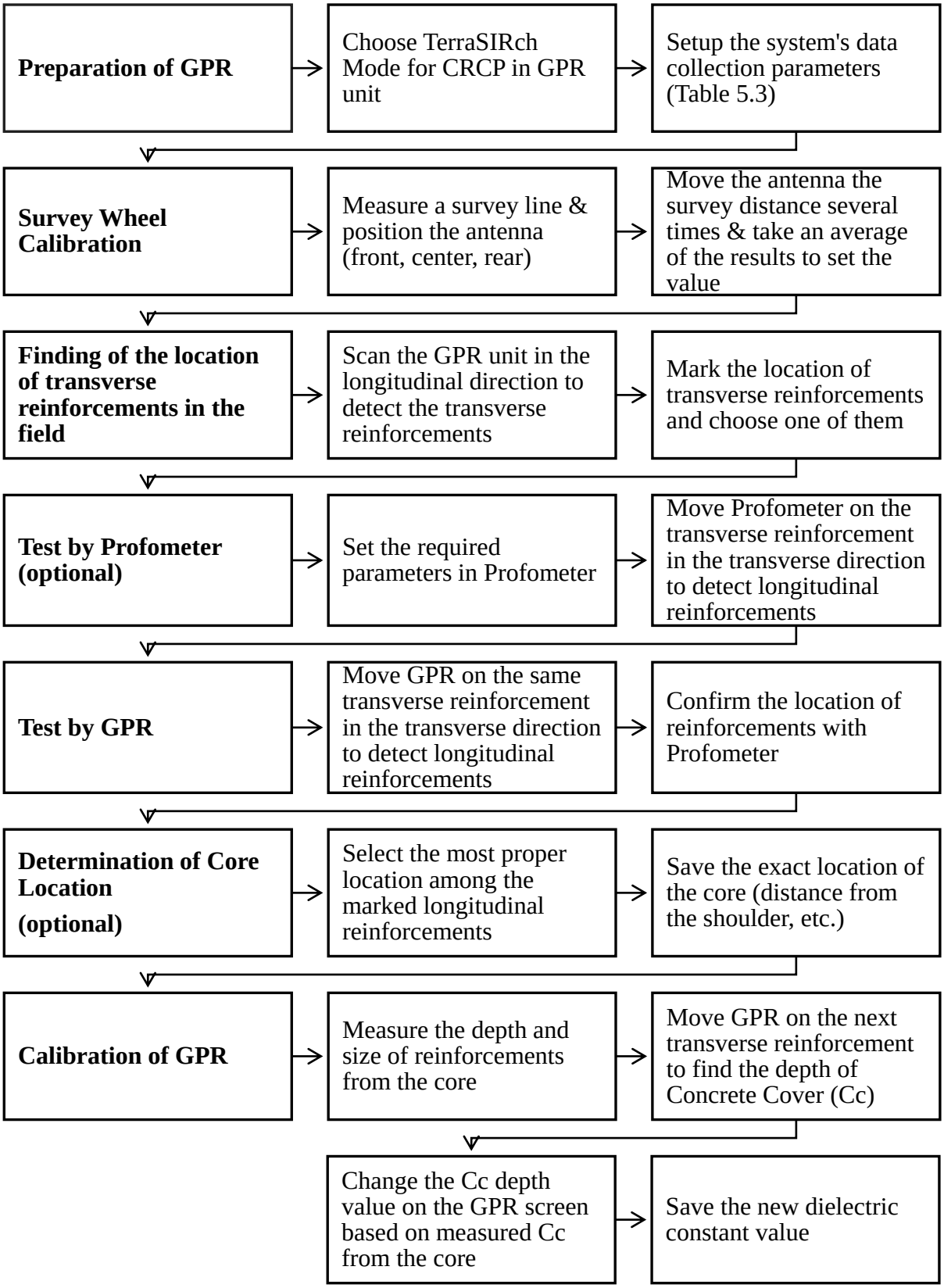


**Figure 5.8 – The Flow Chart of the Steps of the Calibration Process of GPR in the Field**

### 5.3. Project Locations

In this task, a site survey, including six different sites, was conducted to evaluate CRCPs throughout the state of Georgia to identify characteristics of CRCPs having a reliable performance and to determine the potential reasons for significant CRCP distresses such as punchouts. The GPR unit and Profometer recorded the placement of steel reinforcing bars within the CRC pavement slab. GPR images, which showed the location of the transverse cracks, punchout and adjacent areas over four segments throughout 1 mile (1.6 km), were obtained. This task was completed with relatively high frequency for improved resolution of images required to identify the reinforcement height.

After selecting of the project locations, including a review of CRCPs in Georgia that incorporated location, historical information, and pavement condition, a Geographic Information Systems (GIS) database was developed (Figure 5.9). Then, CRCP locations were confirmed through the use of satellite imagery. Through this imagery, specific sections (MPs) were identified for testing.

The six sites were selected based on condition and proximity and were evaluated as being in good/fair or poor conditions. Historical information for many of these sites was found and confirmed through a review of the pavement design/drawings found on Project Search (GeoPI). Based on the original typical sections for some CRCP sections of Interstates in Georgia, some information about pavements was obtained from various sources and projects in the 1990s. The selected CRCP sections and their locations together with their project name used in this study are listed in Table 5.4.

**Table 5.4 - Information of Sites Selected in Georgia**

| Sorting of Site Surveys | Abbreviation of Site Names | Expansion of Site names |
|---|---|---|
| **Site 1** | SR6NBCMP0-1 | **S**tate **R**oute **6** **N**orth **B**ound **C**obb County **M**ilepost **0-1** |
| **Site 2** | I20EBHMP4-5 | **I**nterstate **20** **E**ast **B**ound **H**aralson County **M**ilepost **4-5** |
| **Site 3** | I20WBCMP24-25 | **I**nterstate **20** **W**est **B**ound **C**arroll County **M**ilepost **24-25** |
| **Site 4** | I20EBNMP92-93 | **I**nterstate **20** **E**ast **B**ound **N**ewton County **M**ilepost **92-93** |
| **Site 5** | I75NBCMP267-268 | **I**nterstate **75** **N**orth **B**ound **C**obb County **M**ilepost **267-268** |
| **Site 6** | I75NBTMP57-58 | **I**nterstate **75** **N**orth **B**ound **T**ift County **M**ilepost **57-58** |

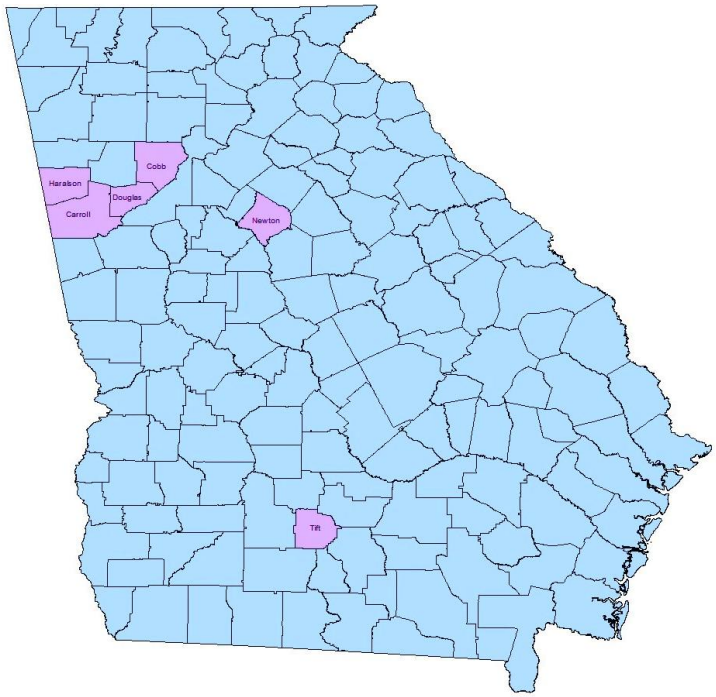


**Figure 5.9 – The Selected Sites in Georgia for RP 16-39 Project**

# CHAPTER 6

# EXPERIMENTAL RESULTS

## 6.1. Analysis of GPR Images Using Post-Processing Software

This study aimed to analyze GPR images recorded during the field investigations by using a post-processing software program and, later, to present an overall summary report showing the details of the images such as the rebar position within the CRCP section, direction of traffic, etc.

Alternatively, the data obtained from survey investigations can be transferred to a PC and analyzed by using a software program. If the post-processing software is used to interpret the graphics, the analysis will be much more accurate and reliable. The primary advantages of using post-processing software is that allows for the user to interpret data visually by (GSSI 2006);

- Obtaining multiple file screen,
- Advancing of processing capabilities;
- Determining the correct velocity with migration,
- Printing the output

In this study, RadView software was used for the post-processing. The data collected from the site was uploaded to the program. Then, images showing steel reinforcement locations, thicknesses of layers and material properties such as frequency, dielectric values, etc., were presented in detail below.

## 6.2. Definition of Terms

The terms needed clarification in terms of meaning were explained below to be able to make their meaning and interpretation clearer.

- *Subsite* – The name given to each of the divided four segments of a site investigation.
- *Transverse direction* – The direction of site investigation performed from the shoulder to inner lane of the roadway.
- *Longitudinal direction* – The direction of site investigation performed in the direction of traffic.
- *Longitudinal Crack* – Crack that is predominantly parallel to the pavement centerline.
- *Single transverse crack* – Each transverse crack that is predominantly perpendicular to the pavement centerline.
- *Cluster of single transverse cracks* – A group of closely spaced transverse cracks.
    - Average of five or more consecutive transverse cracks with spacing less than 2 ft. (61 cm) (Kohler and Roesler 2004)
- *Spacing between single transverse cracks* – The distance measured from one transverse crack to another in a cluster or separately.
- *Spacing between clusters of single transverse cracks* – The distance measured from the last single transverse crack in the cluster to the first single transverse crack in the next cluster

### 6.3. Analysis and Synthesis of Outcomes

The results based on information and knowledge collected from Tasks 1-4 were analyzed to answer the three questions included in the 'Research Objectives' section. In addition, the results were evaluated on whether they are within an acceptable range according to the specifications or not Furthermore, other factors that may affect the formation of distresses were recommended for further investigation, together with outcomes resulting from the field investigation and evaluation of the records.

The NDT methods, GPR and Profometer, were used at each site survey. The GPR unit was moved over the wheel path, which was close to the shoulder, on the outside lane of each site to collect data in longitudinal direction. A 6-inch (152 mm) core was taken on the centerline of slab of each site to measure the depth and size of longitudinal and transverse reinforcements and concrete layer thickness (Figure 6.1). The length of cores varied by depending on the CRC thickness of the sites. The lengths of core specimens were 15 in (381 mm) for Site 2, 4, and 6. It was 15 in (381 mm) for Site 1, as well. However, it looks like 12 in (305 mm) in Figure 6.1 because the core was damaged during the process of taking it. Likewise, the core length for Site 3 looks like 9 in (229 mm). A core 12 in (305 mm) in length was taken from Site 5.


**Figure 6.1– Core Specimens taken from Site Investigations**

### 6.3.1. SR-6 Cobb County

#### 6.3.1.1. Data Collection

Non-destructive testing methods were carried out on State Route 6 in Cobb County using a Ground Penetration Radar (GPR) and Profometer. The detailed information regarding the working procedures of these units is mentioned in Section 5.1.

The outside lane on North Bound (NB) SR-6 located between mileposts 0-1 in Cobb County was selected for inclusion in this study. The CRC pavement was reported to be in good condition, which indicated some visible distresses such as clusters of transverse cracks. The construction drawings obtained from GeoPI (see SR6NBCMP0-1 in Appendix A) indicate that the section was built in 2005. The location of this site is shown in Figure 6.2.


**Figure 6.2 – SR-6 MP 0-1 Cobb County Site Location (Google Maps, 2017)**

The design parameters and distress assessment values are presented in Table 6.1. The site exhibited clusters of transverse cracks. It was detected that the selected section did not have punchout per mile. To confirm the size and location of longitudinal and transverse reinforcements and pavement thickness before collecting data, a 6 in (152.4 mm) core was taken from the site.

**Table 6.1 - CRC Design Parameters and NDT Results for SR6NBCMP0-1**

| | | | | | | | |
|---|---|---|---|---|---|---|---|
| **SR-6 COBB COUNTY** | **Design Parameters** | | | | | | |
| | Site Condition | Age (Years) | CRC Thickness (in) | Longitudinal Rebar Size/ Spacing (in) | Transverse Rebar Size/ Spacing (in) | Longitudinal Rebar Depth (in) | Transverse Rebar Depth (in) |
| | Good | 12 (2005) | 12” | #6 / 5” | #4 / 36” | 3.50” | 4.40” |
| | **Distress Assessment** | | | | | | |
| | Spacing between single transverse cracks (ft.) | Spacing between clusters of transverse cracks (ft.) | | Transverse crack width (in) | | Longitudinal crack width (in) | Number of Punchouts / mile |
| | 1’~ 4’ (typical 1’) | 46’ | | 0.04” ~ 0.14” (typical 0.075”) | | 0 | 0 |

The transverse cracks pattern on the investigated lane is shown in Figure 6.3. The section was constructed as a 12 in (305 mm) CRC slab above a 0.75 in (19 mm) recycled asphaltic concrete layer and 12 in (305 mm) of graded aggregate base. The longitudinal and transverse reinforcements consisted of #6 and #4 rebars, respectively. The concrete cover depth to the top of the longitudinal reinforcement was measured to be 3.50 in (89 mm) from the core specimen. The site was investigated in four stages in terms of density of crack types and existence of other distress types. The stages were named as S1-a, S1-b, S1-c, and S1-d. They

refer the first (a), second (b), third (c), and forth (d) subsite (S) segments of SR6 Cobb County which was the 1st site investigated.

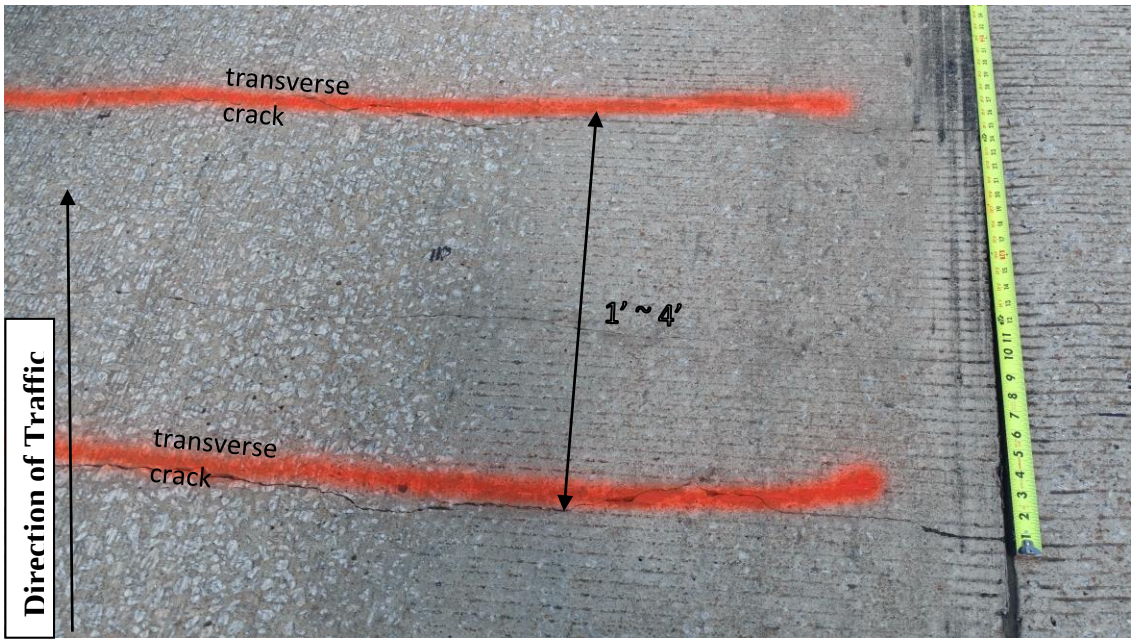


**Figure 6.3 - Typical Single Transverse Crack Pattern (S1-b)**

The site had the cluster transverse cracks as showed in Figure 6.4. Transverse rebars and cracks were marked as 'TC' and 'T' in the clusters, which indicate 'crack on transverse rebar' and 'transverse rebar', respectively (Figure 6.4). The minimum and maximum distance between the clusters of transverse cracks were measured as approximately 46 ft. (1402 cm). The single transverse cracks were spaced at the range of approximately 1 ft. and 4 ft. (30.5 and 122 cm) as it is shown in Figure 5.6. The typical transverse crack width varied in the range of 0.04 in and 0.14 in (1.02 and 3.56 mm) (Figure 6.5). There was no visible longitudinal crack.

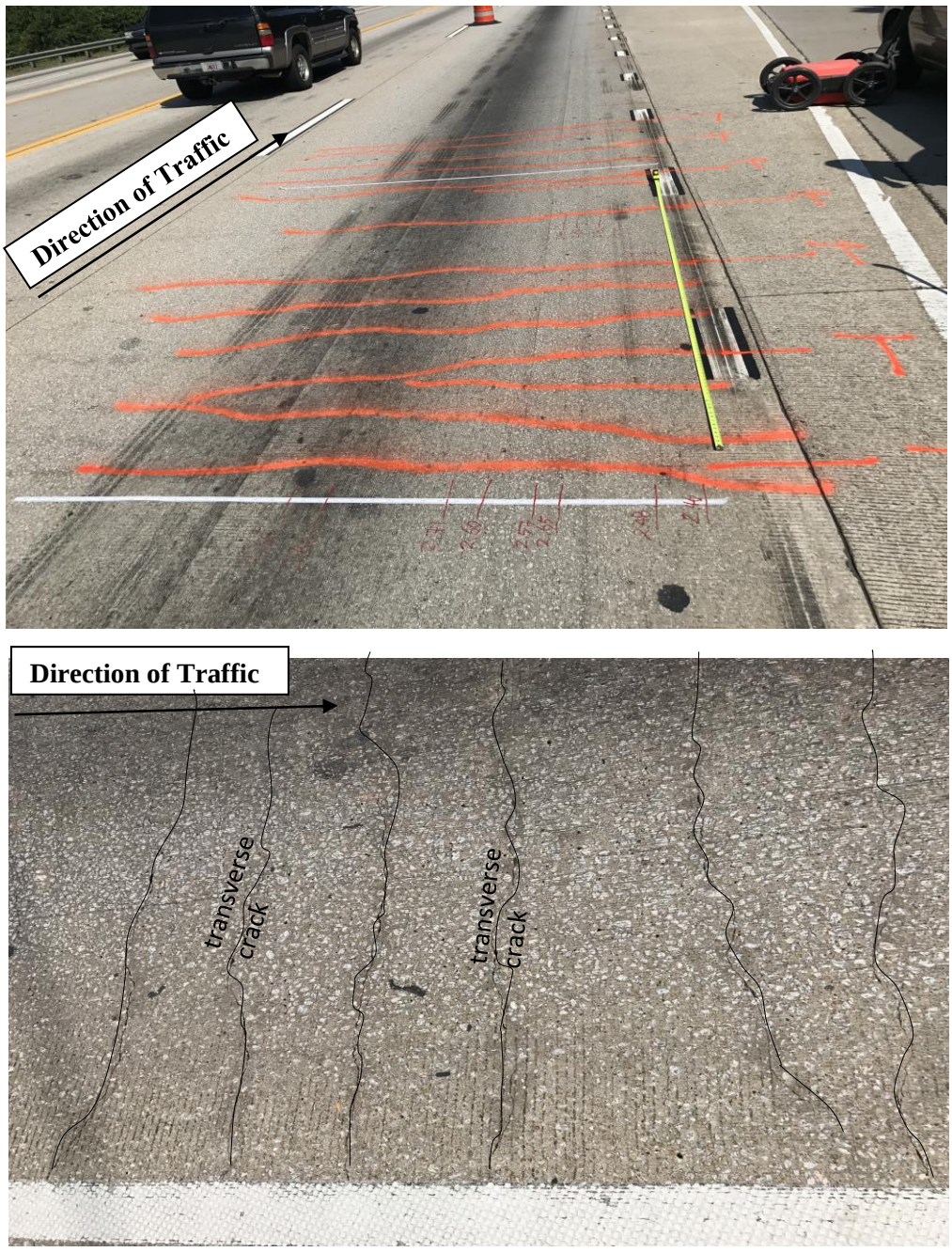


**Figure 6.4 – Typical Cluster Transverse Cracks Pattern at S1-a and S1-b**

**Figure 6.5 – The Measurement of Crack Widths at S1-b, S1-c, and S1-d**

#### 6.3.1.2.Data Post-Processing

The GPR unit scans were visualized in RadView software. Figure 6.6 clearly shows the location of four transverse reinforcements and concrete layer thickness. Based on findings, the sections for which cracks formed were over the steel transverse reinforcements. The site did not show significant depth change of transverse and longitudinal reinforcements across the section scanned. Figure 6.7 indicates the depth of longitudinal reinforcement and CRC thickness in the transverse direction. The longitudinal reinforcements' depth lowered toward the inside lane.

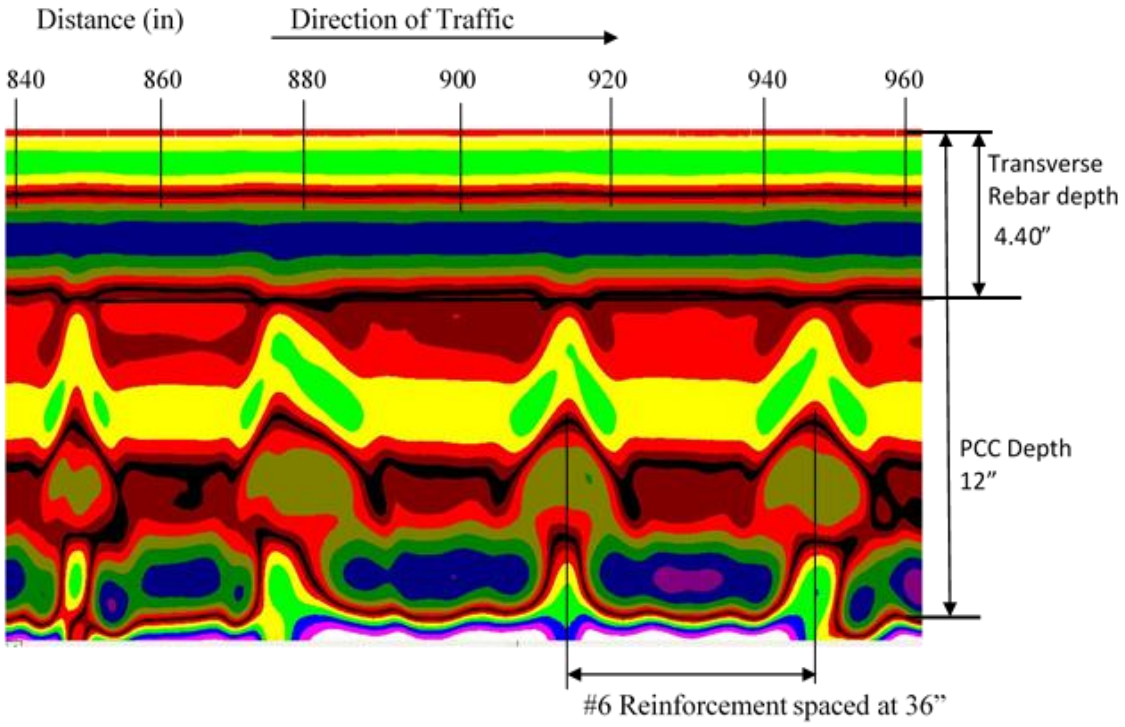


**Figure 6.6 – GPR Scan in the Longitudinal Direction (S1-b)**

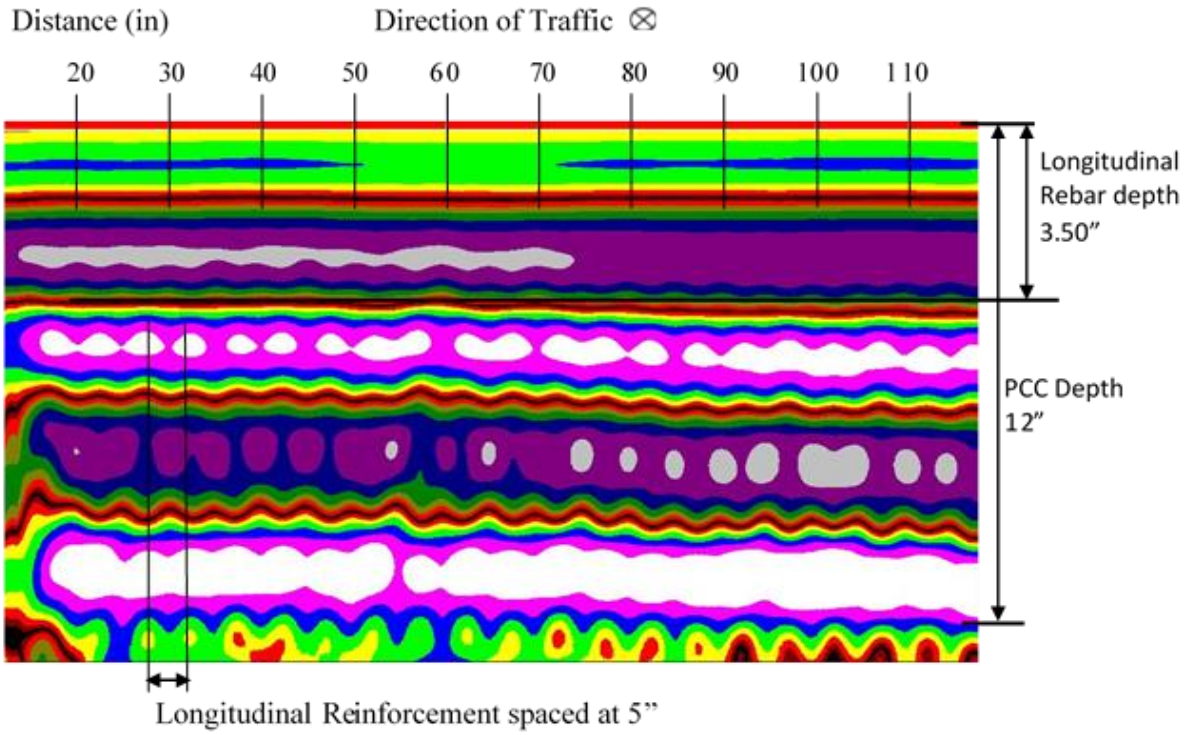


**Figure 6.7 – GPR Scan in the Transverse Direction (S1-b)**

Each subsite segment was scanned by GPR and Profometer because of the existence of a minimum ten single transverse cracks within the cluster. In addition, most cracks were formed over the transverse reinforcements. In the selected site, the depth of longitudinal rebar varied throughout the 1-mile (1.61 km) section because of construction processes. Figure 6.8 illustrates the crack pattern and the change in concrete cover depth along 1 mile (1.60 km). The GPR values in the graph indicates the average depth of longitudinal reinforcements, which were located over one transverse reinforcement selected from the distressed area in each segment. As seen in Figure 6.8, the depth of longitudinal reinforcement at S1-c is deeper than other three segments. In addition, as shown in the crack pattern, the S1-c had the most number of cracks among the four segments. The author believes that this relates to the concrete cover depth and the density of cracks.

The following graphs (Figure 6.9-10) indicates the depths of longitudinal reinforcements, which were detected by GPR and Profometer, between single transverse cracks in the transverse direction (S4-d). Before the GPR unit was calibrated, the depth values collected from the site were deeper than the actual values (Figure 6.9). It means that the concrete cover depth values are far from the actual values without the calibration process. After taking a core from the site, which its location is shown in Figure 6.10, the cover depth was calibrated to measured actual depth, 3.50 in (89 mm). It was shown that the depth values through the survey line in the transverse direction were close to the actual values. In addition, the data collected by GPR unit and Profometer showed the similar pattern in Figure 6.10. In other words, GPR results were confirmed by Profometer results for this site.

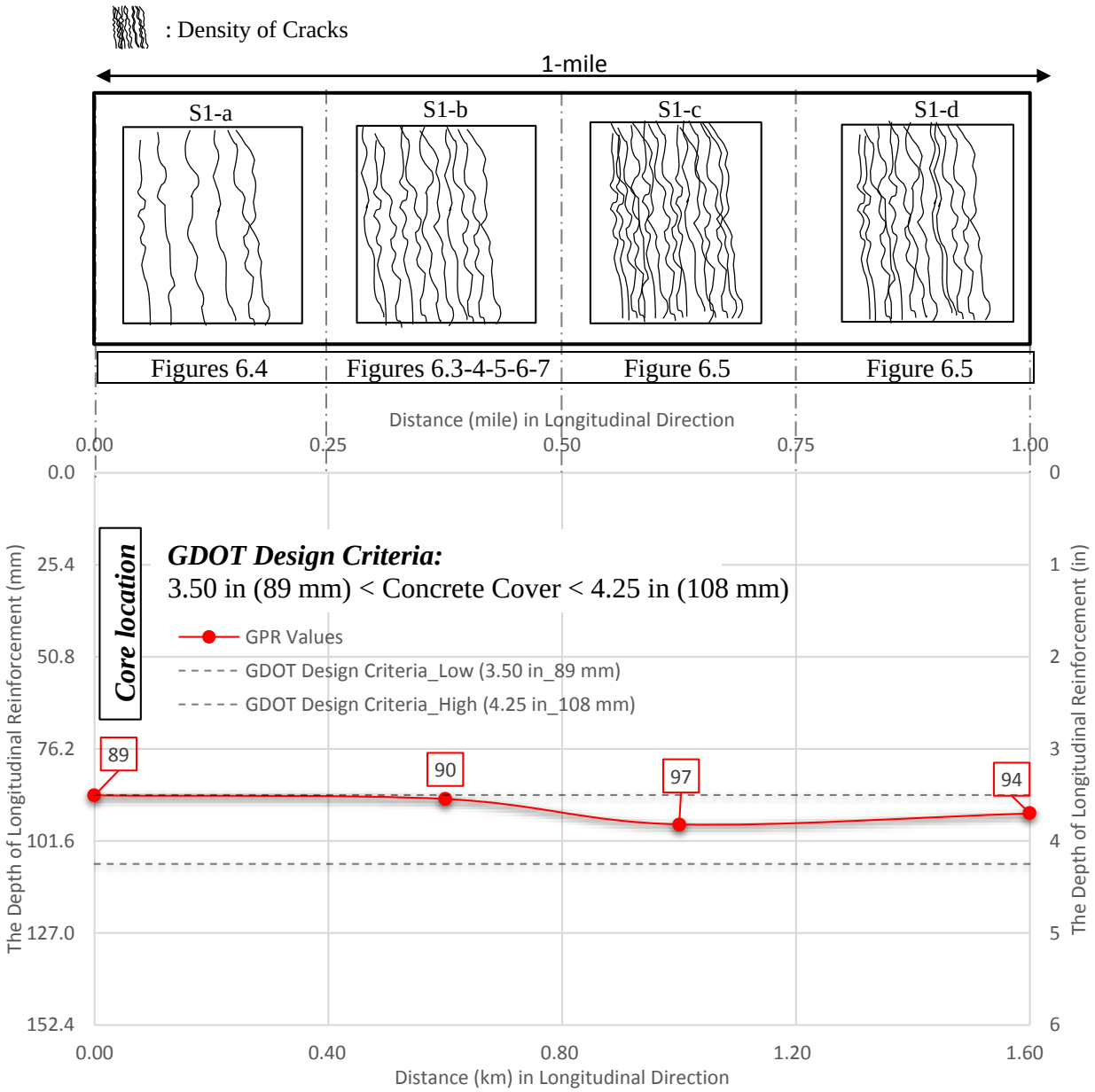


**Figure 6.8 – Stress Pattern and Concrete Cover in Longitudinal Direction in Each Segment Along 1-mile**

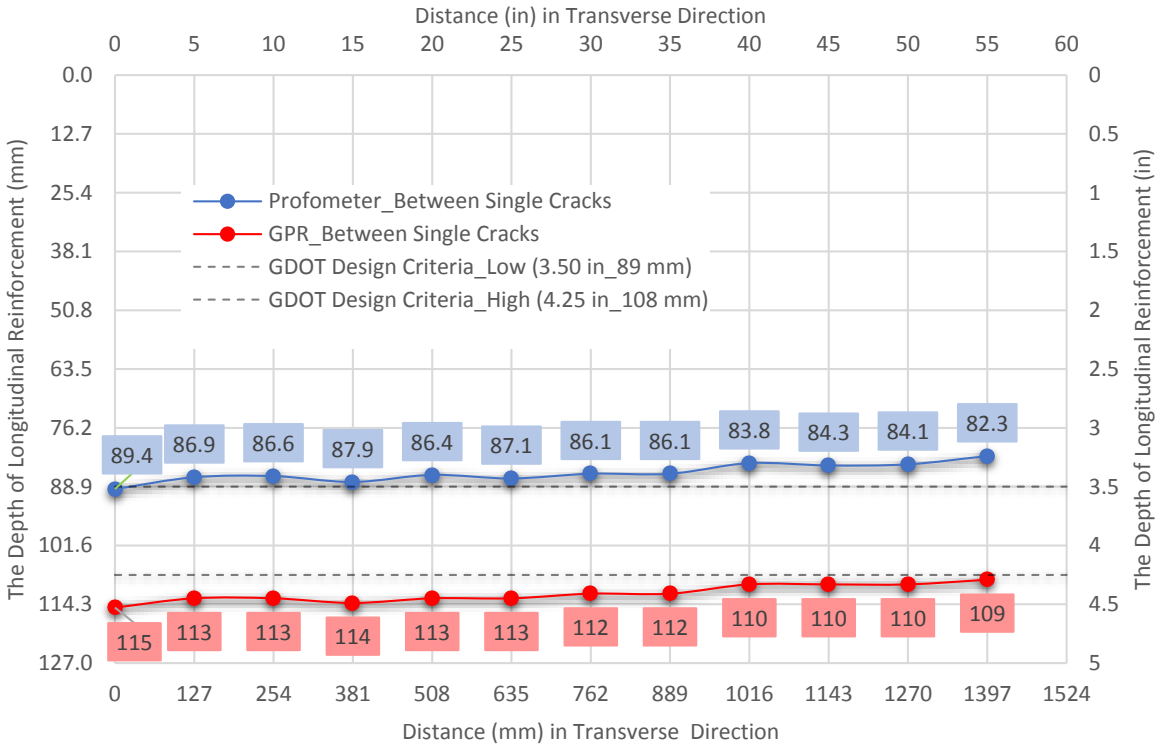


**Figure 6.9 –Concrete Cover Depth Values Detected by non-calibrated GPR and Profometer in Transverse Direction at S1-d**

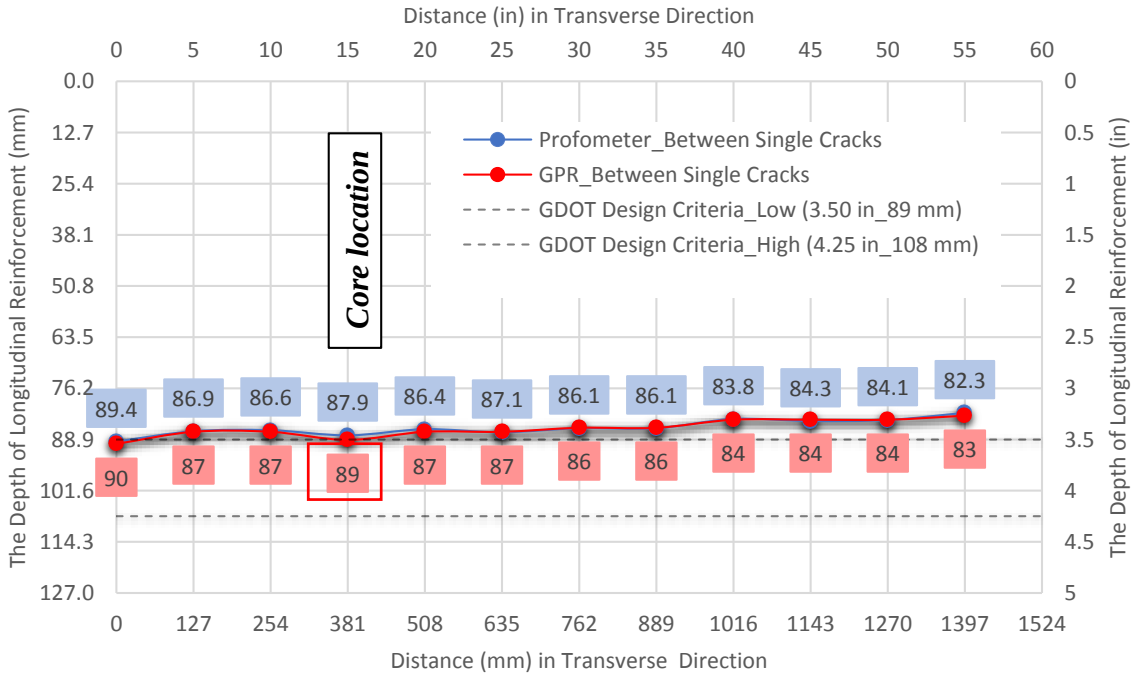


**Figure 6.10 –Concrete Cover Depth Values Detected by calibrated GPR and Profometer in Transverse Direction at S1-d**

### 6.3.2. I-20 - Haralson County

#### 6.3.2.1. Data Collection

Non-destructive testing methods were carried out on Interstate 20 in Haralson County using a Ground Penetration Radar (GPR) and Profometer. The detailed information regarding the working procedures of these units is mentioned in Section 5.1.

The outside lane on East Bound (EB) I-20 located between mileposts 4-5 in Haralson County was selected for inclusion in this study. The CRC pavement was reported to be in good condition, which indicated clusters of transverse cracks. The construction drawings obtained from GeoPI (see I20EBHMP4-5 in Appendix A) indicate that the section was built in 1980. The location of this site is shown in Figure 6.11.


**Figure 6.11 – I-20 MP 4-5 Haralson County Site Location (Google Maps, 2017)**

The design parameters and distress assessment values are presented in Table 6.2. The site exhibited clusters of transverse cracks. It was detected that the selected section did not have punchout per mile. To confirm the size and location of longitudinal and transverse reinforcements and pavement thickness before collecting data, a 6 in (152.4 mm)-core specimen was taken from the site.

**Table 6.2 - CRC Design Parameters and NDT Results for I20EBHMP4-5**

| | | | | | | | |
|---|---|---|---|---|---|---|---|
| **HARALSON COUNTY** | **Design Parameters** | | | | | | |
| | Site Condition | Age (Year) | CRC Thck. (in) | Longitudinal Rebar Size/ Spacing (in) | Transverse Rebar Size/ Spacing(in) | Longitudinal Rebar Depth (in) | Transverse Rebar Depth (in) |
| | Good | 37 (1980) | 12” | #6 / 4” ~ 8” | #6 / 23” ~ 46” (typical 39”) | 4.25” | 5” |
| | **Distress Assessment** | | | | | | |
| | Spacing between single transverse cracks (ft.) | Spacing between clusters of transverse cracks (ft.) | | Transverse crack width (in) | | Longitudinal crack width (in) | Number of Punchouts / mile |
| | 1.6’ ~ 4.0’ (typical 1.63’) | 24’ | | 0.03” ~ 0.10” (typical 0.08”) | | 0 | 0 |

The transverse cracks pattern on the investigated lane is shown in Figure 6.12. The section was constructed as an 11 in (280 mm) CRC slab above a 0.75 in (19 mm) asphaltic concrete layer and 12 in (305 mm) of graded aggregate (cement stabilized) subbase. However, the concrete layer thickness was measured 12 in (305 mm) from the core specimen. The longitudinal and transverse reinforcements consisted of #6 rebars. The concrete cover depth to the top of the longitudinal reinforcement was measured to be 4.25 in (108 mm) from the core specimen. The site was investigated in four stages in terms of density of crack types and existence of other distress types. The stages were named as S2-a, S2-b, S2-c and S2-d. They refer

the first (a), second (b), third (c), and forth (d) subsite (S) segments of Haralson County which was the 2nd site investigated.

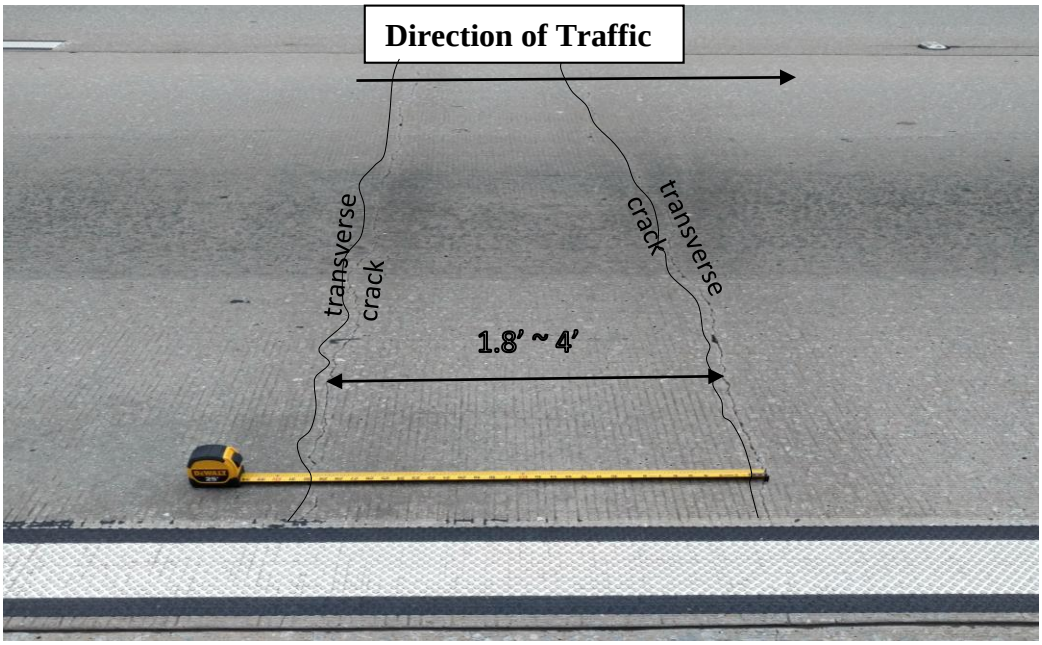


**Figure 6.12 - Typical Single Transverse Crack Pattern (S2-a)**

The site had the cluster transverse cracks as showed in Figure 6.13. Transverse cracks were marked in the clusters (Figure 6.13). The distance between the clusters of transverse cracks was measured approximately 24 ft. (732 cm). The single transverse cracks were spaced at the range of approximately 1.8 ft. and 4.0 ft. (55 and 122 cm) as it is shown in Figure 6.12. The typical transverse crack width varied in the range of 0.03 in and 0.10 in (0.76 and 2.54 mm). The site had many visible holes on the pavement by sizing maximum 1.5 in x 3 in (38 mm x 76 mm) (Figure 6.14). The longitudinal cracks were not noticed visibly.


**Figure 6.13 – Typical Cluster Transverse Cracks Pattern at S2-a and S2-c**

**Figure 6.14 – The Measurement of Crack Widths at S2-a and S2-c**

### 6.3.2.2.Data Post-Processing

The GPR unit scans were visualized in RadView software. Figure 6.15 clearly shows the location of four reinforcements and the layer thickness. An issue to be considered is the depth difference among the top points of reflections of transverse reinforcements. Based on findings, the last transverse reinforcement in the image showed the existence of crack on the reinforcement. It means that as the transverse reinforcements go deeper, more transverse cracks are formed. Figure 6.16 indicates the depth of longitudinal reinforcement and CRC thickness in the transverse direction. It is clear to see that the levelling was appeared on the longitudinal reinforcements, as well.

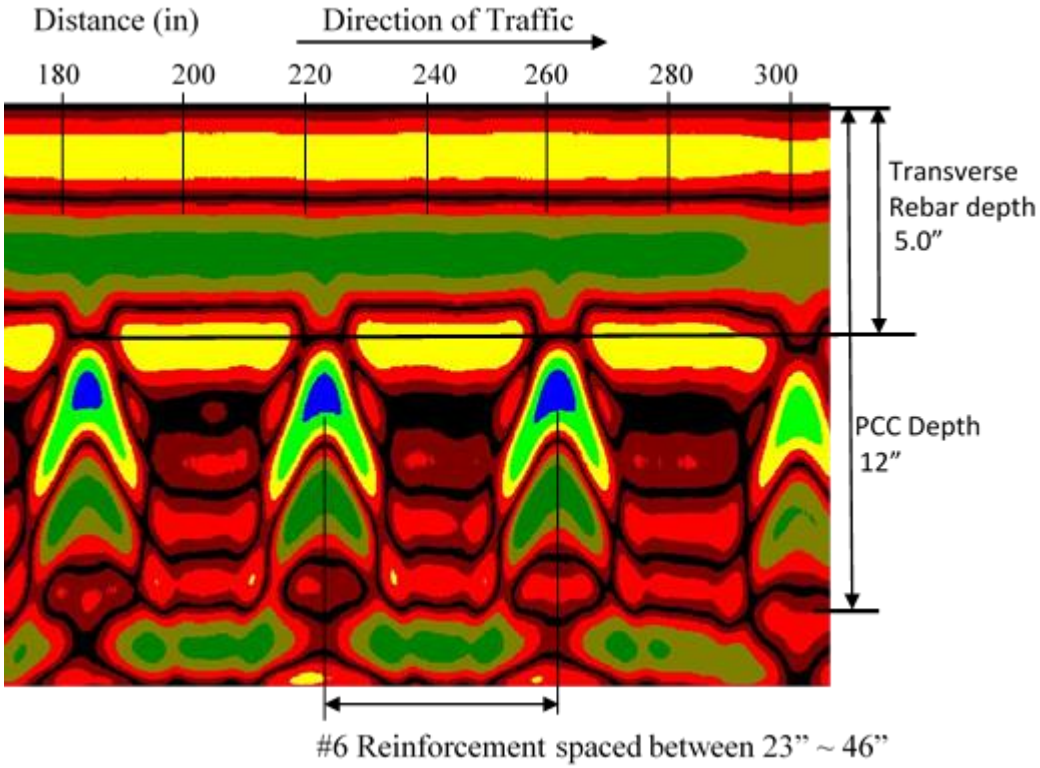


**Figure 6.15 – GPR Scan in the Longitudinal Direction (S2-b)**

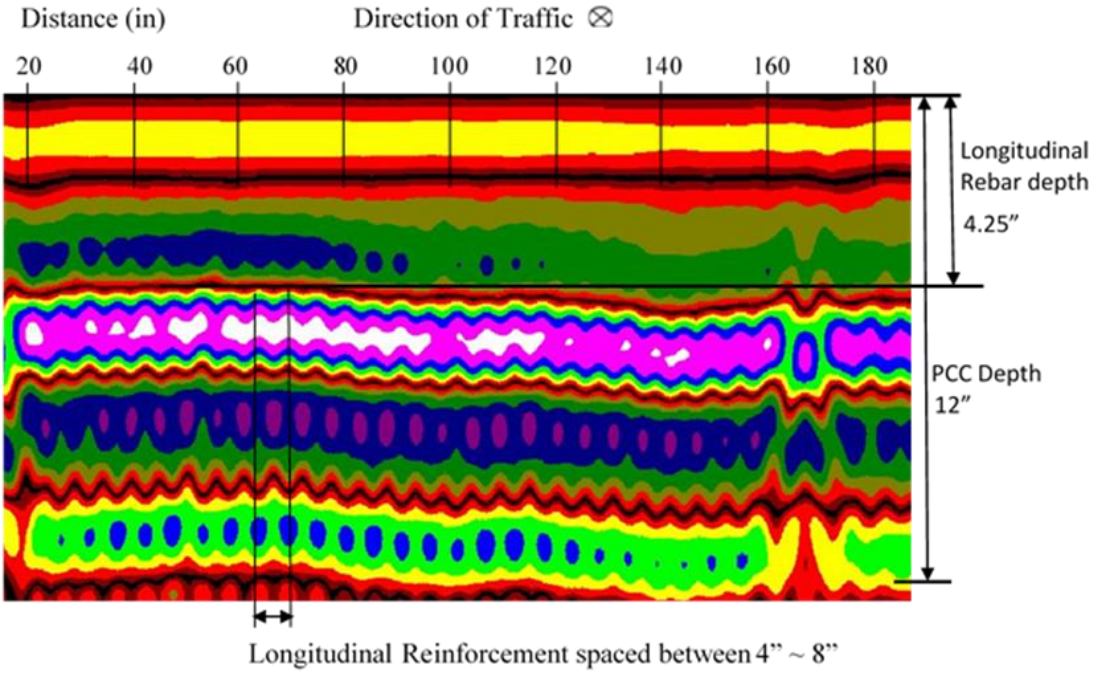


**Figure 6.16 – GPR Scan in the Transverse Direction (S2-c)**

In the selected site, the depth of longitudinal rebar is varied throughout the 1-mile section because of construction processes. The S2-a and S2-c were determined to be scanned by GPR and Profometer because of the existence over ten single transverse cracks in the cluster. In addition, the most of these cracks were placed on the transverse reinforcements. The S2-b and S2-d indicated the same repetitive crack distress pattern. Based on observations, the S2-c indicated the most crack formation over the pavement, and the following segment was the S2-a as seen in Figure 6.17. The reason for this might be that the reinforcements at S2-a and S2-c were placed at 4.25 in (108 mm) and 4.45 in (113 mm) in depth, which were out of the recommended range by GDOT.

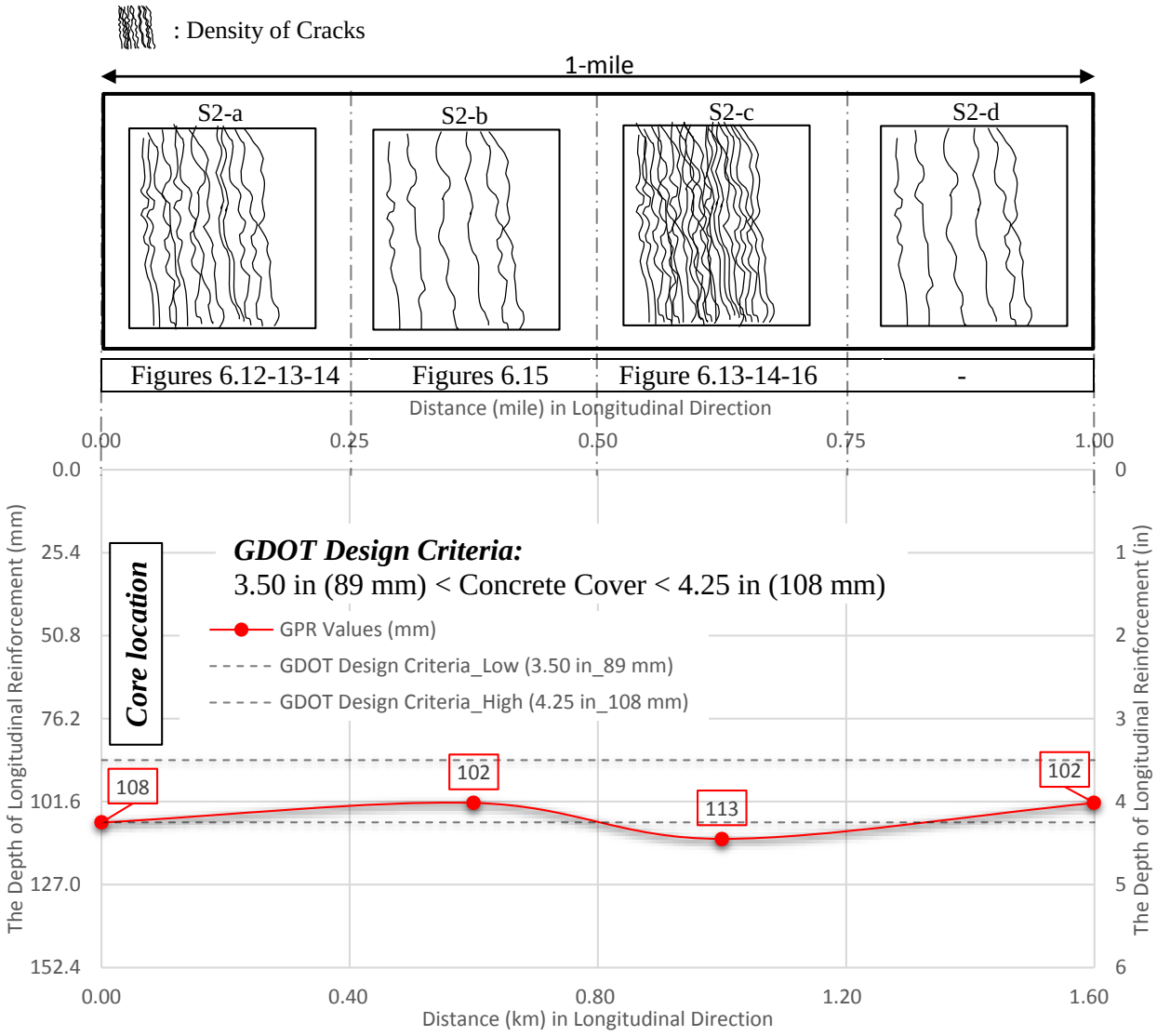


**Figure 6.17 – Stress Pattern and Concrete Cover in Longitudinal Direction in Each Segment Along 1-mile**

The following graph (Figure 6.18) indicates the depths of longitudinal reinforcements, which were detected from the core location (S2-a) in the transverse direction, from the shoulder to the inner lane, by GPR and Profometer. Although the depth values taken by both techniques show a similar pattern in the graph, these values are not matched exactly (Figure 6.18). The reason for this is believed to be the result of varied materials, such as metal or other pieces of steel, which can be detected easily by Profometer units forming a basis for this error margin. In addition, the cracks were observed to continue into the shoulder. As shown in the graph, the depth of longitudinal reinforcements was lower near the shoulder. Thus, it is believed that the concrete cover affects the density and/or severity of cracks.

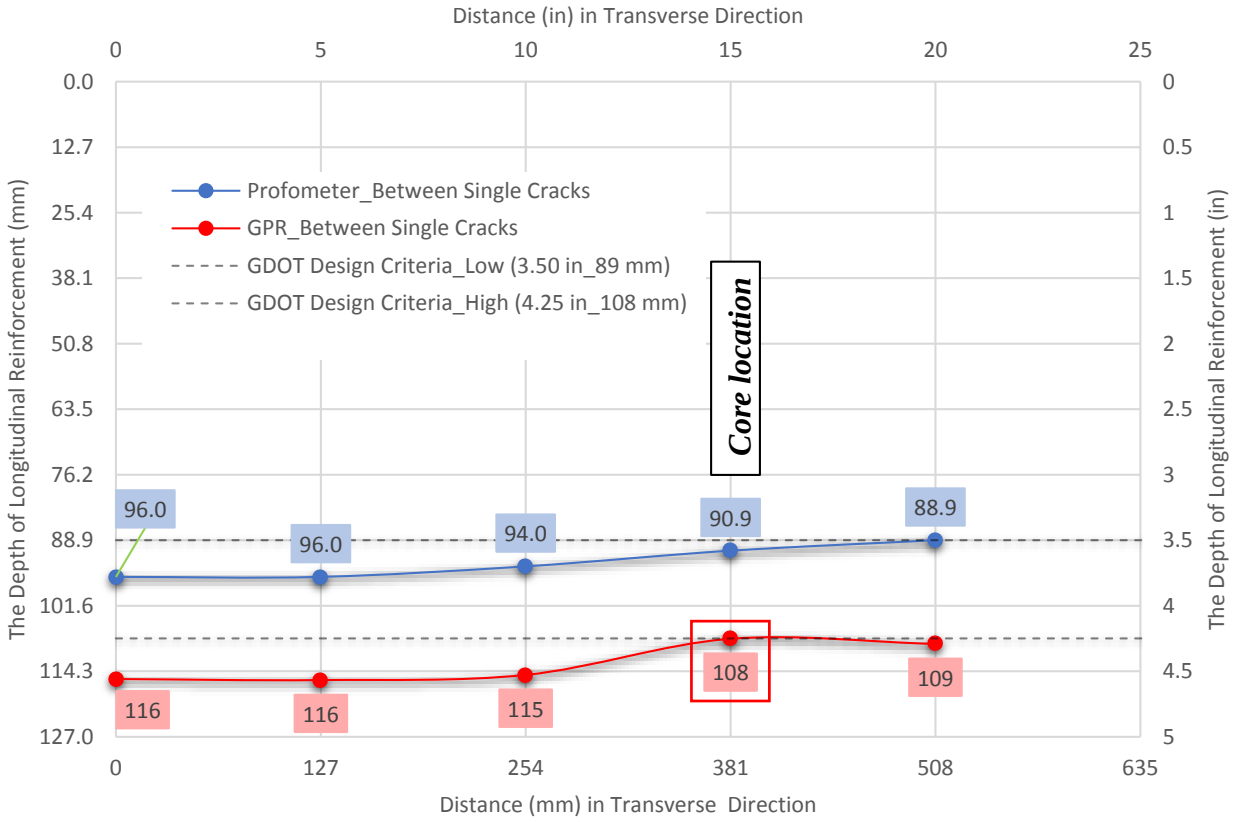


**Figure 6.18 – Concrete Cover Depth Values Detected by calibrated GPR and Profometer in Transverse Direction at S2-a**

### 6.1.1. I-20 - Carroll County

#### 6.1.1.1. Data Collection

Non-destructive testing methods were carried out on Interstate 20 in Carroll County using a Ground Penetration Radar (GPR) and Profometer. The detailed information regarding the working procedures of these units is mentioned in Section 5.1.

The outside lane on West Bound (WB) I-20 located between mileposts 24-25 in Carroll County was selected for inclusion in this study. The CRC pavement was reported to be in poor condition, which indicated many visible distresses such as transverse cracks, punchouts, and patched areas. The construction drawings obtained from GeoPI (see I20WBCMP24-25 in Appendix A) indicate that the section was built in 1972, and, later, the constructional drawings were revised in 1976. The location of this site is shown in Figure 6.19.


**Figure 6.19 – I-20 MP 24-25 Carroll County Site Location (Google Maps, 2017)**

The design parameters and distress assessment values are presented in Table 6.3. The site exhibited several punchout, patched areas, and a few severe cracks. It was detected that the selected section had 10 punchout per mile. Based on the investigation, there is a relation between the occurrence of punchouts and patched areas.

**Table 6.3 - CRC Design Parameters and NDT Results for I20WBCMP24-25**

| | **Design Parameters** | | | | | | |
|---|---|---|---|---|---|---|---|
| **CARROLL COUNTY** | Site Condition | Age (Years) | CRC Thickness (in) | Longitudinal Rebar Size/ Spacing (in) | Transverse Rebar Size/ Spacing (in) | Longitudinal Rebar Depth (in) | Transverse Rebar Depth (in) |
| | Poor | 45 (1972) | 8.70” | #6 / 8” | - | 4.00” | - |
| | **Distress Assessment** | | | | | | |
| | Spacing between single transverse cracks (ft.) | | Spacing between clusters of transverse cracks (ft.) | Transverse crack width (in) | Number of Punchouts / mile | | |
| | 1’ | | 10’ ~ 20’ | 0.06” ~ 0.12” (typical 0.1”) | 10 | | |

The transverse cracks pattern on the investigated lane is shown in Figure 6.20. The section was constructed as a 9 in (229 mm) CRC slab above a 1 in (25.4 mm) asphaltic concrete layer and 5 in (127 mm) of graded aggregate (cement stabilized) subbase. However, the concrete layer thickness was measured 8.70 in (221 mm) from the core specimen. The longitudinal and transverse reinforcement consisted of #6 rebar. It was observed that there was no transverse reinforcement throughout the investigated section except for two transverse reinforcement bars located at irregular locations. The concrete cover depth to the top of the longitudinal reinforcement was measured to be 4.00 in (102 mm) from the core specimen. The site was investigated in four stages in terms of density of crack types and existence of other distress types.

The stages were named as S3-a, S3-b, S3-c, S3-d. They refer the first (a), second (b), third (c), and forth (d) subsite (S) segments of Carroll County which was the 3rd site investigated.

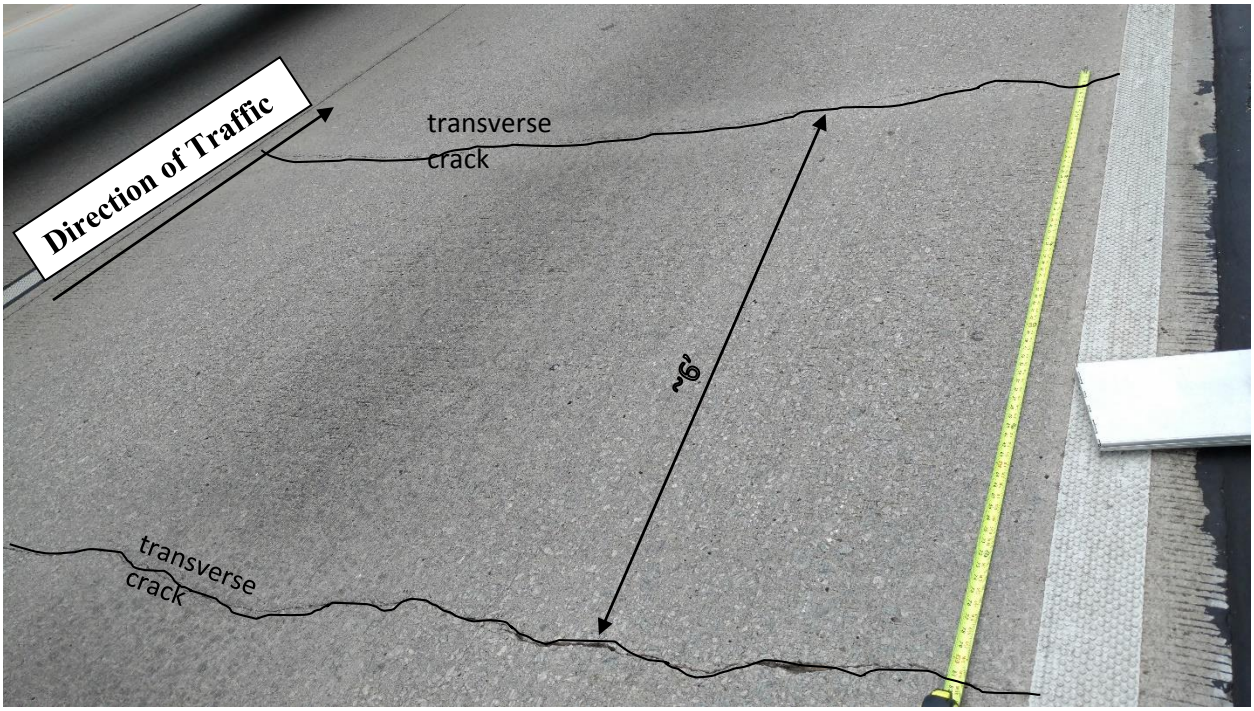


**Figure 6.20 - Typical Single Transverse Crack Pattern (S3-a)**

The site had a considerable number of cluster transverse cracks as showed in Figure 6.21. The minimum and maximum distance between the clusters of transverse cracks were measured to range from 10 ft. to 20 ft. (305 and 610 cm). The single transverse cracks were spaced at the range of approximately 5 ft. and 6.5 ft. (152 and 198 cm) as it is shown in Figure 6.20. It was detected that the site had the punchouts at the location of the cluster transverse cracks (Figure 6.21). The crack width varied in the range of 0.06 in and 0.12 in (1.5 and 3 mm) indicated in Figure 6.22.

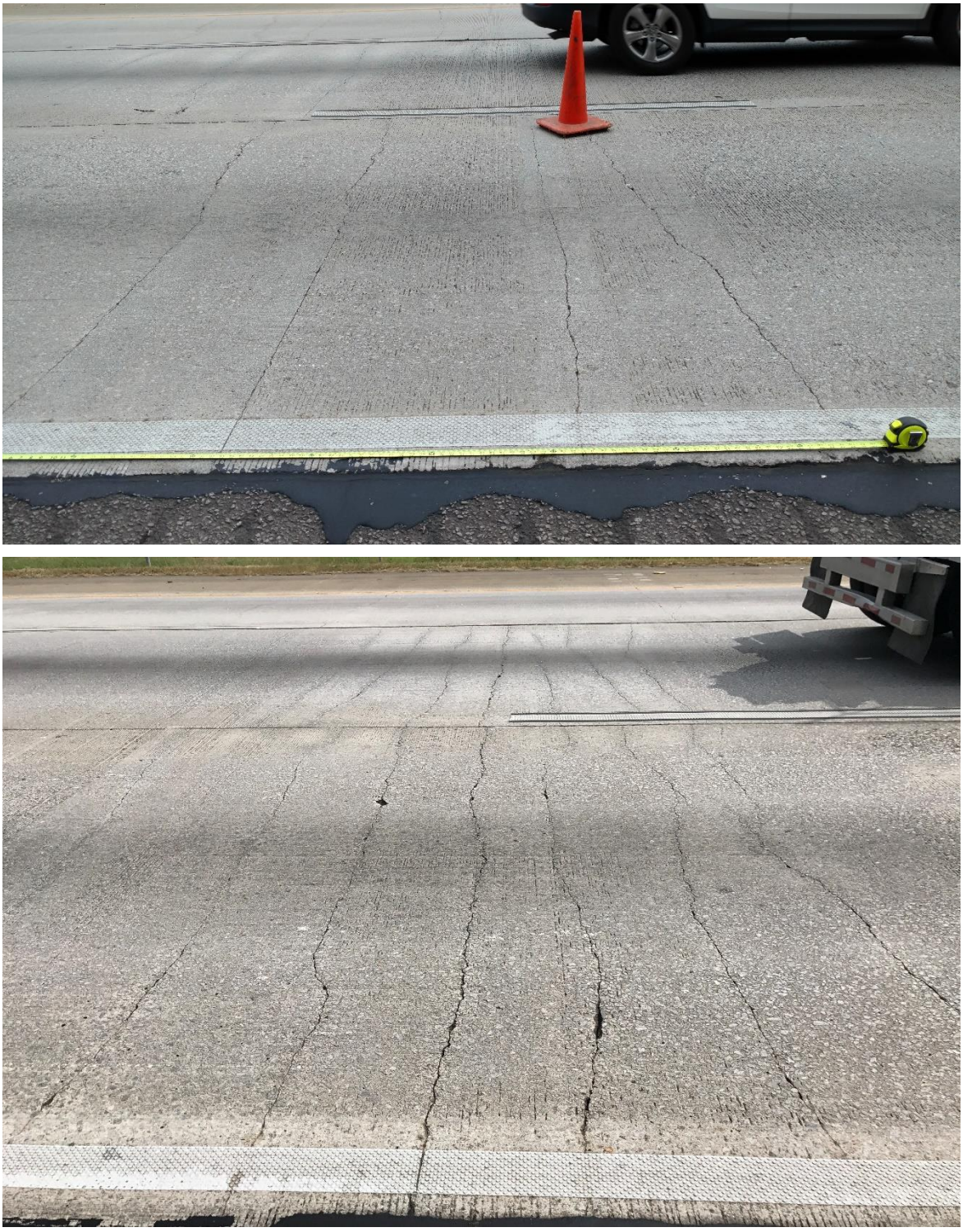

**Figure 6.21 – Typical Cluster Transverse Cracks Pattern at S3-a and S3-c**

**Figure 6.22 – The Measurement of Crack Widths at S3-a**

A few patched areas observed in this project were examined using GPR and Profometer. It should be noted that while the punchout areas had been previously patched, the repairs had become severity distressed again with significant punchouts observed during the field investigation. Figures 6.23-24 show the patched area with punchout at S3-b during investigation. Another problem area was located near MP 24 WB. This area had a few punchouts on the wheel-path which was on the patched area near the inside lane (S3-d), as seen in Figures 6.25-26.

**Figure 6.23 – A Patched Area at Outside Lane at S3-b**


**Figure 6.24 – A Patched Area at Outside Lane at S3-b (Google Maps, 2017)**

**Figure 6.25 – A Patched Area at Outside Lane at S3-d**


**Figure 6.26 – A Patched Area at Outside Lane at S3-d (Google Maps, 2017)**

### 6.1.1.2. Data Post-Processing

While the GPR unit scans the varied materials having the different dielectric constant values, the results show the different reflections and color in the GPR images. The following images were obtained by using RadView software. Figure 6.27 clearly shows the layer thickness since this location does not have transverse reinforcement. Figure 6.28 indicates the depths of longitudinal reinforcements and layer thicknesses in the transverse direction.

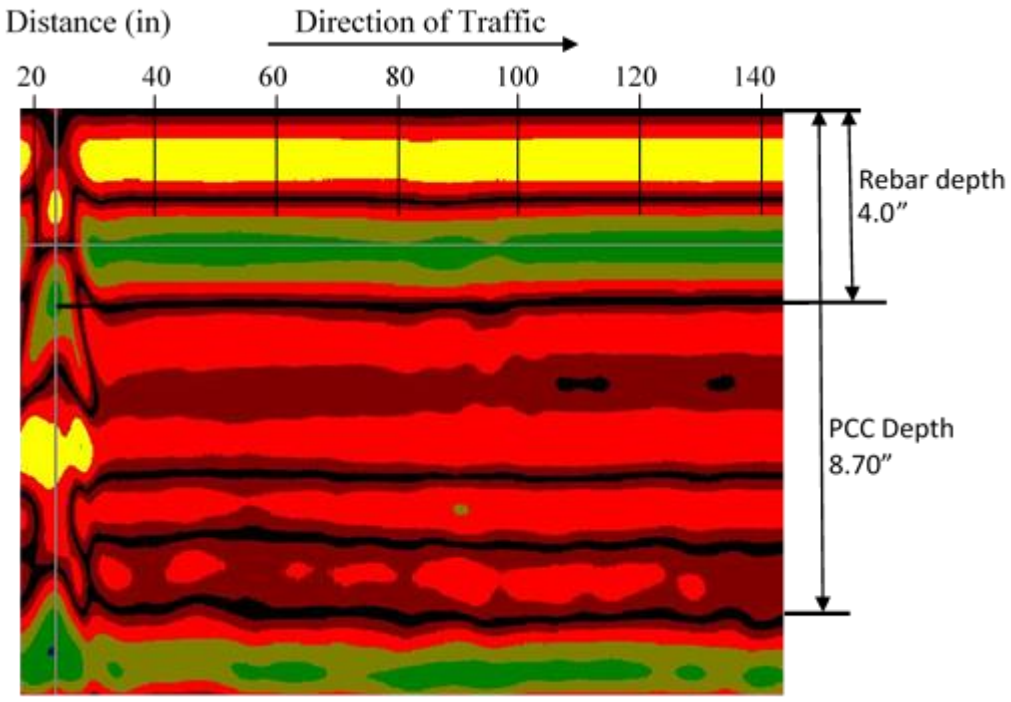


**Figure 6.27 – GPR Scan in the Longitudinal Direction (S3-a)**

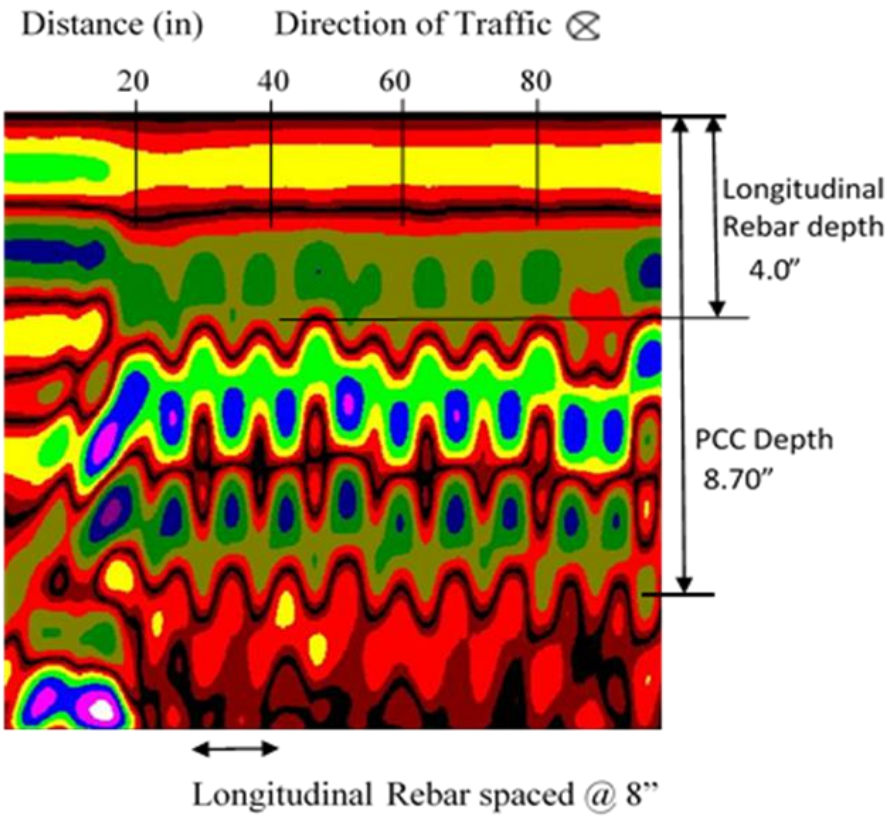


**Figure 6.28 – GPR Scan in the Transverse Direction (S3-a)**

In the selected site, there was no transverse reinforcement throughout the 1-mile section. The S3-a was determined to be scanned by GPR and Profometer because of the existence of the single and cluster cracks. The S3-b had an increased number of punchouts and patched area rather than cracks. Along the site, the section which had many irregular cracking was S3-c. The section exhibiting significant punchout and patched areas was as S3-d.

The graph in Figure 6.29 indicates the location of core, patched area, and transverse cracks. The GPR values at S3-b and S3-d were obtained from left, over, and right of patched area having high severity punchouts at the edges. It showed that the longitudinal reinforcements were deeper at the location of patched area than one of left and right. The S3-c, surveyed over cluster

cracking area, had the deepest longitudinal reinforcements, relatively more cracks. In addition, the concrete cover depth values were reasonably out of the range recommended by GDOT.

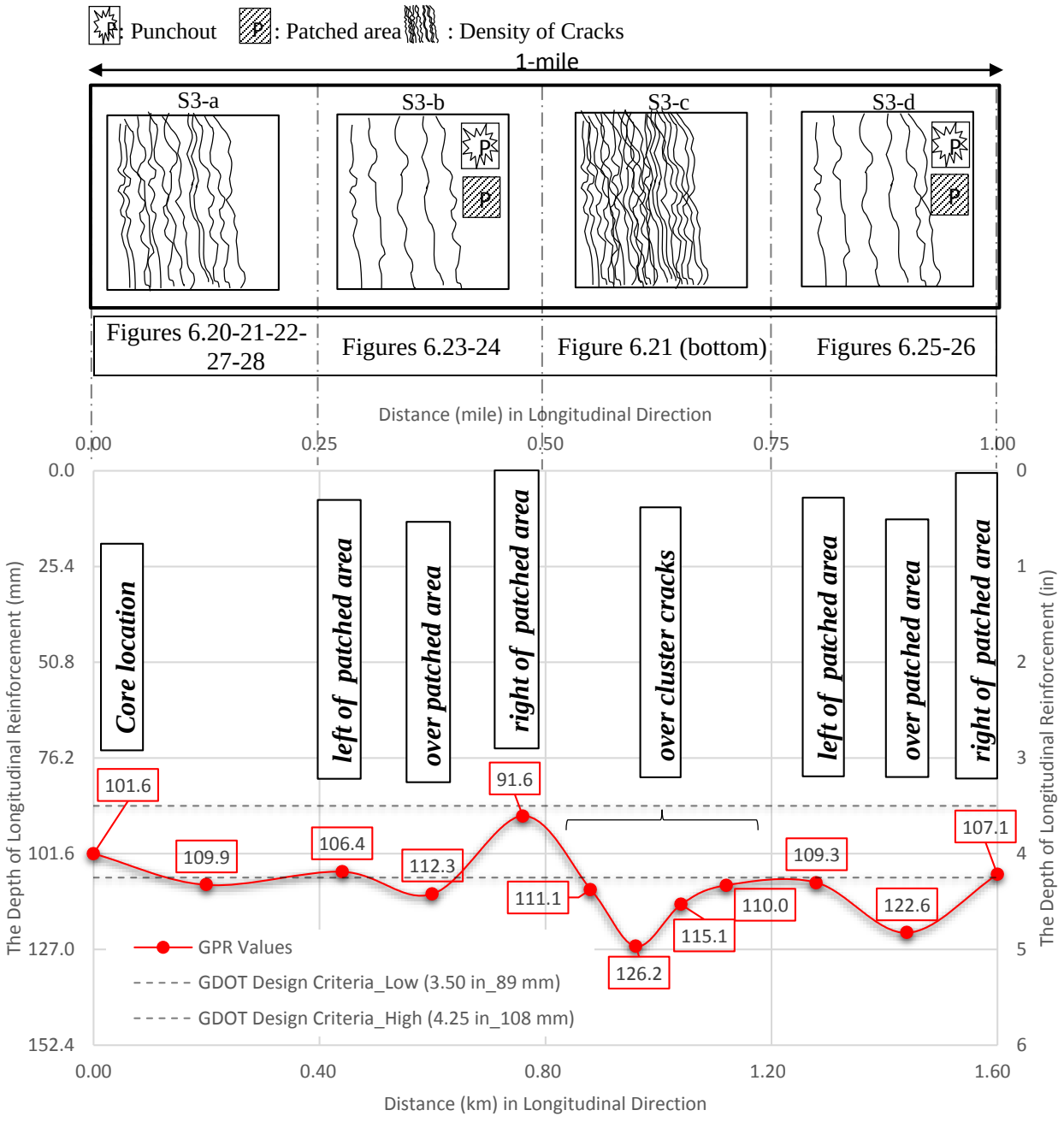


**Figure 6.29 – Stress Pattern and Concrete Cover in Longitudinal Direction in Each Segment Along 1-mile**

The following graph (Figure 6.30) indicates the depths of longitudinal reinforcements, which were obtained from between the single transverse cracks using GPR and Profometer (S3-a). The depth values taken by both techniques almost overlapped and showed the similar pattern in the graph. Likewise, the compared data for S3-b indicates the similar pattern as seen in Figures 6.31 and 6.32 although the data was not calibrated. The S3-b has the data taken from over, left and right of patched area (see in Figure 6.23). It means that GPR unit and Profometer might give the similar results for the locations of reinforcements if the units are calibrated.

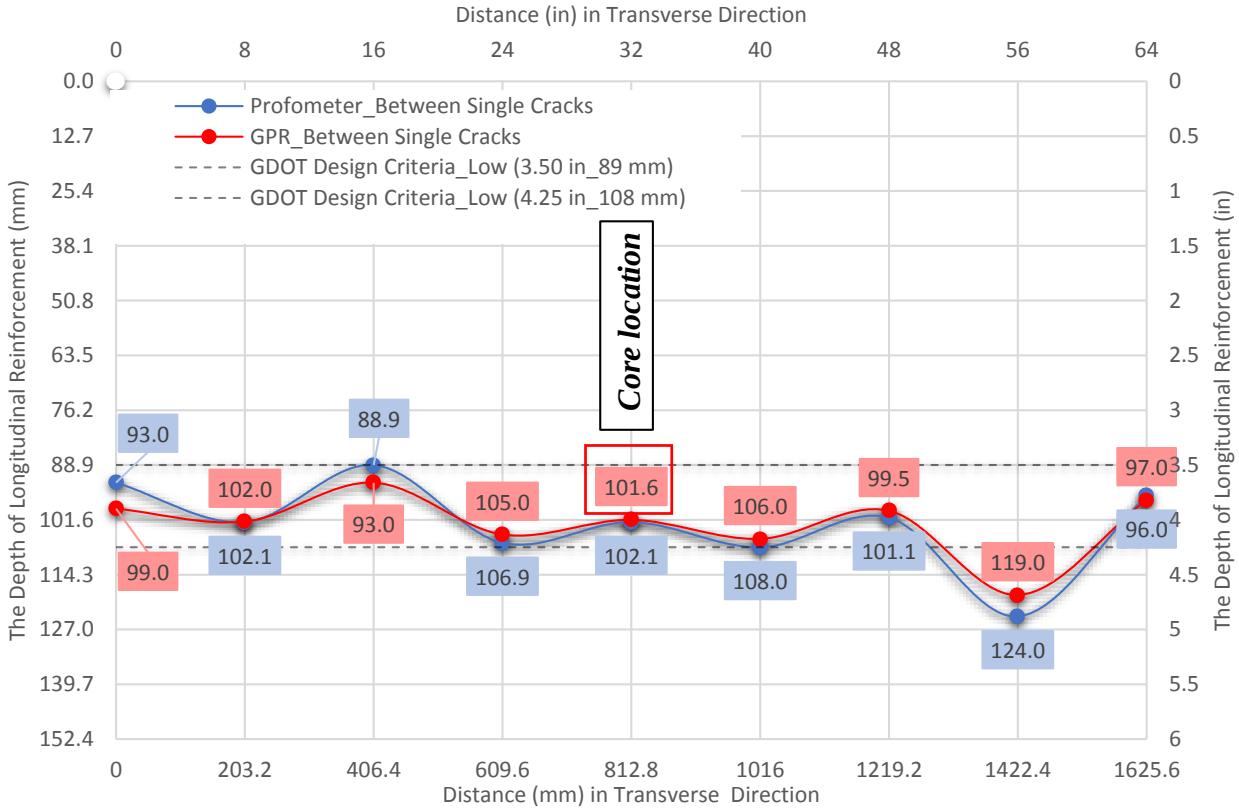


**Figure 6.30 –Concrete Cover Depth Values Detected by calibrated GPR and Profometer in Transverse Direction at S3-a**

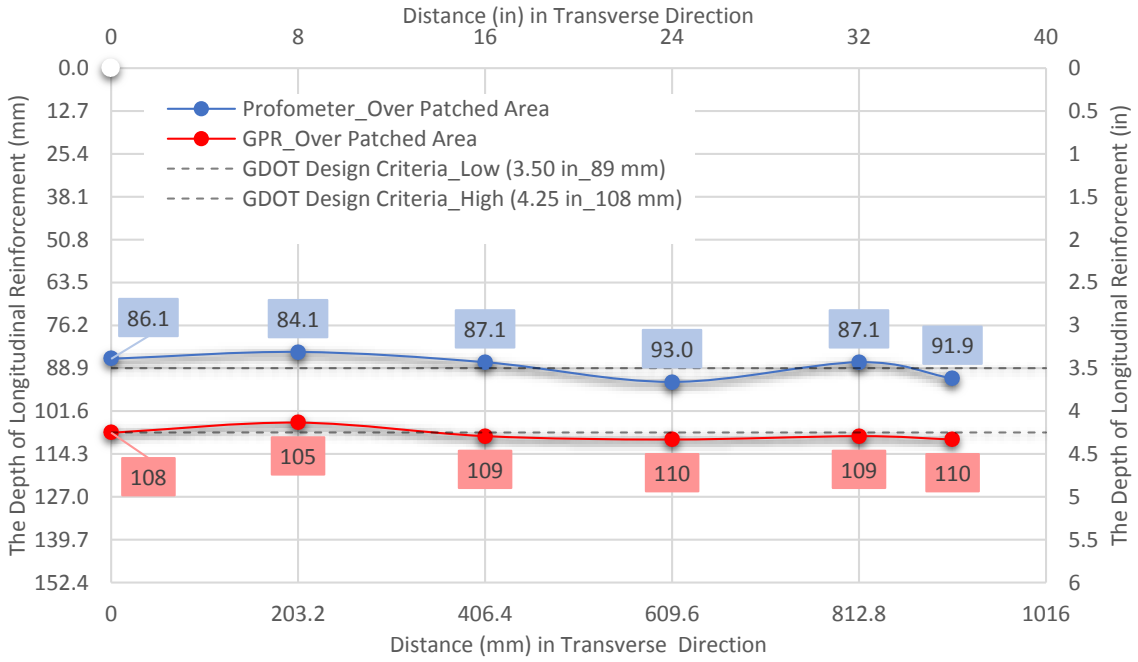


**Figure 6.31 –Concrete Cover Depth Values over Patched Area, Detected by non-calibrated GPR and Profometer in Transverse Direction at S3-b**

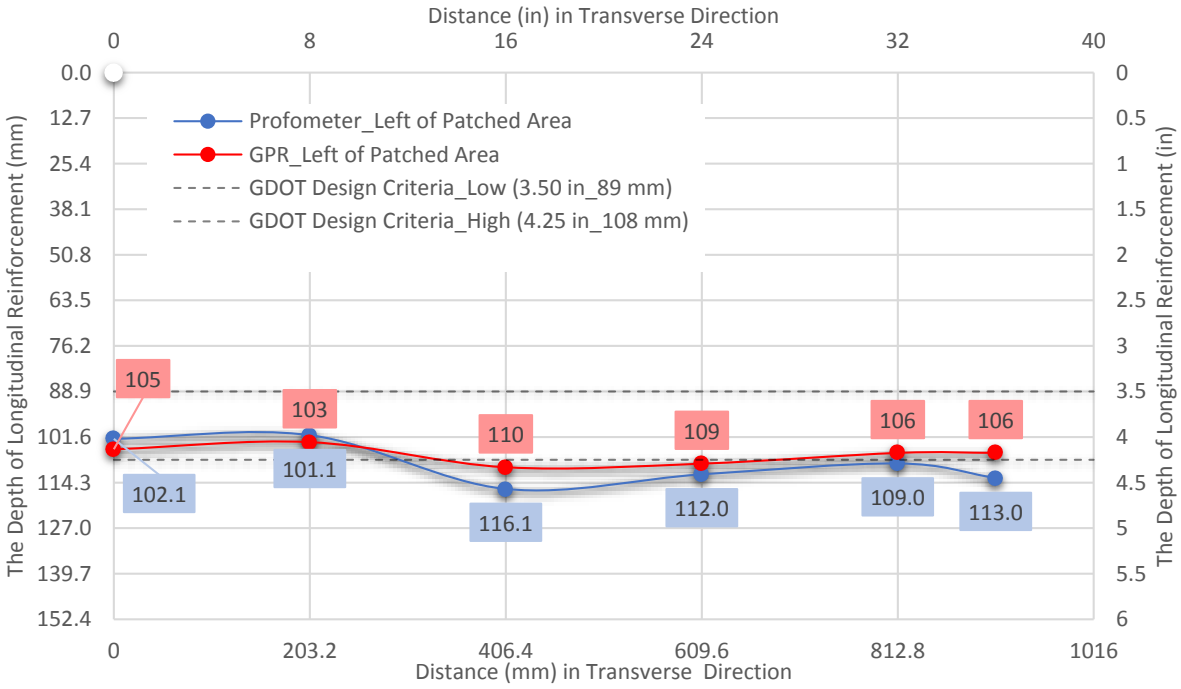


**Figure 6.32 –Concrete Cover Depth Values over left of Patched Area, Detected by non-calibrated GPR and Profometer in Transverse Direction at S3-b**

### 6.1.2. I-20 - Newton County

#### 6.1.2.1. Data Collection

Non-destructive testing methods were carried out on Interstate 20 in Newton County using a Ground Penetration Radar (GPR) and Profometer. The detailed information regarding the working procedures of these units is mentioned in Section 5.1.

The outside lane on East Bound (EB) I-20 located between mileposts 92-93 in Newton County was selected for inclusion in this study. The CRC pavement was reported to be in fair condition, which indicated many visible distresses such as clusters of transverse cracks, longitudinal cracks, and possibly material issues. The construction drawings obtained from GeoPI (see I20EBNMP92-93 in Appendix A) indicate that the section was built in 2005. The location of this site is shown in Figure 6.33.


**Figure 6.33 – I-20 MP 92-93 Newton County Site Location (Google Maps, 2017)**

The design parameters and distress assessment values are presented in Table 6.4. The site exhibited clusters of transverse cracks, and a few longitudinal cracks on the wheel-paths. It was detected that the selected section did not have punchout per mile. To confirm the size and location of longitudinal and transverse reinforcements and pavement thickness before collecting data, a-6 in (152.4 mm) core was taken from the site.

**Table 6.4 - CRC Design Parameters and NDT Results for I20EBNMP92-93**

| | | | | | | | |
|---|---|---|---|---|---|---|---|
| **NEWTON COUNTY** | **Design Parameters** | | | | | | |
| | Site Condition | Age (Year) | CRC Thickness (in) | Longitudinal Rebar Size/ Spacing (in) | Transverse Rebar Size/ Spacing (in) | Longitudinal Rebar Depth (in) | Transverse Rebar Depth (in) |
| | Fair | 12 (2005) | 12” | #6 / 5” | #4 / 36” | 4.00” | 4.75” |
| | **Distress Assessment** | | | | | | |
| | Spacing between single transverse cracks (ft.) | | Spacing between clusters of transverse cracks (ft.) | Transverse crack width (in) | Longitudinal crack width (in) | Number of Punchouts / mile | |
| | 1’~ 10’ (typical 1’) | | 12’ ~ 60’ (typical 12’) | 0.03” ~ 0.12” (typical 0.04”) | 0.01~0.08” | 0 | |

The transverse cracks pattern on the investigated lane is shown in Figure 6.34. The section was constructed as a 12 in (305 mm) CRC slab.The longitudinal and transverse reinforcement consisted of #6 and #4 rebars, respectively. The concrete cover depth to the top of the longitudinal reinforcement was measured to be 4.00 in (102 mm) from the core specimen. The site was investigated in four stages in terms of density of crack types and existence of other distress types. The stages were named as S4-a, S4-b, S4-c, and S4-d. They refer the first (a), second (b), third (c), and forth (d) subsite (S) segments of Newton County which was the 4$^{th}$ site investigated.

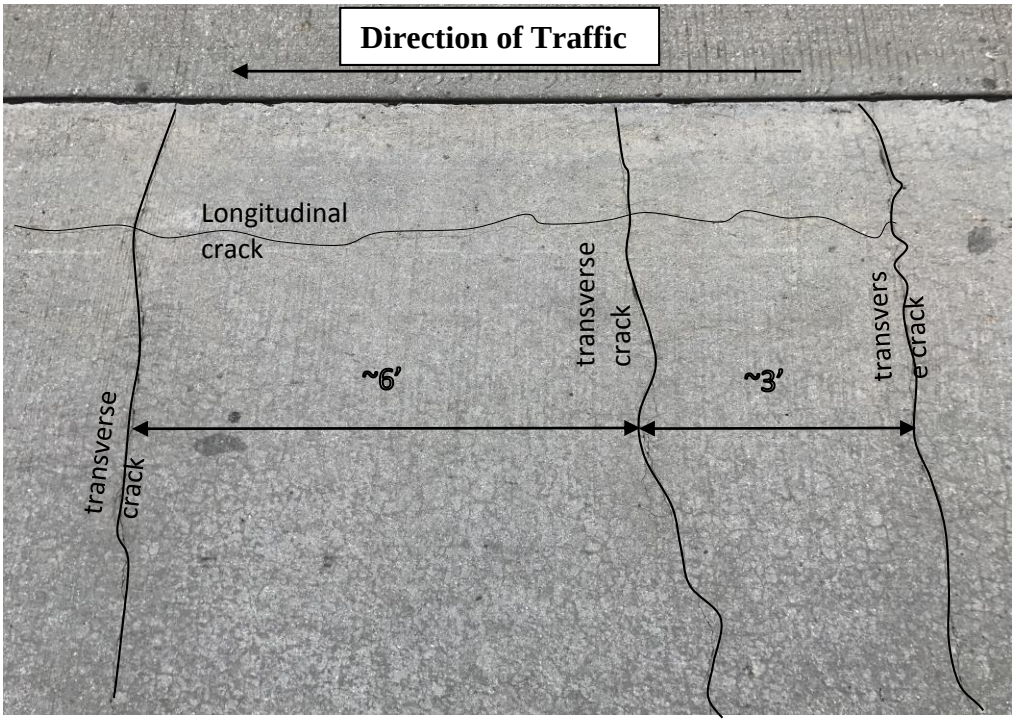


**Figure 6.34 - Typical Single Transverse Crack Pattern (S4-a)**

The site had the cluster transverse cracks as showed in Figure 6.35. Transverse rebars and cracks were marked as 'TC' and 'T' in the clusters, which mean 'crack on transverse rebar' and 'transverse rebar', respectively (Figure 6.35). The minimum and maximum distance between the clusters of transverse cracks were measured to range from 12 ft. to 60 ft. (366 and 1829 cm). The single transverse cracks were spaced at the range of approximately 1 ft. and 12 ft. (30.5 and 366 cm) as an example of the crack spacing is shown in Figure 6.34. The typical transverse crack width varied in the range of 0.03 in and 0.12 in (0.76 and 3.05 mm) and the maximum transverse crack width was 0.5 in (12.7 mm) (Figure 6.36). The S4-a, S4-b, and S4-d had the longitudinal crack, ranged between 0.03 in (0.76 mm) and 0.1 in (2.54mm) in width although the longitudinal crack was not appeared at S4-c. It was detected that the site had the signs of potential longitudinal cracks at the location of the cluster transverse cracks in S4-c.

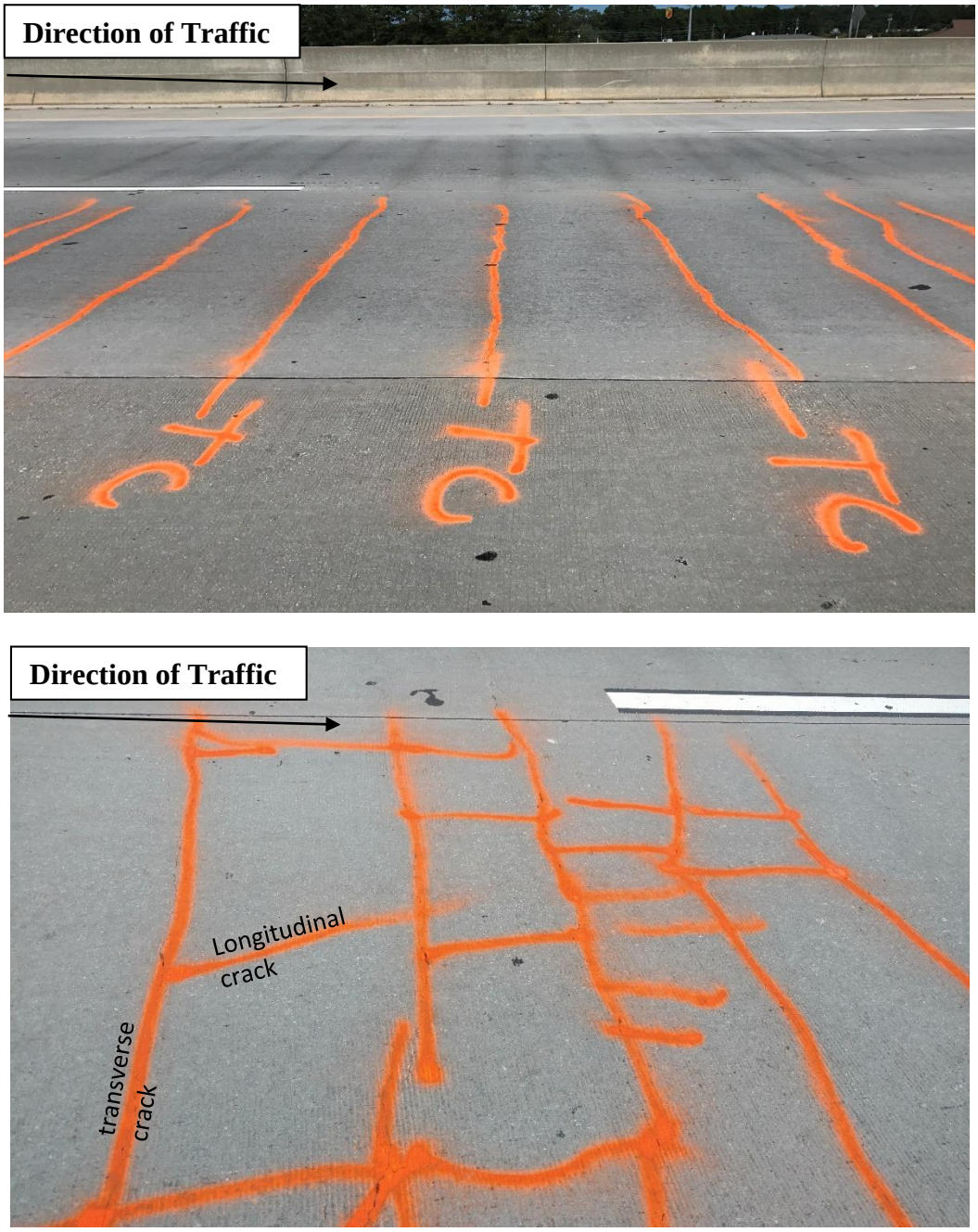


**Figure 6.35 – Typical Cluster Transverse Cracks Pattern at S4-b and S4-d**

**Figure 6.36 – The Measurement of Crack Widths at S4-a and S4-c**

### 6.1.2.2. Data Post-Processing

The GPR unit scans were visualized in RadView software. Figure 6.37 clearly shows the location of six reinforcements and the layer thickness. An issue to be considered is the depth difference among the top points of reflections of transverse and longitudinal reinforcements. Based on findings, there was no crack on 1$^{st}$, 2$^{nd}$, and 6$^{th}$ steel transverse reinforcements while some transverse cracks appeared on 3$^{rd}$, 4$^{th}$, and 5$^{th}$ transverse reinforcements were detected. As it is seen in the GPR scan (Figure 6.37), the deeper transverse reinforcements, the more transverse cracks. Figure 6.38 indicates the depth of longitudinal reinforcement and CRC thickness in the transverse direction. An increase of the depth of transverse reinforcements causes deeper longitudinal reinforcements. The result of this movement creates transverse cracks on the pavement. Figure 6.39 shows the comparison of images obtained by scanning over transverse reinforcements located in pavement formed with no crack and crack, which was consecutive area. It is clear to see that the reinforcements are deeper where the cracks appear.

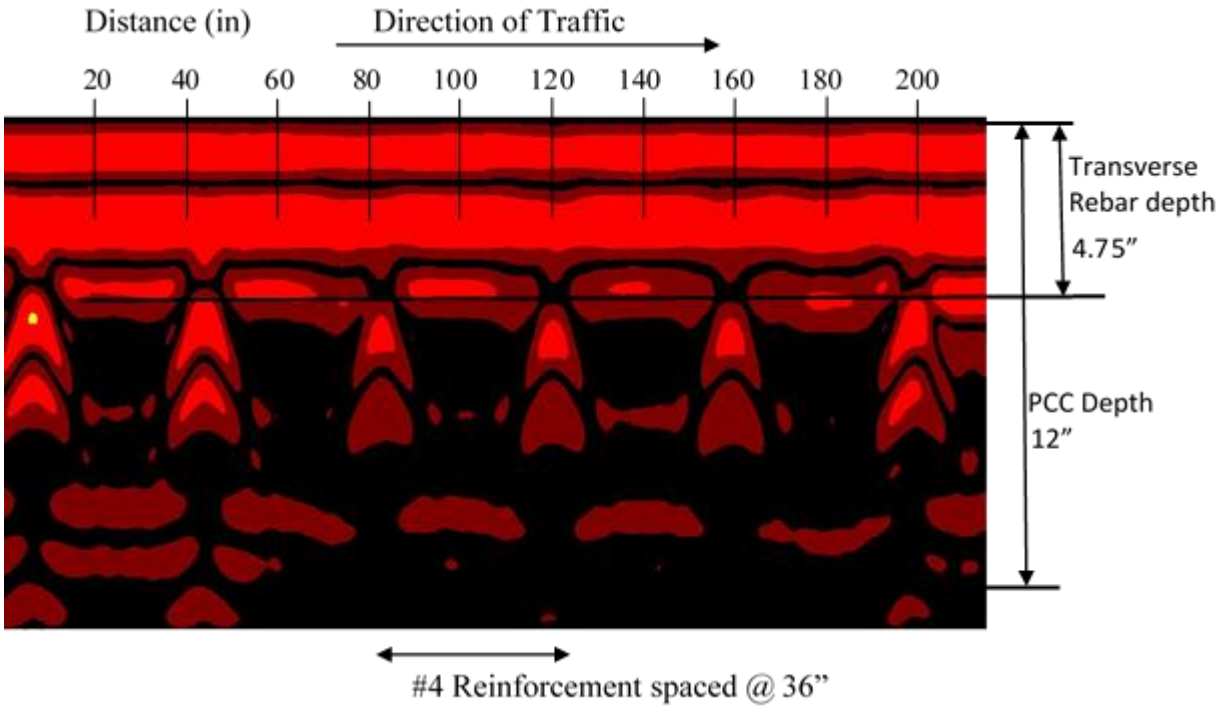


**Figure 6.37 – GPR Scan in the Longitudinal Direction (S4-a)**

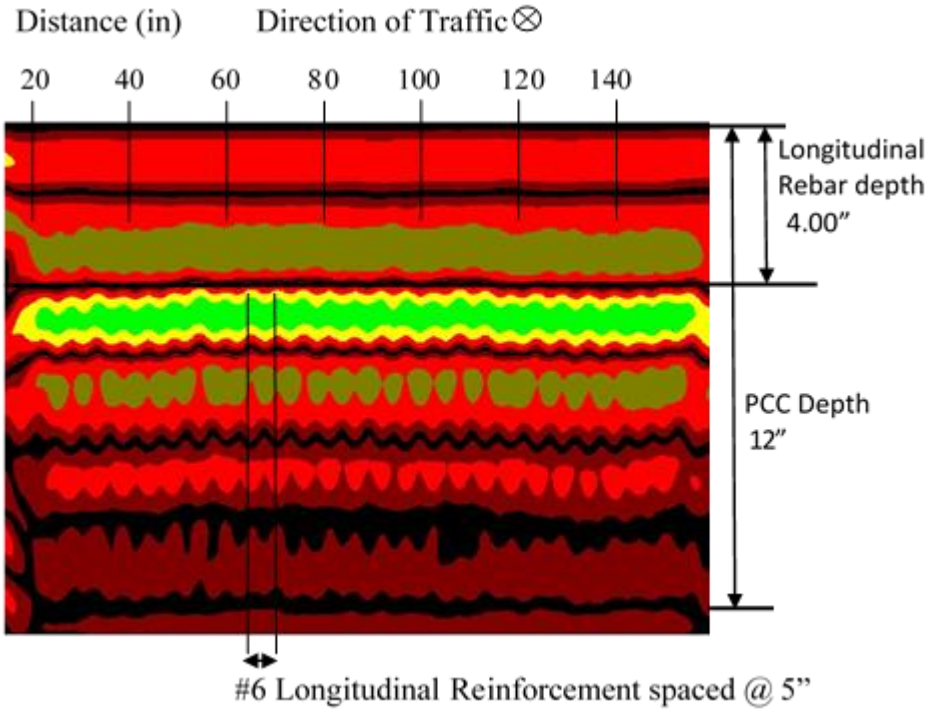


**Figure 6.38 – GPR Scan in the Transverse Direction (S4-b)**

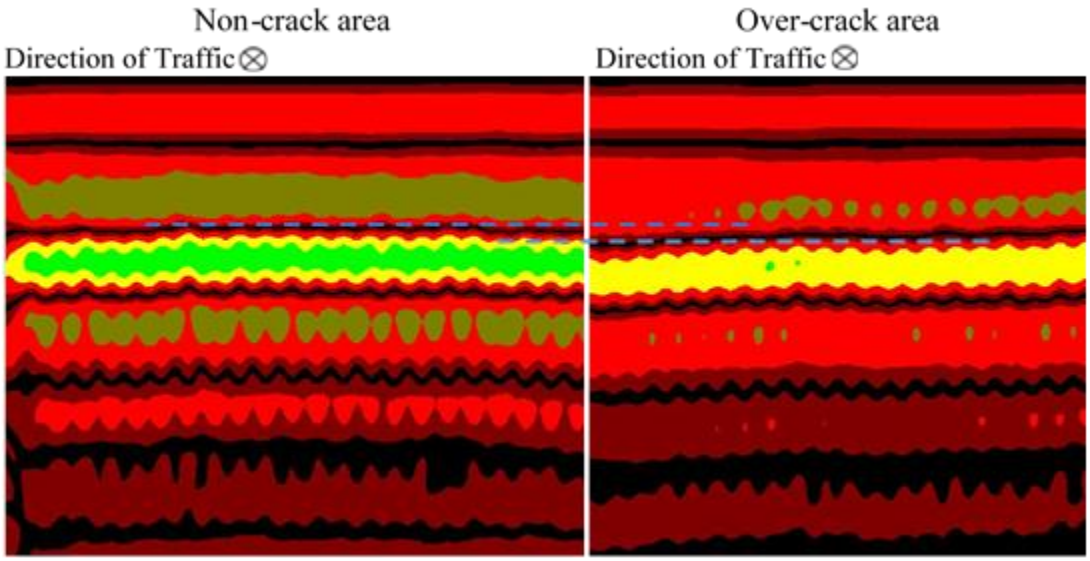


**Figure 6.39 – Comparison of GPR Scans obtained from non-crack area and over-crack area in the Transverse Direction (S4-a)**

In the selected site, the depth of longitudinal rebar is varied throughout the 1-mile section because of construction processes. The S4-a was determined to be scanned by GPR and Profometer because of the existence over ten single transverse cracks in the cluster. In addition, most cracks formed over the transverse reinforcement locations. The S4-b has a large distance, 10 ft. (305 cm), between two single transverse cracks in a cluster cracking. The S4-c was chosen because of the existence of many transverse cracks. This cluster had more than twenty cracks, which twelve cracks of them formed on transverse reinforcements. This segment had no longitudinal cracks. The section location exhibiting five transverse cracks and many longitudinal cracks was named as S4-d.

The concrete cover depth significantly decreased while traveling from S4-b to S4-d. It was believed that the sudden change in depth between S4-b and S4-c caused numerous transverse cracks at S4-c. In addition, as the reinforcements moved higher in the pavement cross-section, the quantity of longitudinal cracks increased instead of transverse cracks.

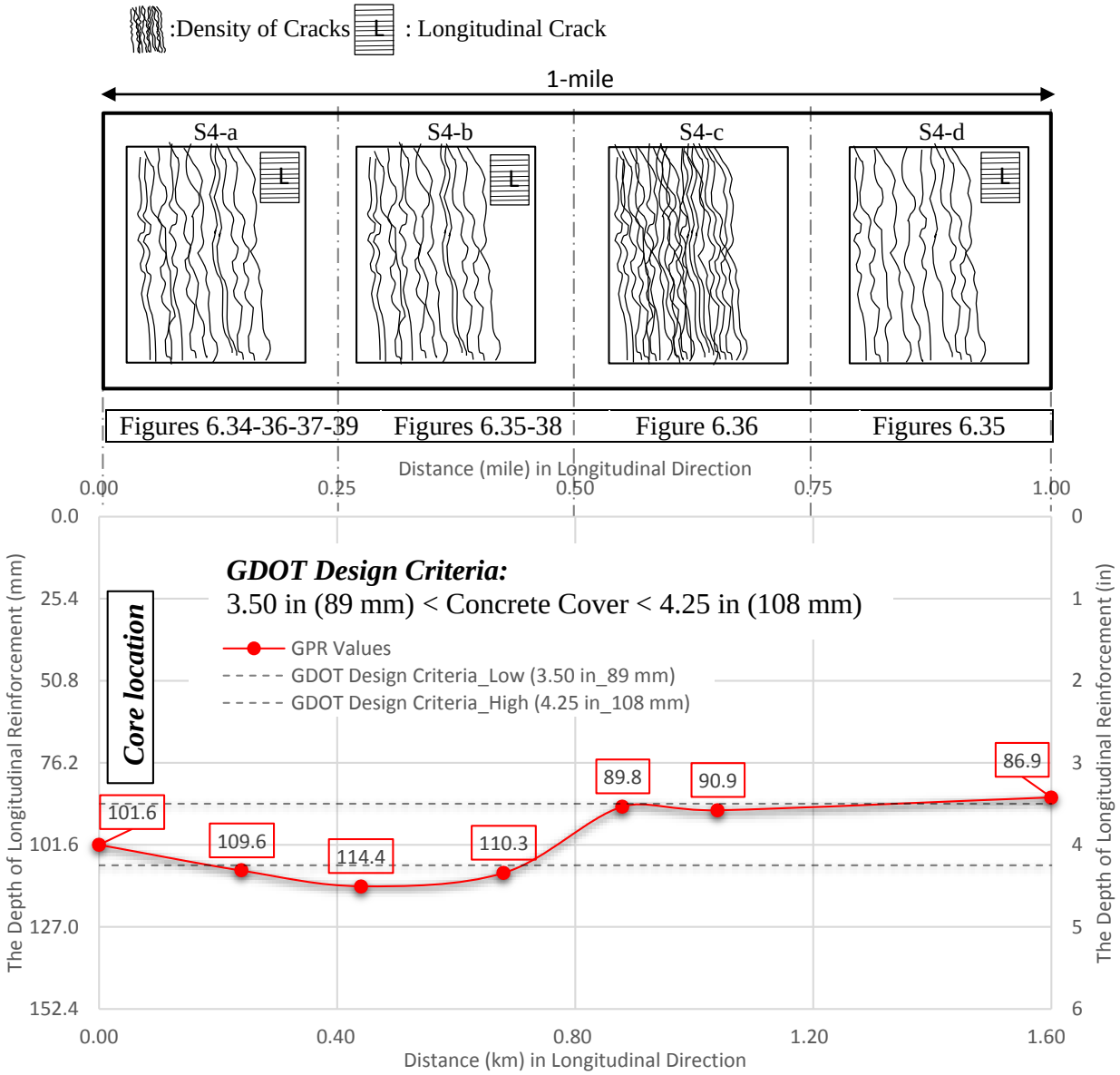


**Figure 6.40 – Stress Pattern and Concrete Cover in Longitudinal Direction in Each Segment Along 1-mile**

The following graph (Figure 6.41) indicates the depths of longitudinal reinforcements, which were detected from the section located between the single transverse cracks using GPR and Profometer (S4-a). Although the depth values taken by both techniques show the similar pattern in the graph, these values are not matched exactly (Figure 6.41). The reason for this is believed to be the result of varied materials, such as metal or other pieces of steel, which can be detected easily by GPR and Profometer units, and forms the basis for this error.

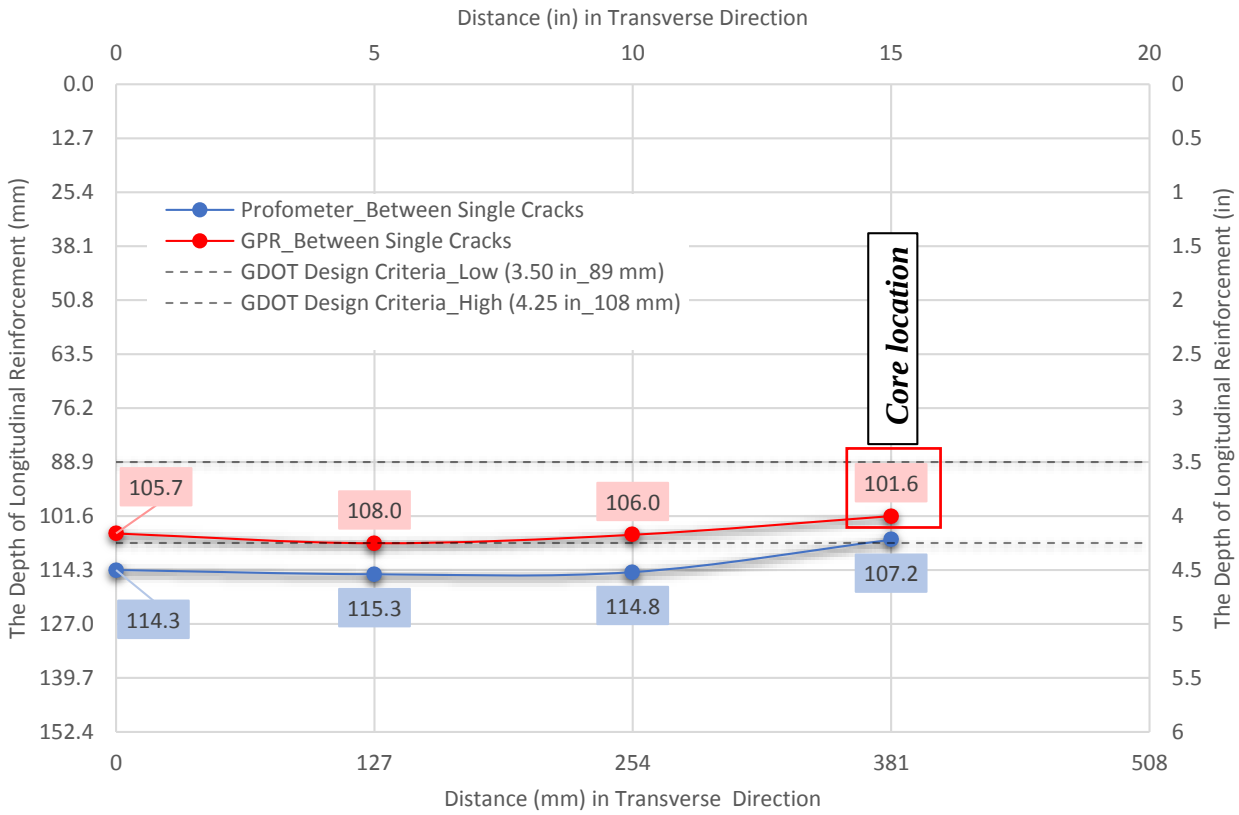


**Figure 6.41–Concrete Cover Depth Values Detected by calibrated GPR and Profometer in Transverse Direction at S4-a**

### 6.1.1. 3I-75 Cobb County

#### 6.1.1.1. Data Collection

Non-destructive testing methods were carried out on Interstate 75 in Cobb County using a Ground Penetration Radar (GPR) and Profometer. The detailed information regarding the working procedures of these units is mentioned in Section 5.1.

The outside lane on North Bound (NB) I-75 located between mileposts 267-268 in Cobb County was selected for inclusion in this study. The CRC pavement was reported to be in poor condition, which indicated many visible distresses such as transverse and longitudinal cracks, potential punchouts, and map cracking. The construction drawings obtained from GeoPI (see I75NBCMP267-268 in Appendix A) indicate that the plans of the section were completed in 1979, and, later, the constructional drawings were revised in 1985. The location of this site is shown in Figure 6.42. The design parameters and distress assessment values are presented in Table 6.5. It was detected that the selected section had no punchouts per mile.


**Figure 6.42 – I-75 MP 267-268 Cobb County Site Location (Google Maps, 2017)**

**Table 6.5 - CRC Design Parameters and NDT Results for I75NBCMP267-268**

| | Design Parameters | | | | | | |
|---|---|---|---|---|---|---|---|
| **COBB COUNTY** | Site Condition | Age (Years) | CRC Thickness (in) | Longitudinal Rebar Size/ Spacing (in) | Transverse Rebar Size/ Spacing (in) | Longitudinal Rebar Depth (in) | Transverse Rebar Depth (in) |
| | Poor | 32 (1985) | 10.25” | #6 / 5” ~ 9.5” | #4 / 25” ~ 40” (typical 39”) | 4.50” | 5.25” |
| | **Distress Assessment** | | | | | | |
| | Spacing between single transverse cracks (ft.) | | Spacing between clusters of transverse cracks (ft.) | Transverse crack width (in) | | Longitudinal crack width (in) | Number of Punchouts / mile |
| | 1.5’~ 4.25’ (typical 3.25’) | | No Grouping (typical 1’) | 0.10” ~ 0.15” (typical 0.15”) | | 0.05” | 0 |

The transverse cracks pattern on the investigated lane is shown in Figure 6.43. The section was planned as a 9 in (229 mm) CRC slab above a 1 in (25.4 mm) asphaltic concrete layer, 5 in (127 mm) of graded aggregate (cement stabilized) subbase, and 6 in (152 mm) crushed aggregate subgrade. Then, based on the revised constructional drawings, the pavement was redesigned as a 9 in (229 mm) CRC slab above a 5 in (127 mm) asphaltic concrete base (or alternatively Portland cement concrete base), 7 in (178 mm) of graded aggregate (cement stabilized) subbase. However, the concrete layer thickness was measured 10.25 in (260 mm) from the core specimen. The longitudinal and transverse reinforcements consisted of #6 with 0.6% cross sectional area and #4 rebars, respectively. The concrete cover depth to the top of the longitudinal reinforcement was measured to be 4.50 in (114 mm) from the core specimen. The site was investigated in four stages in terms of density of crack types and existence of other distress types. The stages were named as S5-a, S5-b, S5-c, S5-d. They refer the first (a), second (b), third (c), and forth (d) subsite (S) segments of Cobb County which was the 5th site investigated.

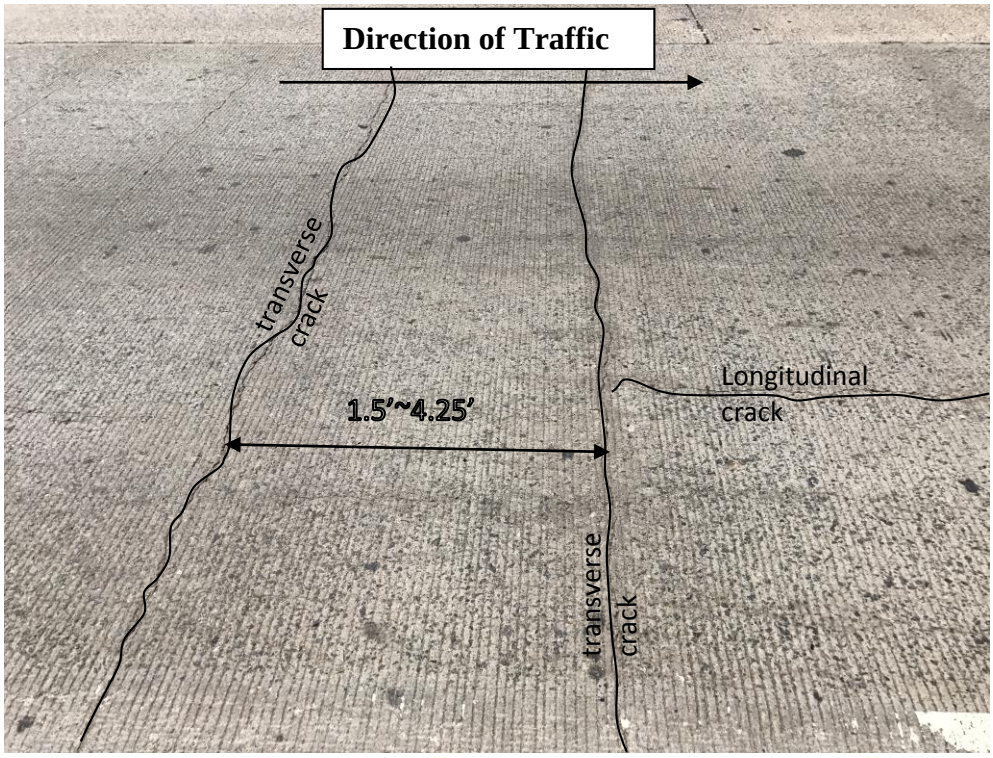


**Figure 6.43 - Typical Single Transverse Crack Pattern (S5-a)**

The site had cluster transverse cracks as showed in Figure 6.44. Transverse rebars and cracks were marked as 'TC' and 'T' in the clusters, which mean 'crack on transverse rebar' and 'transverse rebar', respectively (Figure 6.44). There is no clear distance between the clusters of transverse cracks because the site indicated the continuous pattern of cluster transvers cracks. The single transverse cracks were spaced at the range of approximately 1.5 ft. and 4.25 ft. (46 and 130 cm). The typical transverse crack width varied in the range of 0.1 in and 0.15 in (2.54 and 3.81 mm) and the maximum transverse crack width was 1 in (25.4 mm). Although the longitudinal crack typically ranged between 0.03 in (0.76 mm) and 0.1 in (2.54mm) in width, it was observed that the maximum longitudinal crack width was 0.5 in (12.7 mm) (Figure 6.45). It was detected that the site had signs of potential punchouts at the location of the cluster transverse cracks in S5-c.


**Figure 6.44 – Typical Cluster Transverse Cracks Pattern at S5-a and S5-d**

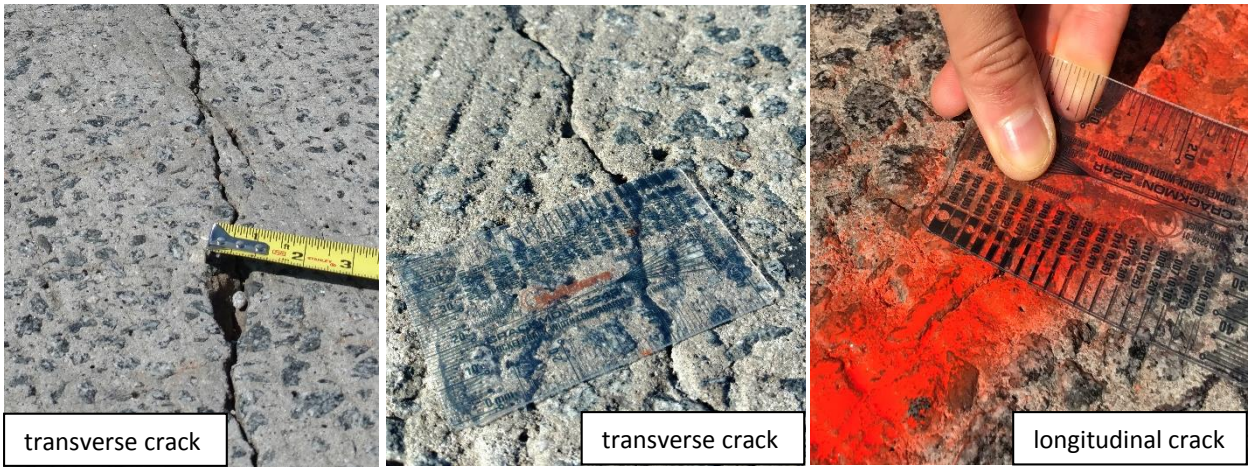


**Figure 6.45 – The Measurement of Non-Typical Crack Widths at S5-a and S5-d**

It is predicted that S5-c potentially has a risk of forming a punchout in near future because of existence of high severity longitudinal cracks between transverse cracks (Figure 6.46).

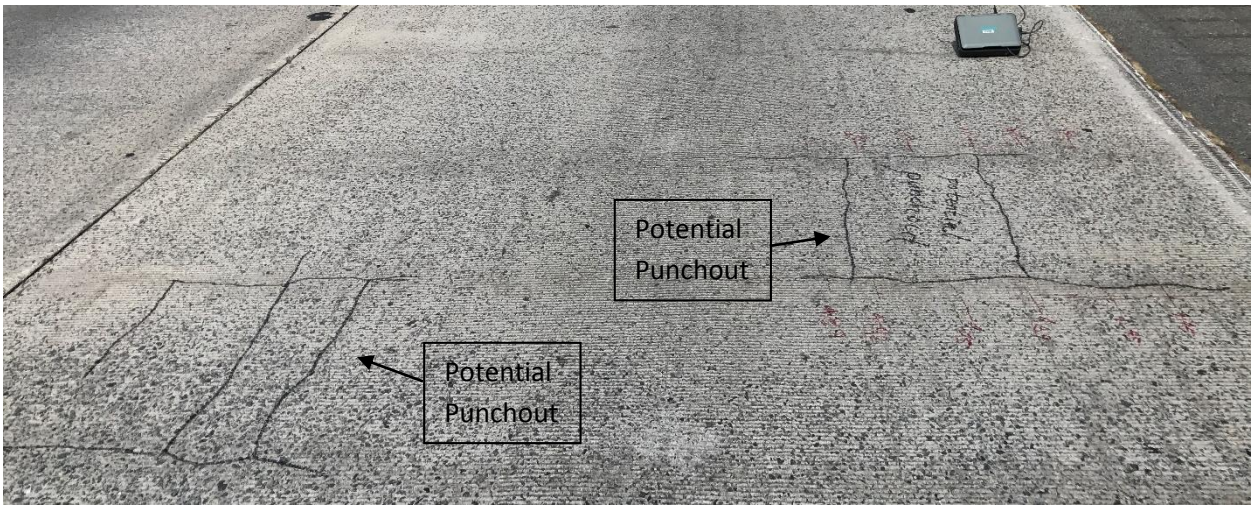


**Figure 6.46 – Potential Punchout Sections at S5-c**

### 6.1.1.2. Data Post-Processing

The GPR unit scans were visualized in RadView software. Figure 6.47 clearly shows the location of six reinforcements and the layer thickness. The depth difference among the top points of reflections of transverse reinforcements indicates a sign of distress on the pavement. Based on findings from the site investigation and, later, post-processing in the software (Figure 6.47), there was no crack on the 4$^{th}$ transverse reinforcement while some transverse cracks appeared on the rest of transverse reinforcements were detected. It means that, the deeper the transverse reinforcements, the more the transverse cracks. Figure 6.48 indicates the depths of longitudinal reinforcements and CRC thickness in the transverse direction. The deeper the transverse reinforcements go, the deeper the longitudinal reinforcements must accompany. The result of this movement causes the transverse cracks on the pavement.

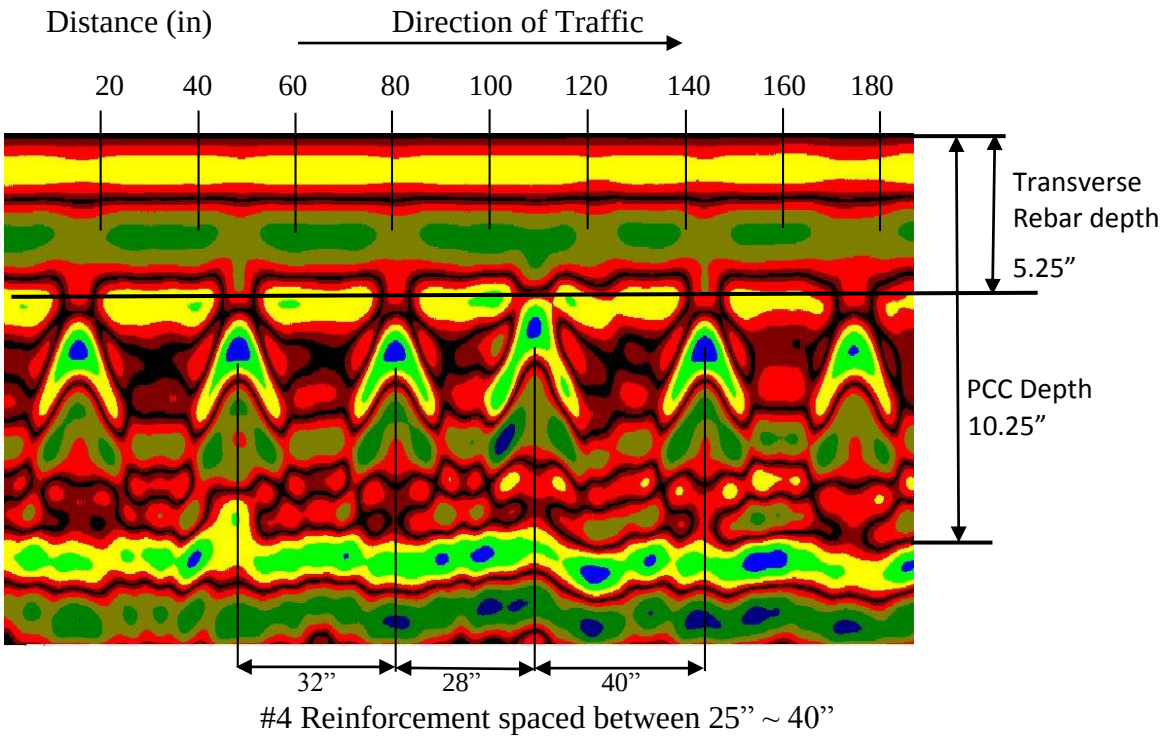


**Figure 6.47 – GPR Scan in the Longitudinal Direction (S5-a)**

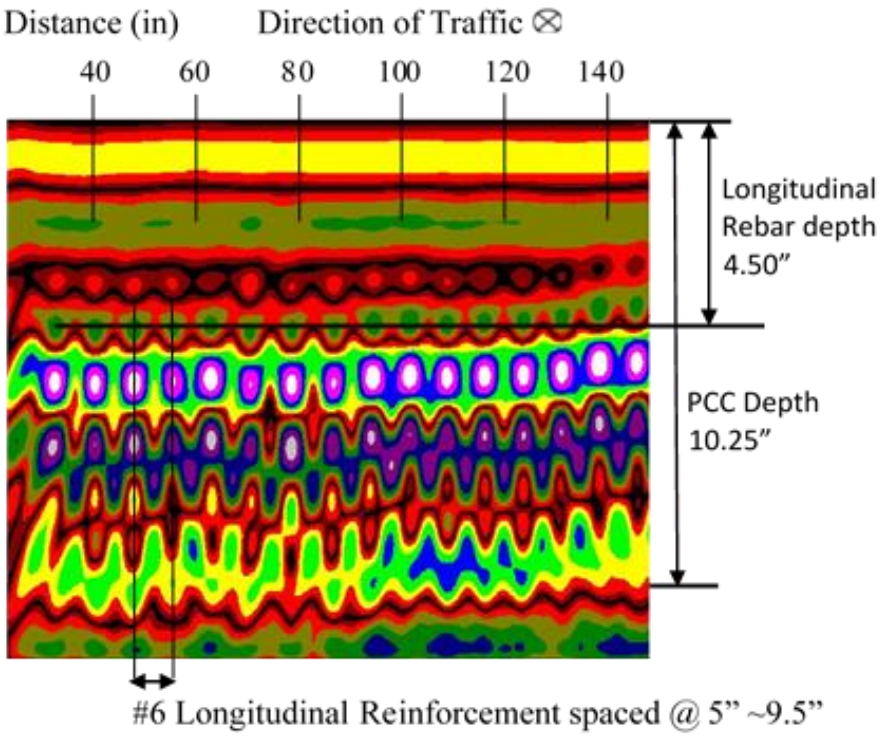


**Figure 6.48 – GPR Scan in the Transverse Direction (S5-d)**

In the selected site, the depth of longitudinal reinforcement is varied throughout the 1-mile (1.61 km) section because of construction processes. The S5-a was determined to be scanned by GPR and Profometer because of the existence of around twenty single transverse cracks in the cluster. In addition, the most of these cracks formed on the transverse reinforcements. The S5-b had a map cracking distress together with transverse cracks and longitudinal cracks over the wheel path. The S5-c was chosen because of the occurrence of potential punchout areas. The section showing many longitudinal cracks and transverse cracks was named as S5-d. It was found that this segment has deeper transverse reinforcements than other segments at around 6.5 in (165 mm) in depth. Likewise, when compared the longitudinal reinforcements in S5-b and S5-d, it was clear to see the change in the cover depth between these segments (Figure 6.49). Therefore, large crack openings with 1 in (25.4 mm) in width were appeared. As seen in Figure 6.50, the concrete cover

depths obtained from over cracked areas were higher than one from non-cracked area (S5-a and S5-d).

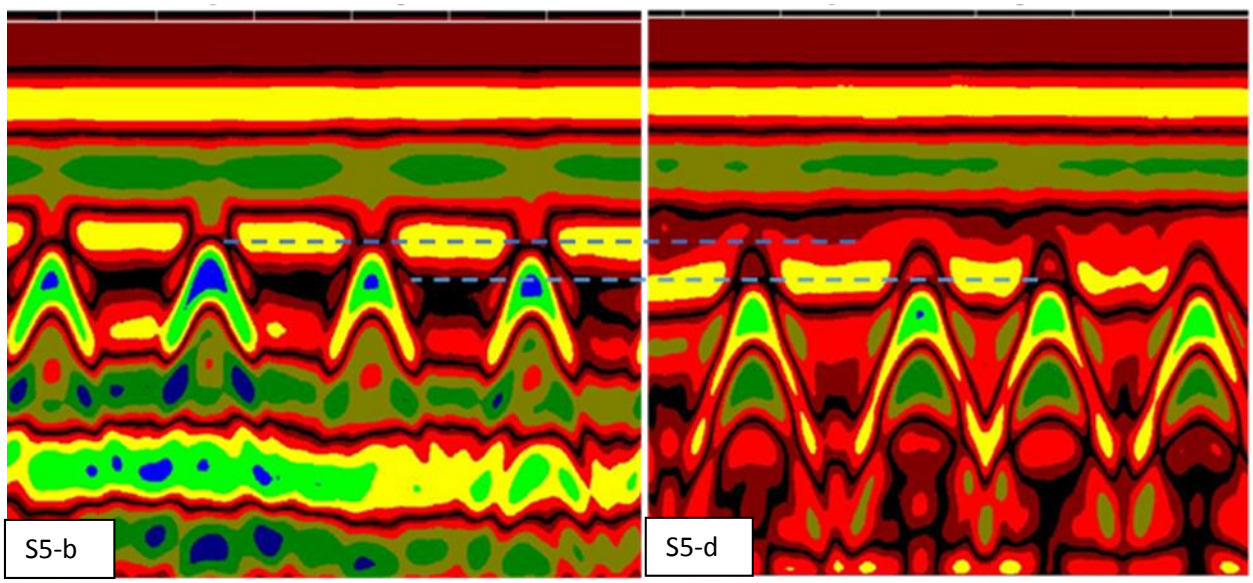


**Figure 6.49 – The Comparison of Transverse Reinforcements in Depth for S5-b and S5-d**

The following graph (Figure 6.51) indicates the depths of longitudinal reinforcements, which were detected from between the single transverse cracks by GPR and Profometer (S5-a). Although the depth values taken by both techniques show the similar pattern in the graph, these values are not matched exactly (Figure 6.51). The Profometer showed that it worked more precisely by finding more variable values. The reason for this is believed to be the result of varied materials, such as metal or other pieces of steel, which can be detected easily by GPR and, particularly, Profometer units, and forms the basis for our error margin.

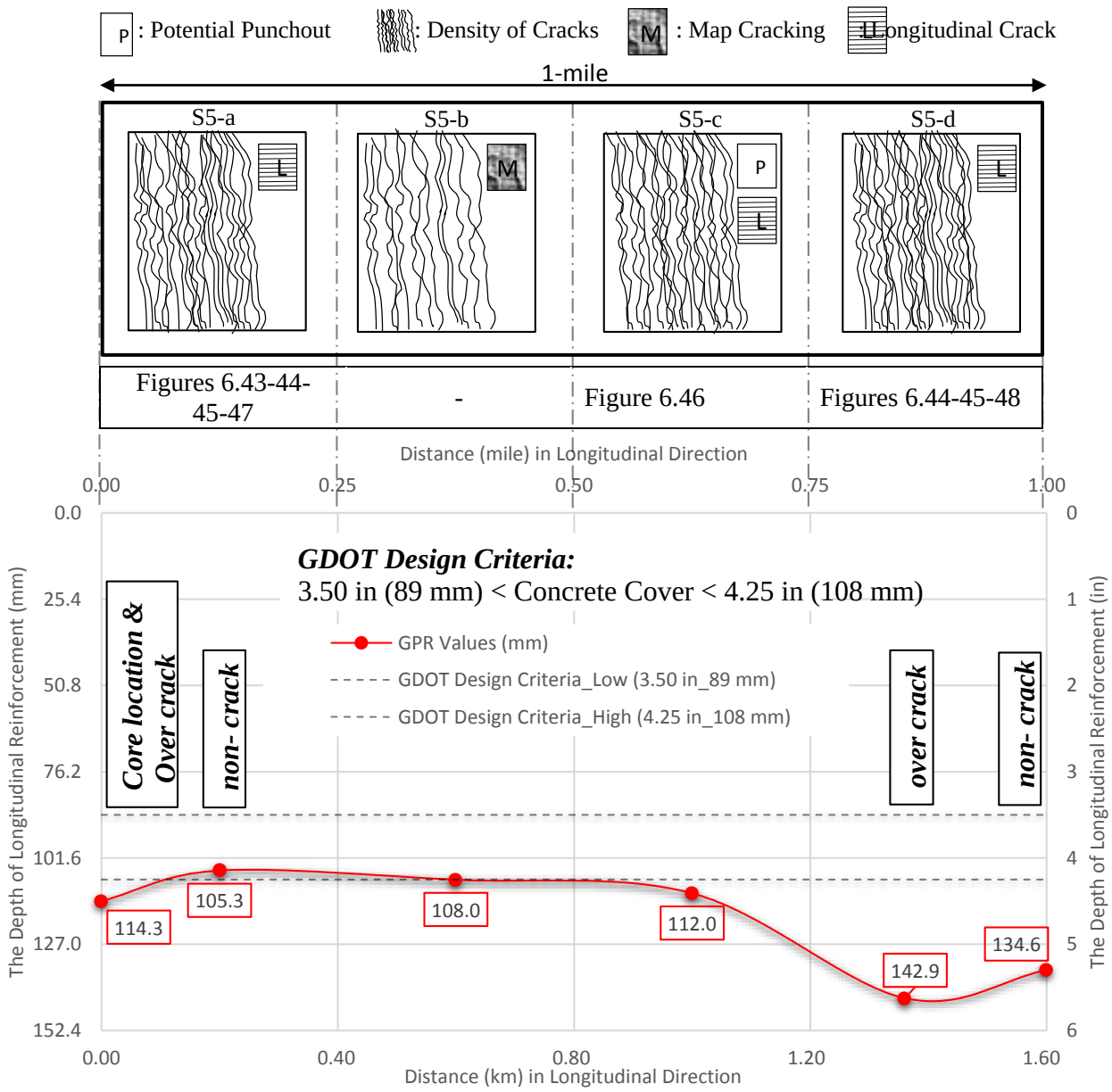


**Figure 6.50 – Stress Pattern and Concrete Cover in Longitudinal Direction in Each Segment Along 1-mile**

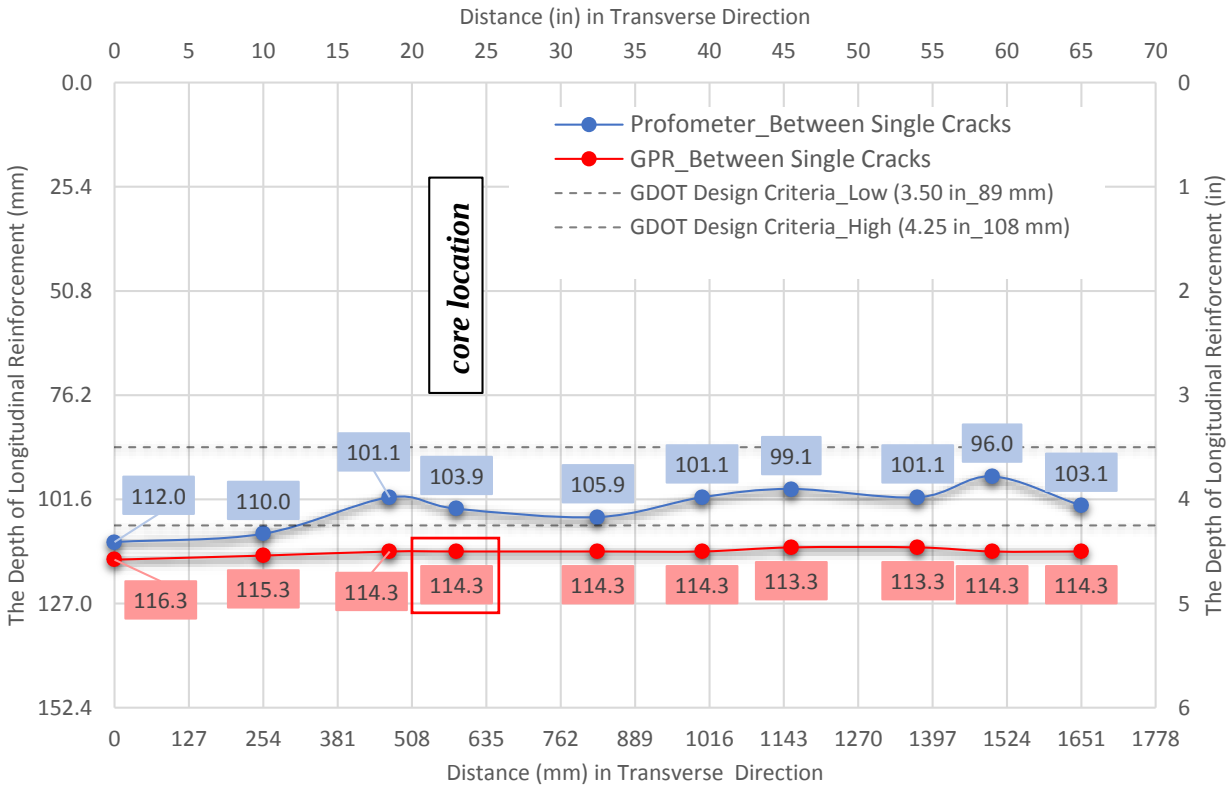


**Figure 6.51 –Concrete Cover Depth Values Detected by calibrated GPR and Profometer in Transverse Direction at S5-a**

### 6.1.2. I-75 Tift County

#### 6.1.2.1. Data Collection

Non-destructive testing methods were carried out on Interstate 75 in Tift County using a Ground Penetration Radar (GPR) and Profometer. The detailed information regarding the working procedures of these units is mentioned in Section 5.1.

The outside lane on North Bound (NB) I-75 located between mileposts 57-58 in Tift County was selected for inclusion in this study. The CRC pavement was reported to be in fair condition, which indicated continuous clusters of transverse cracks. The construction drawings obtained from GeoPI (see I75NBTMP57-58 in Appendix A) indicate that the plans of the section were completed in 2006, and, later, the constructional drawings were revised in 2008. The location of this site is shown in Figure 6.52. The design parameters and distress assessment values are presented in Table 6.6. It was detected that the selected section had no punchout per mile.

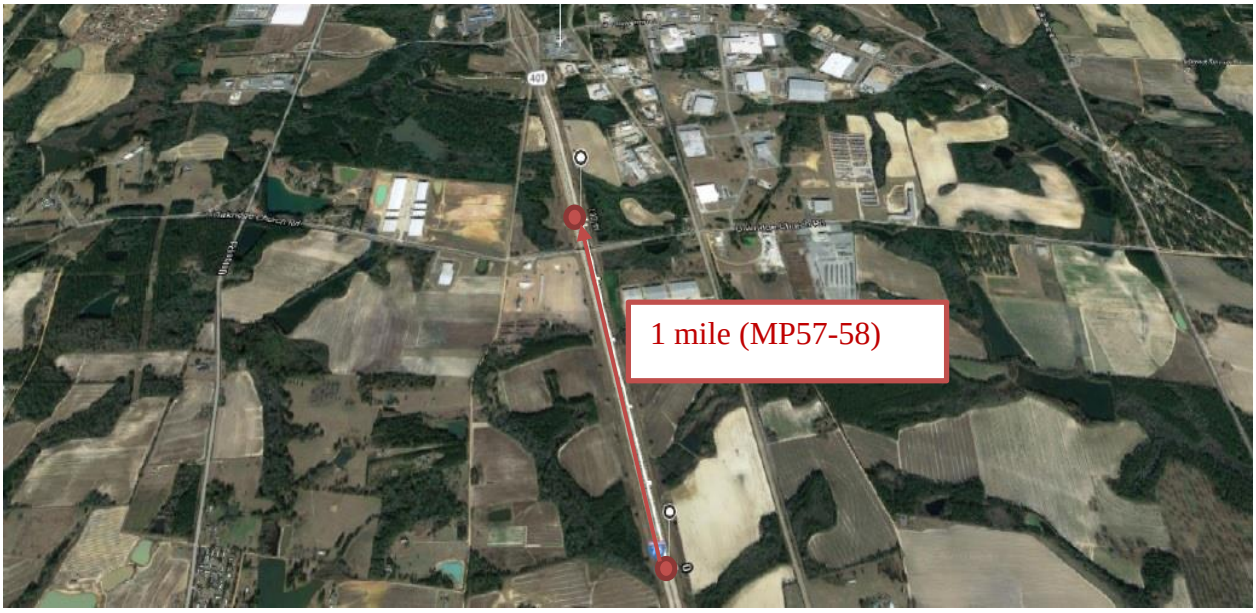


**Figure 6.52 – I-75 MP 57-58 Tift County Site Location (Google Maps, 2017)**

**Table 6.6 - CRC Design Parameters and NDT Results for I75NBTMP57-58**

| | Design Parameters | | | | | | |
|---|---|---|---|---|---|---|---|
| **TIFT COUNTY** | Site Condition | Age (Years) | CRC Thickness (in) | Longitudinal Rebar Size/ Spacing (in) | Transverse Rebar Size/ Spacing (in) | Longitudinal Rebar Depth (in) | Transverse Rebar Depth (in) |
| | Fair | 9 (2008) | 12” | #6 / 5” | #4 / 36” ~ 40” (typical 36”) | 3.75” | 4.50” |
| | **Distress Assessment** | | | | | | |
| | Spacing between single transverse cracks (ft.) | | Spacing between clusters of transverse cracks (ft.) | | Transverse crack width (in) | Longitudinal crack width (in) | Number of Punchouts / mile |
| | 1’~ 3’ (typical 1’) | | 6’ ~ 12’ (typical 6’) | | 0.01” ~ 0.08” (typical 0.06”) | 0.06” | 0 |

The transverse cracks’ pattern on the investigated lane is shown in Figure 6.53. The section was constructed as a 12 in (305 mm) CRC slab above a 0.75 in (19 mm) asphaltic concrete superpave, 12 in (305 mm) of graded aggregate base. The longitudinal and transverse reinforcements consisted of #6 and #4 rebars, respectively. The concrete cover depth to the top of the longitudinal reinforcement was measured to be 3.75 in (95 mm) from the core specimen. The site was investigated in four stages in terms of density of crack types and existence of other distress types. The stages were named as S6-a, S6-b, S6-c, S6-d. They refer the first (a), second (b), third (c), and forth (d) subsite (S) segments of Tift County which was the 6$^{th}$ site investigated.

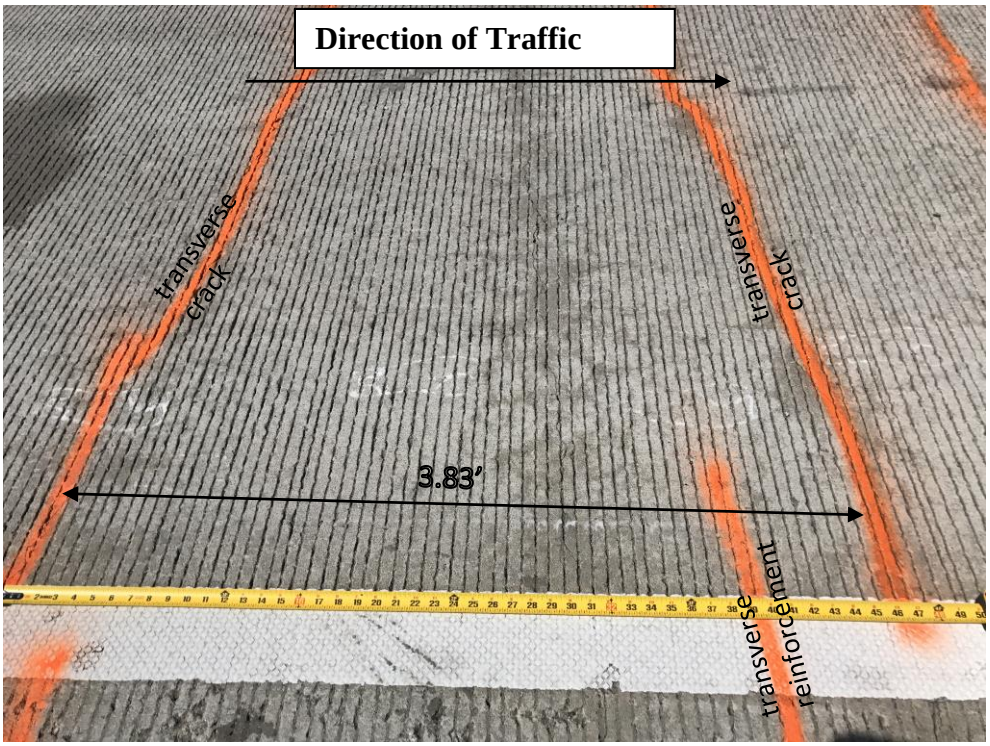


**Figure 6.53 - Typical Single Transverse Crack Pattern (S6-a)**

The site indicated the same pattern along a one-mile (1.61 km) stretch, which were continuous clusters of transverse cracks at regular intervals (Figure 6.54). Transverse reinforcements and cracks were marked as 'TC' and 'T' in the clusters, which meant 'crack on transverse reinforcement' and 'transverse reinforcement,' respectively (Figure 6.54). The distance between the clusters of transverse cracks changed from 6 ft. (183 cm) to 12 ft. (366 cm). The single transverse cracks were spaced at the range of approximately 1.25 ft. and 3 ft. (38 and 92 cm) (Figure 6.53). The typical transverse crack width varied in the range of 0.01 in and 0.08 in (0.25 and 2.03 mm) while the typical longitudinal crack width was approximately 0.006 in (0.15 mm) (Figure 6.55). It was detected that the site had signs of potential punchouts at the location of the cluster of transverse cracks in S6-c.

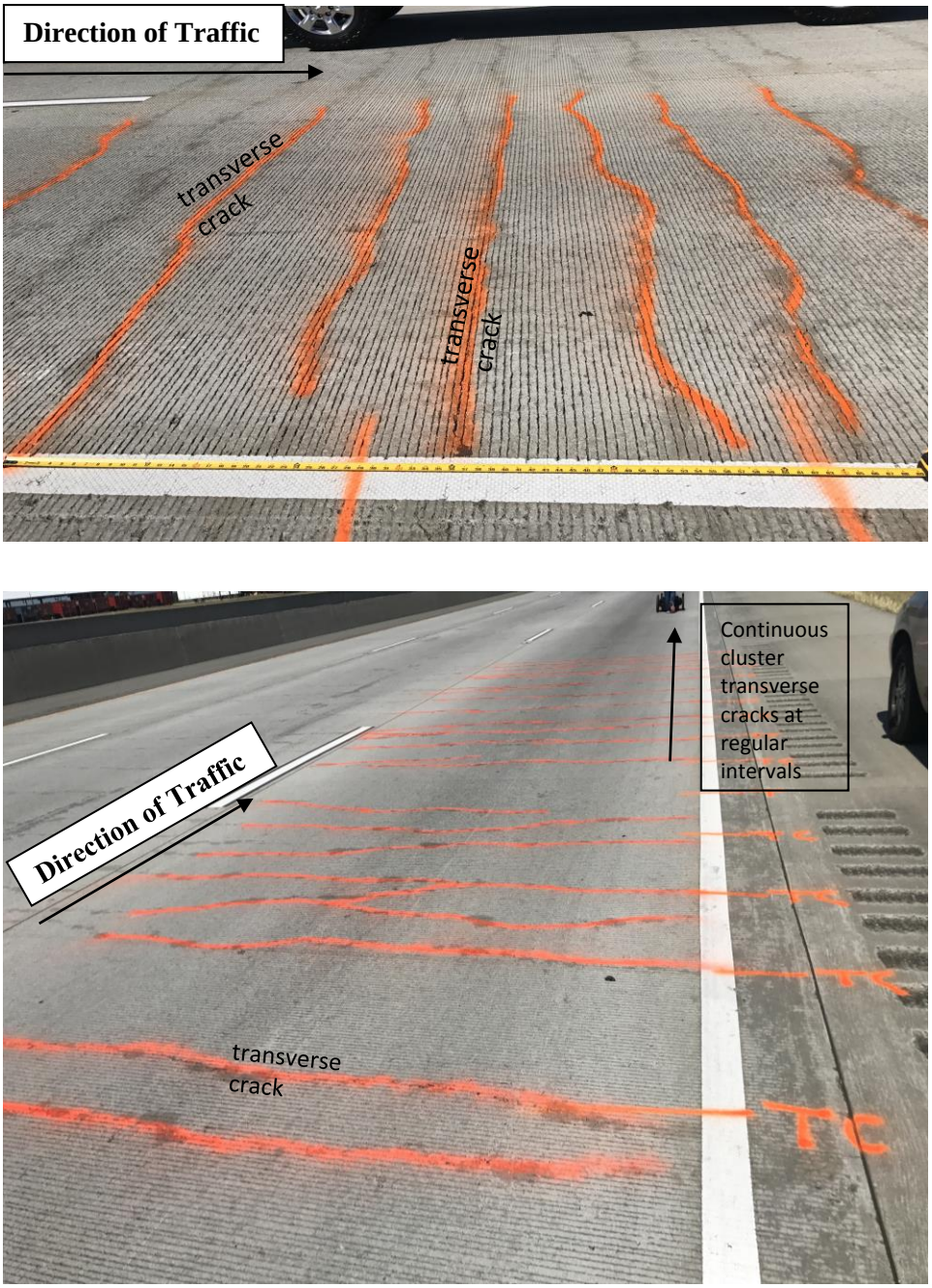


**Figure 6.54 – Typical Cluster Transverse Cracks Pattern at S6-a and S6-c**

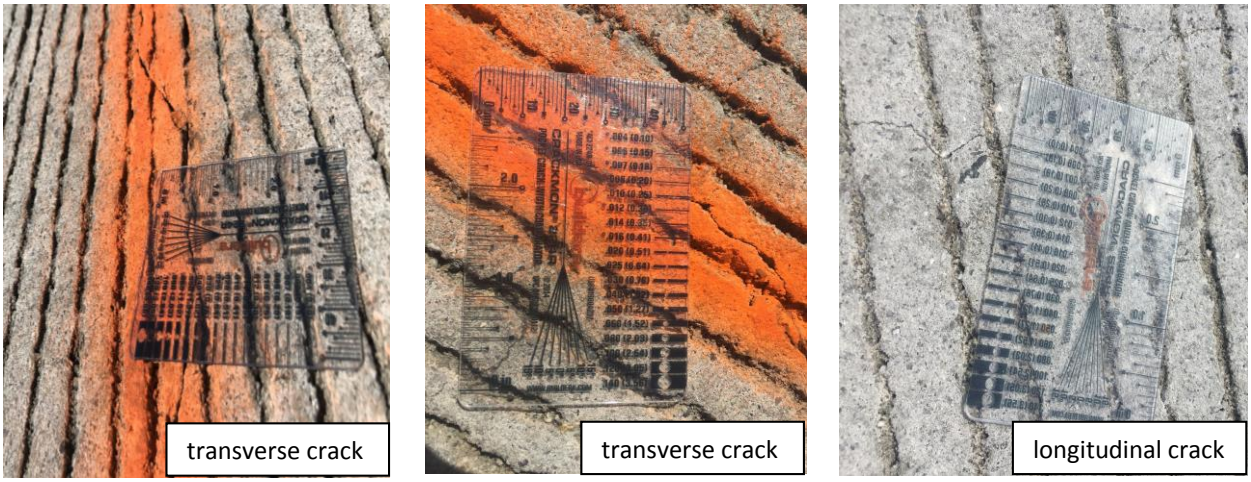


**Figure 6.55 – The Measurement of Typical Crack Widths at S6-a and S6-b**

It is predicted that the S6-c will form a punchout in the near future because of the existence of high severity longitudinal cracks between transverse cracks (Figure 6.56).

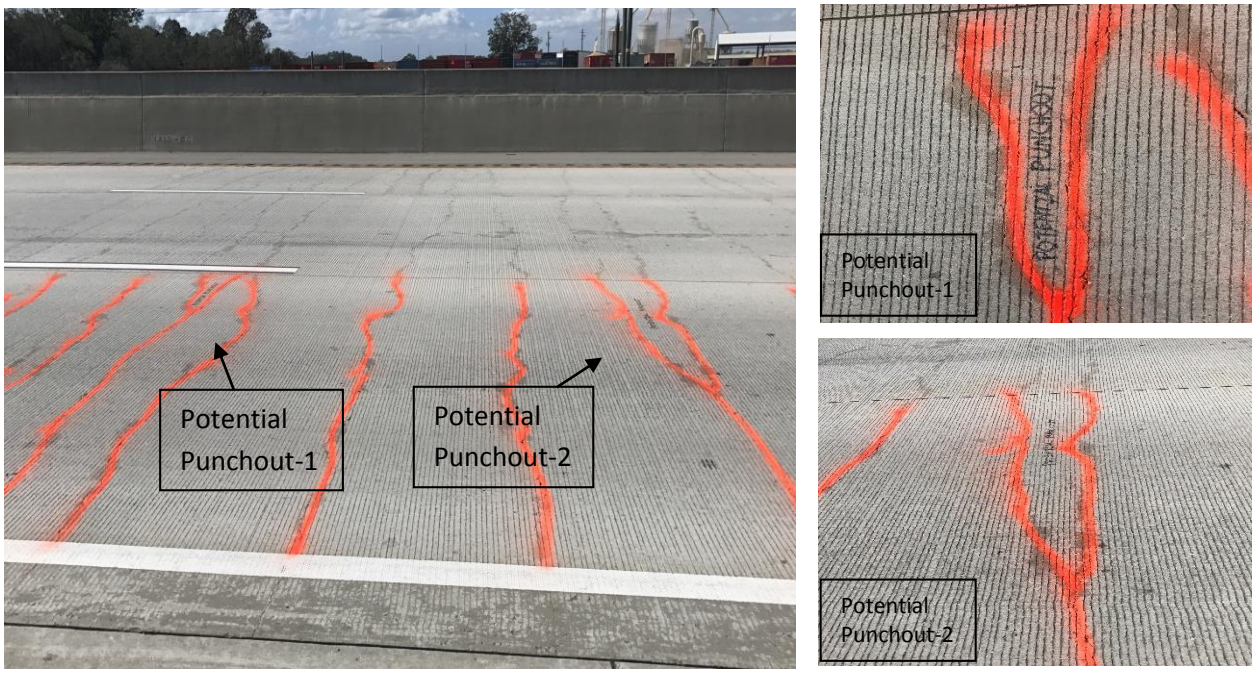


**Figure 6.56 – Potential Punchout Sections at S6-c**

### 6.1.2.2. Data Post-Processing

The GPR unit scans were visualized in RadView software. Figure 6.57 clearly shows the location of six reinforcements and concrete layer thickness. The depth difference among the top points of reflections of transverse reinforcements indicated a sign of distress formed at the pavement surface. Based on findings obtained from the site investigation and the GPR scan image, there was no crack on the 4$^{th}$, 5$^{th}$, and 6$^{th}$ transverse reinforcements while some transverse cracks appeared on the rest of transverse reinforcements. As it is shown in the GPR scan (Figure 6.57), the lower the transverse reinforcements within the pavement section, the lower the longitudinal reinforcements must accompany. Therefore, more transverse cracks appear on the surface. Figure 6.58 indicates the depths of longitudinal reinforcements and CRC thickness in the transverse direction.

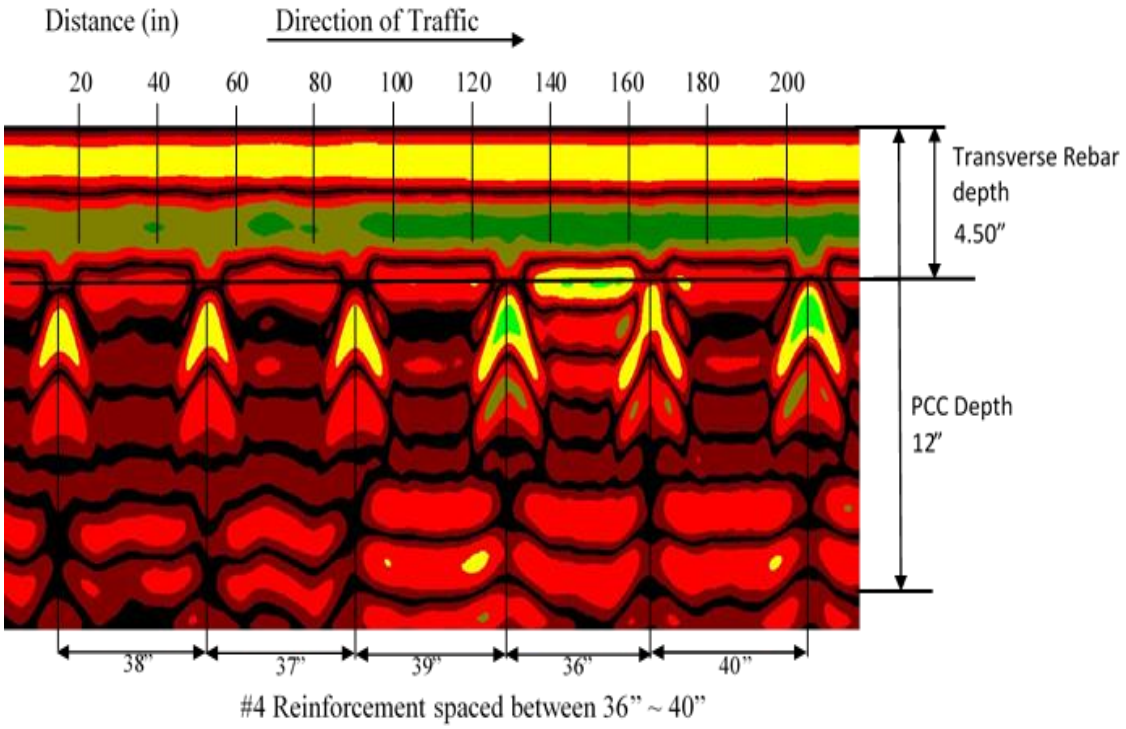


**Figure 6.57 – GPR Scan in the Longitudinal Direction (S6-a)**

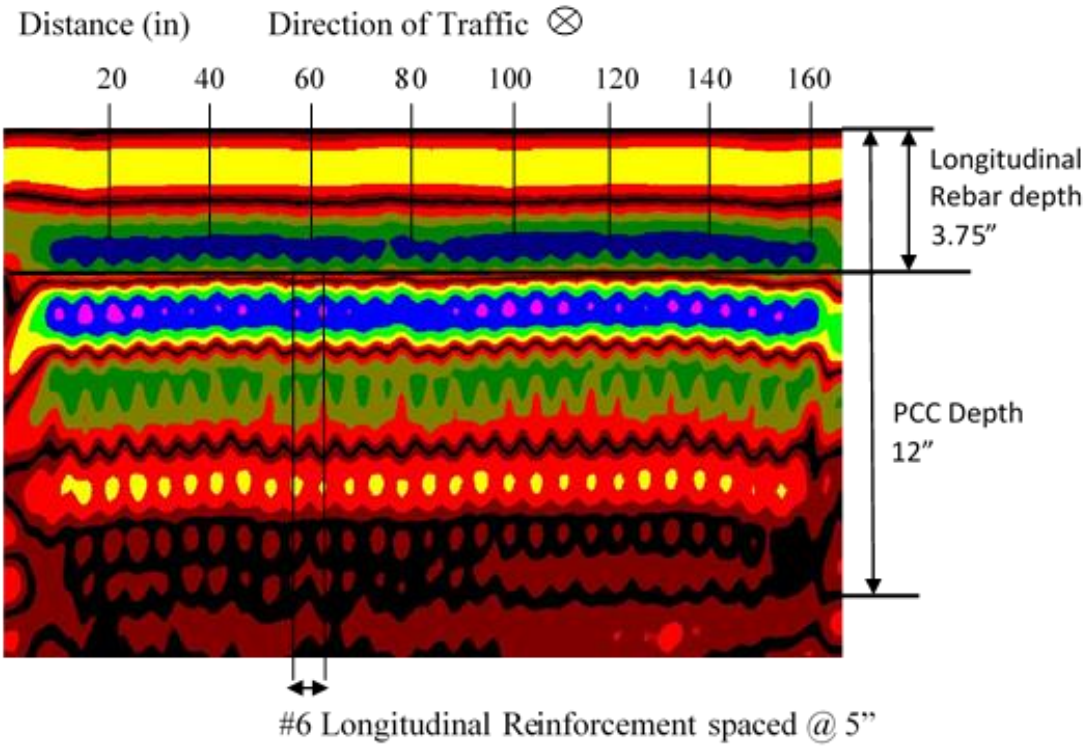


**Figure 6.58 – GPR Scan in the Transverse Direction (S6-a)**

In the selected site, the depth of longitudinal reinforcement varied throughout the 1-mile (1.61 km) section because of construction processes. The S6-a was determined to be scanned by GPR and Profometer because of the existence of approximately twenty single transverse cracks in the cluster with presence of longitudinal cracks. In addition, most of these cracks formed over the transverse reinforcements. The S6-b had cluster transverse cracks and fewer longitudinal cracks over the wheel path which was close to the shoulder. The S6-c was chosen because of the occurrence of potential punchout areas. It was determined that the S6-a and S6-c sections have deeper longitudinal reinforcements than other segments at approximately 3.75 in (95 mm) in depth (Figure 6.59). Finally, the section with the joint connection was named as S6-d.

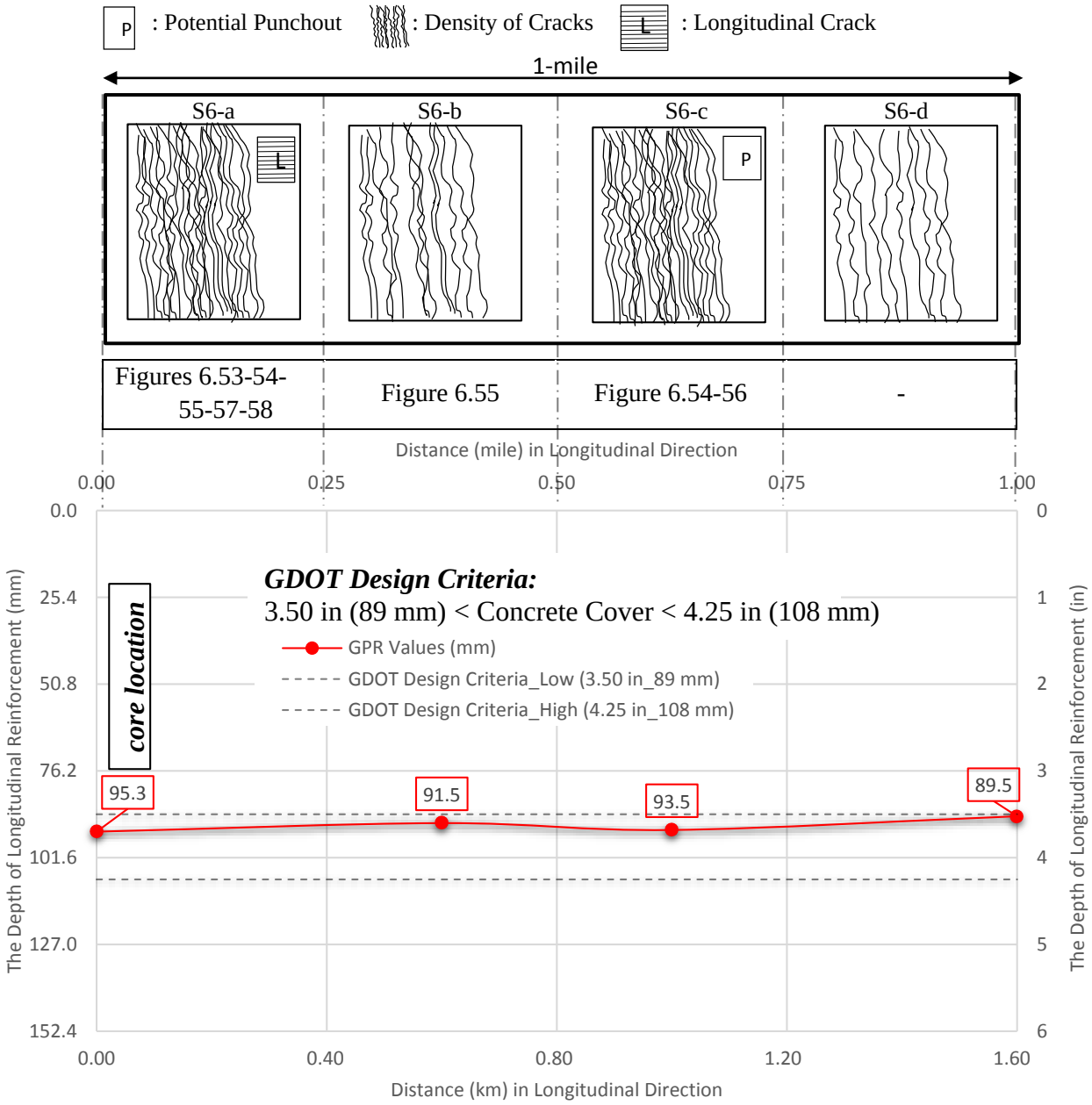


**Figure 6.59 – Stress Pattern and Concrete Cover in Longitudinal Direction in Each Segment Along 1-mile**

The following graph (Figure 6.60) indicates the depths of longitudinal reinforcements, which were detected from over a single transverse crack by GPR and Profometer (S6-a). Although the depth values taken by both techniques show similar patterns in the graph, these values are not matched exactly (Figure 6.60). The reason for this is believed to be the result of varied materials, such as metal or other pieces of steel, which can be detected easily by GPR and Profometer units, and forms the basis for this error.

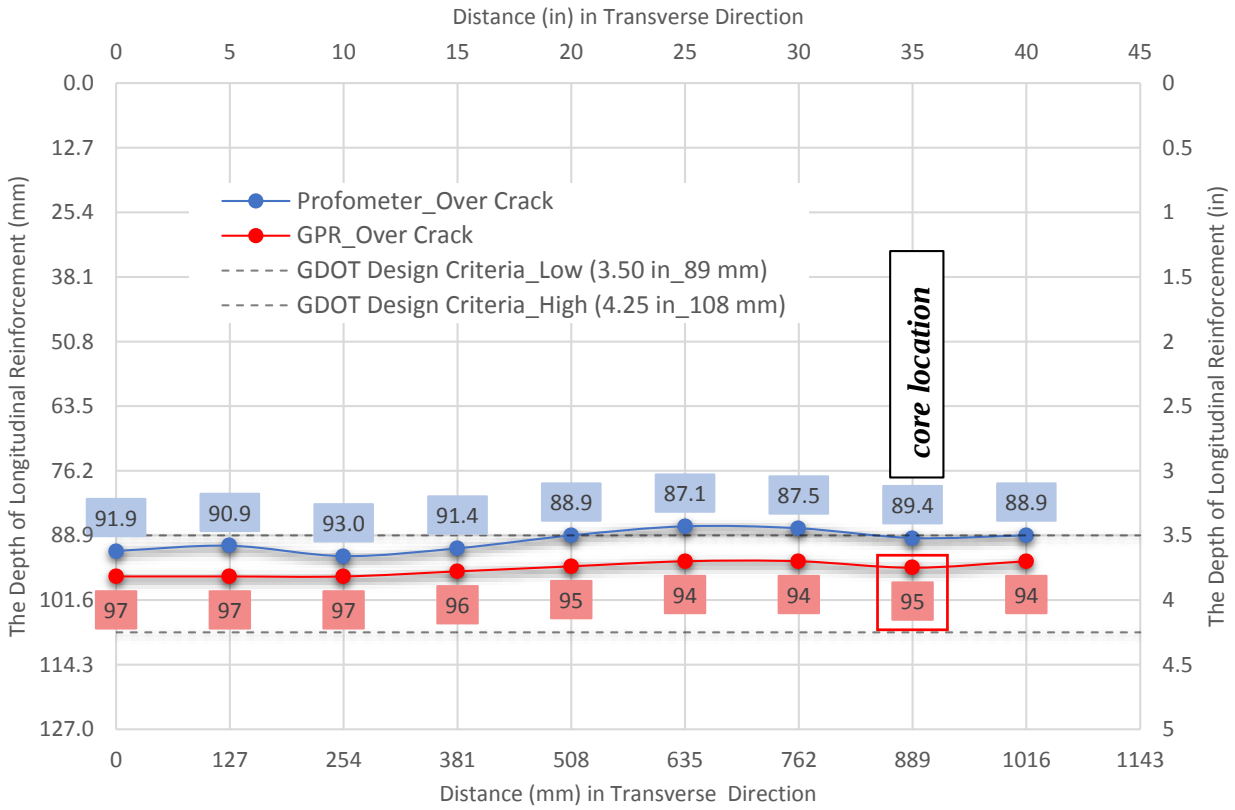


**Figure 6.60 –Concrete Cover Depth Values Detected by calibrated GPR and Profometer in Transverse Direction at S6-a**

## 6.4. The Comparison of Results Obtained from All Site Investigations

### 6.4.1. Evaluation of the Accuracy of Profometer

To confirm the accuracy of the eddy current technique, Profometer, for detecting the rebar cover depth, the results found from this instrument were compared with the cover depths measured directly from cores extracted from six test sections. Table 6.7 presents the actual concrete cover and the depth estimated by Profometer together with the percentage of error in detection.

**Table 6.7 – The Accuracy of Profometer**

| | Site Names | Core Cover Depth, in (mm) | Profometer Cover Depth, in (mm) | Difference Depth Values between both technique, in (mm) | Error in detection (%) |
|---|---|---|---|---|---|
| Site 1 | SR6NBCMP0-1 | 3.5 (88.9) | 3.46 (87.88) | 0.04 (1.02) | 1.1 |
| Site 2 | I20EBHMP4-5 | 4.25 (107.95) | 3.58 (90.93) | 0.67 (17.02) | 15.8 |
| Site 3 | I20WBCMP24-25 | 4 (101.6) | 4.02 (102.11) | -0.02 (-0.51) | -0.5 |
| Site 4 | I20EBNMP92-93 | 4 (101.6) | 4.22 (107.19) | -0.22 (-5.59) | -5.5 |
| Site 5 | I75NBCMP267-268 | 4.5 (114.3) | 4.09 (103.89) | 0.41 (10.41) | 9.1 |
| Site 6 | I75NBTMP57-58 | 3.7 (93.98) | 3.52 (89.41) | 0.18 (4.57) | 4.9 |

In addition, Table 6.7 includes the difference in depth values between the actual cover depths measured on the core specimens and the estimated cover depth from Profometer. Although the Profometer mostly indicated less values of cover depths than the measured cover depths from the core specimens, it sometimes estimated the higher concrete cover than the measured one. Based on the difference of the measured and estimated concrete covers, the percentage error in detection was calculated.

The manufacturer recommends that the cover measuring accuracy might vary from ±0.04 in to ±0.16 in (1 to 4 mm). Based on the results, the 15.8% and 9.1% errors in detection of the concrete cover for Site 2 and 5, respectively, were high. This error may be a result of Site 2 and 5 having the deepest concrete covers with 4.25 in (107.95 mm) and 4.5 in (114.3 mm). However, Site 3 and 4 had the same concrete cover depth, the Profometer indicated the different errors in detection (-0.5% and -5.5%), which might be in the acceptable range. Based on these results, it is clear that even though there was no a linear relationship between an increase in depth and the percentage of error, the accuracy of Profometer decreases as the depth of concrete cover increases. The manufacturer's manual and many studies supported this result with their research.

### 6.4.2. Correlation between Distresses and the Normalized Cover Depth and CRC Thickness

The relationship between the concrete cover depth ($C_c$) and pavement thickness (D) might affect the formation of distresses on the pavement. Therefore, this relationship was evaluated by comparing the six sites having different concrete layer thicknesses and cover depths (Table 6.8). Based on the correlation between cover depth and concrete layer thickness, as the thickness decreases and the cover depth increases, the pavement has more distresses such as cluster cracking and punchouts.

**Table 6.8 – The Normalized Concrete Cover Depth / Concrete Thickness**

| | Site Names | Core Cover Depth, in (mm) | Concrete Pavement Thickness, in (mm) | Normalized $1 - C_c / D$ |
|---|---|---|---|---|
| Site 1 | SR6NBCMP0-1 | 3.5 (88.9) | 12 (305) | 0.71 |
| Site 2 | I20EBHMP4-5 | 4.25 (107.95) | 12 (305) | 0.65 |
| Site 3 | I20WBCMP24-25 | 4 (101.6) | 8.7 (221) | 0.54 |
| Site 4 | I20EBNMP92-93 | 4 (101.6) | 12 (305) | 0.67 |
| Site 5 | I75NBCMP267-268 | 4.5 (114.3) | 10.25 (260.35) | 0.56 |
| Site 6 | I75NBTMP57-58 | 3.7 (93.98) | 12 (305) | 0.69 |

The concrete cover depths recommended by GDOT is in the range of 3.5 in (89 mm) and 4.25 in (108 mm) and the concrete thickness is 11 in (279 mm) or 12 in (305 mm). These are the factors affecting the density and severity of distresses (Figure 6.61).

**Figure 6.61 – The Density of Transverse Cracks in Sites 1, 3, and 5, respectively**

Based on the literature review, the Mechanistic-Empirical Pavement Design Guide (MEPDG) recommends the ideal range of the mean crack spacing is between 3 ft. (91 cm) and 6 ft. (183 cm). A range of 3.5 ft. (107 cm) to 8 ft. (244cm) is recommended by the 1993 AASHTO

CRCP design guide. The Site 1, Site 3, Site 4, and Site 6 had similar transverse cracks' spacing, typically with 1 ft. (25.4 cm). The transverse crack spacings of Site 2 and Site 5 were typically 1.63 ft. (50 cm) and 3.25 ft. (99 cm), respectively. Therefore, according to MEPDG, the transverse crack spacings of the investigated sites were out of the recommended range, except for Site 5. In addition, based on AASHTO design guide, all pavement sections evaluated in this study were out of the acceptable range. Thus, if the spacing of transverse rebar is less than 3.5 ft. (107 cm), the probability of punchout formation increases. The potential for punchouts was observed in Sites 5 and 6.

Figure 6.62 indicates the relation of normalized ratios (1-Cc/D) between six sites. As presented in this graph, the sites having the low value of the normalized ratio showed the poor performance when compared to each other relatively. This study demonstrates the importantace of placing the longituindal steel reinforcement at the top-third of the concrete thickness. If this is performend, the concrete pavement might have better performance than concrete having the steel placement at the mid-depth of concrete thickness.

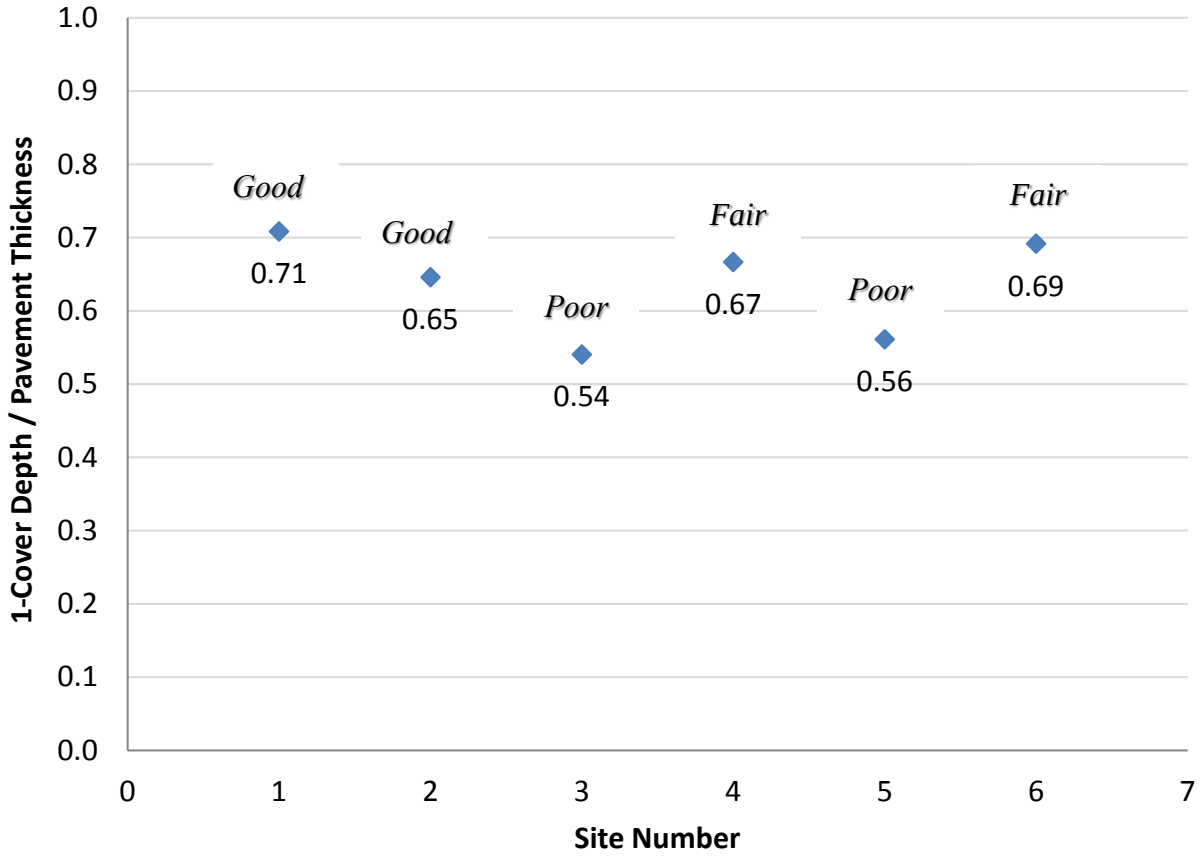


**Figure 6.62 – The Relation between the Normalized Ratio (1 - Cc /D) and Sites**

Figure 6.63 indicates the relationship between crack width of transverse cracks (CW) and the normalized ratios (1-Cc/D). As the steel is placed at or around the mid-depth of concrete thickness, the concrete pavement produces wider transverse cracks. The sites in poor conditions indicated wider transverse cracks with 0.10 in (2.54 mm) and 0.15 in (3.81 mm), as seen in Figure 6.63.

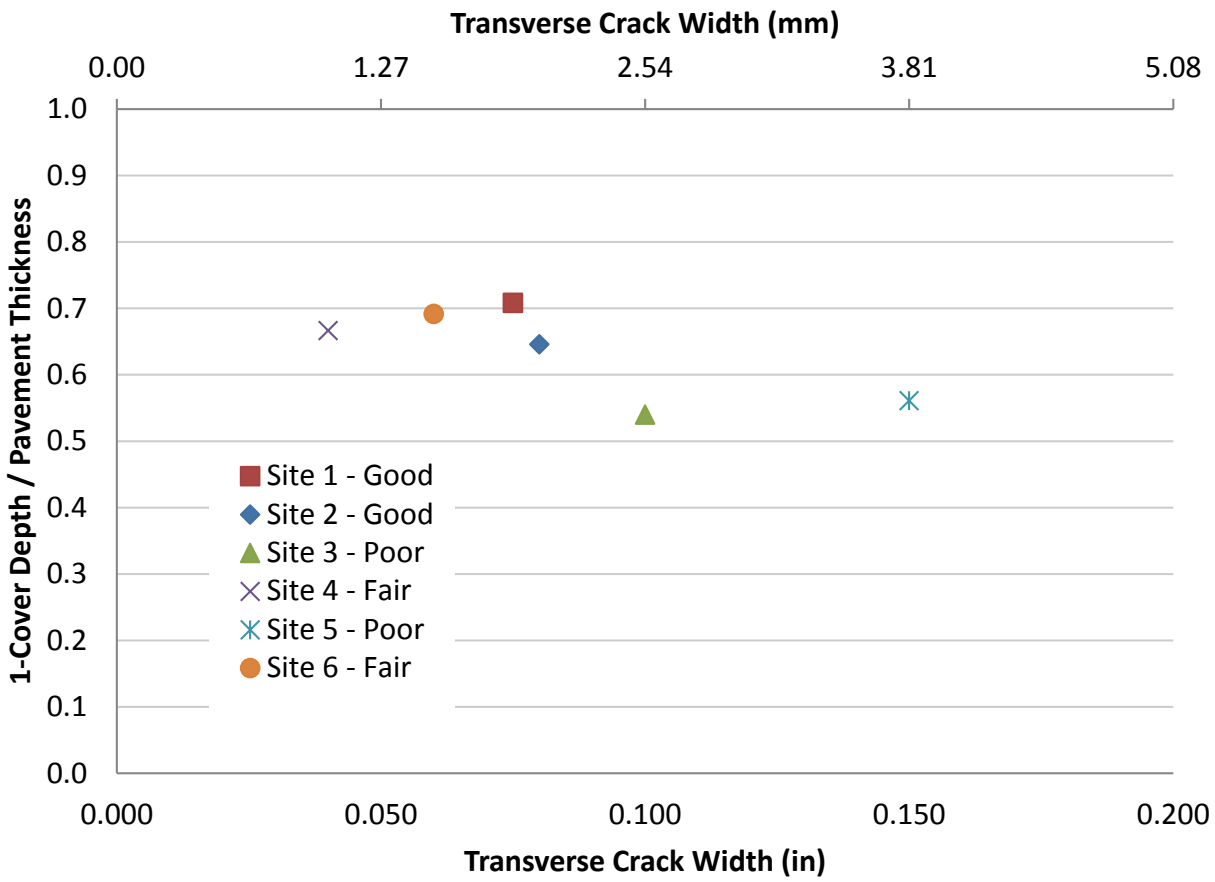


**Figure 6.63 – The Relation between the Normalized Ratio (1 - Cc /D) and Transverse Crack Width**

If the concrete cover depth and concrete thickness were not in the recommended range, the transverse crack width might be wider. The Site 5 in Figure 6.64 had the highest value of concrete cover with 4.5 in (114 mm) and its concrete thickness was 10.25 in (260 mm), which is not a recommended thickness. At this site, the average width of transverse cracks typically was 0.15 in (3.81 mm) even though it locally had a few cracks with 0.5 in (12.7 mm) in maximum width. The reason for this is that as the steel is placed lower within the pavement depth, the cracks will not be held tight by steel reinforcement. Thus, the reinforcements will not be close to the surface and wider transverse cracks will be formed on the pavement surface. Thus, the data

recorded in this study verified the hypothesis which was that wider cracks result from deeper reinforcement.

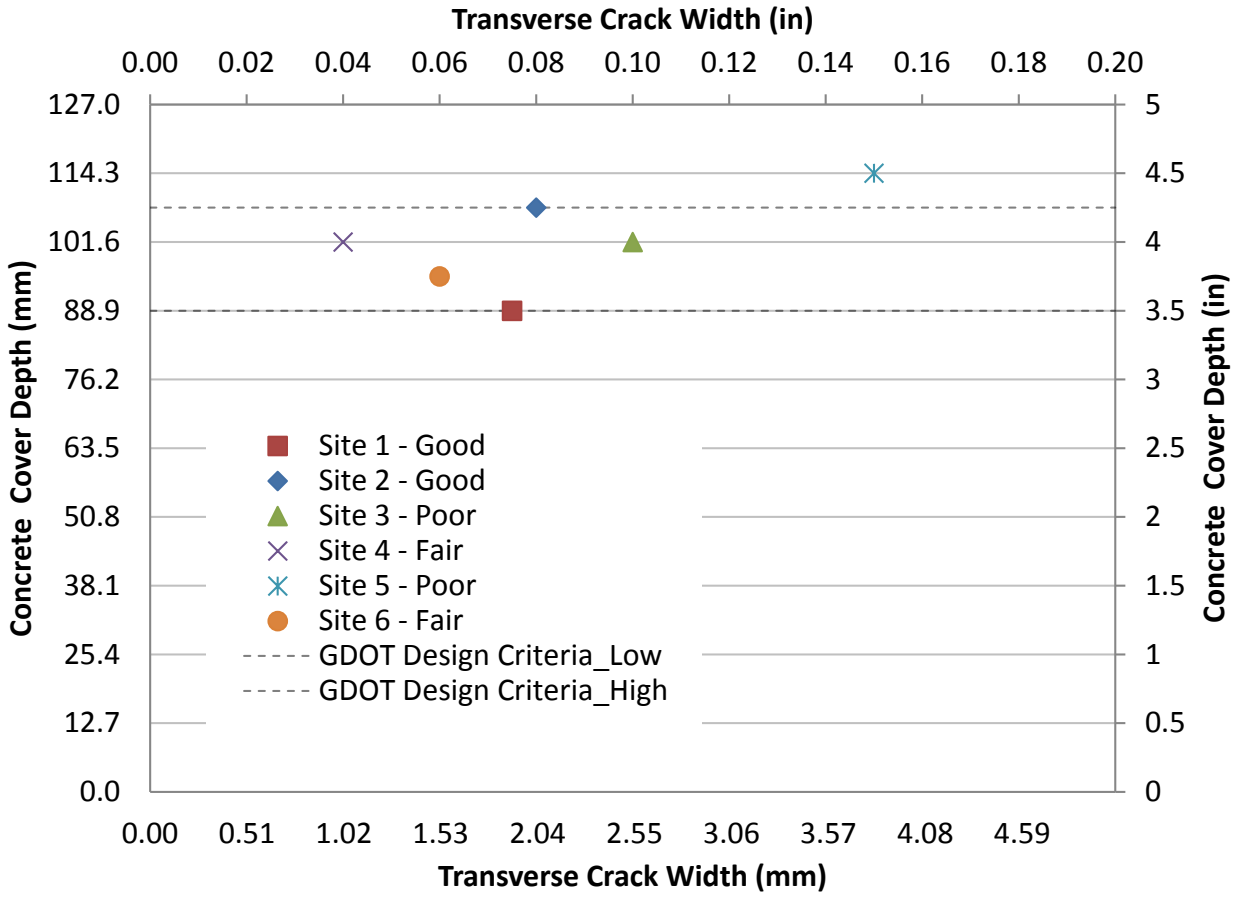


**Figure 6.64 – The Relation between the Concrete Cover Depth and Transverse Crack Width**

In this research, each site was evaluated into four divided segments. Most of each segment had clusters of transverse cracks. Based on the clusters of transverse cracks and crack spacings, how many transverse cracks were formed in 100 ft. (3048 cm) section were detected. According to the results, the sites in fair condition had a significant number of transverse cracks within a 100 ft. (3048 cm) section (Figure 6.65). However, it was expected that the sites in poor condition would have more cracks and distresses. Therefore, it was understood that both the transverse cracks and the longitudinal cracks must be evaluated together to be able to assess truly the condition of fields as relatively to each other.

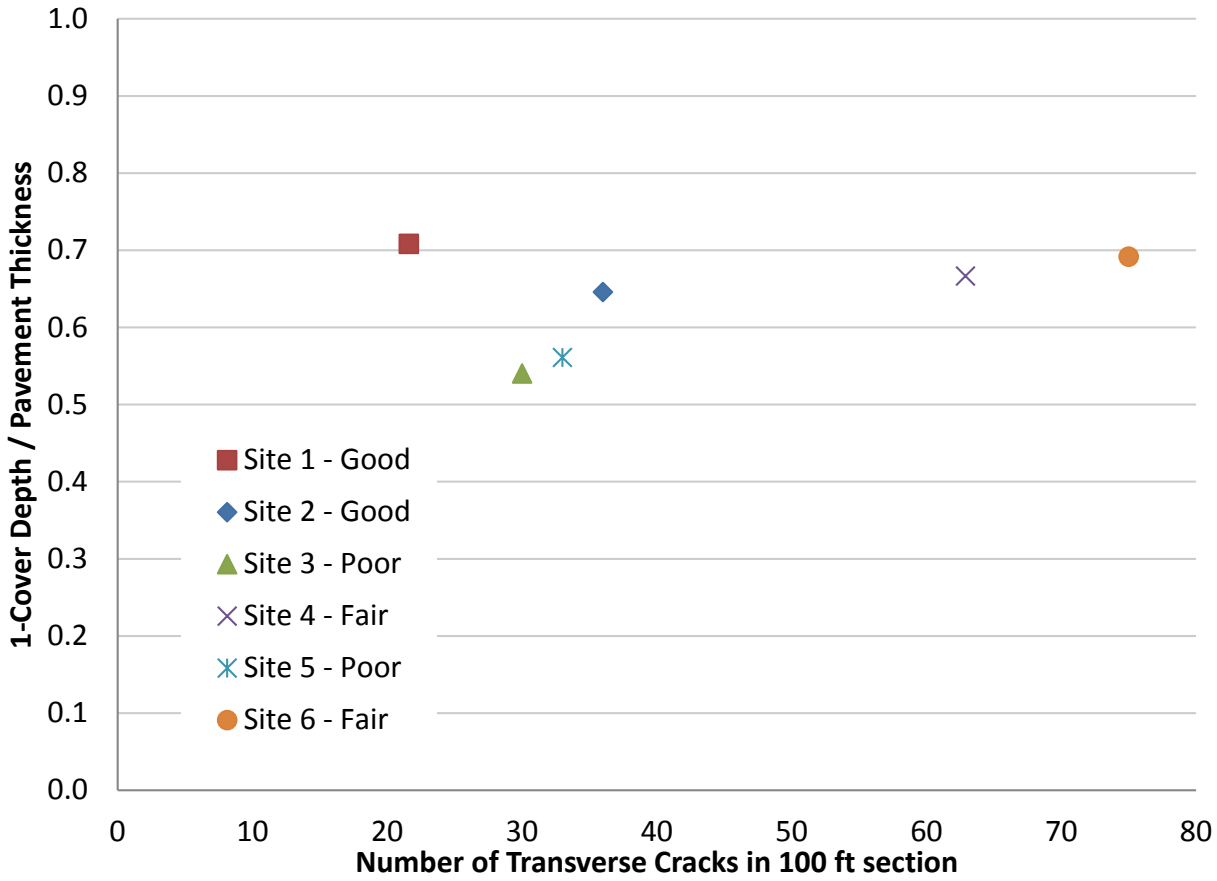


**Figure 6.65 – The Relation between the Normalized Ratio and Number of Transverse Cracks in 100 ft. Section**

Although there were no visible longitudinal cracks in the Site 1,2, and 3 (except for the cracks causing punchouts in Site 3), Site 4,5, and 6 had visible longitudinal cracks with 0.045 in (1.14 mm), 0.05 in (1.27 mm), and 0.06 in (1.52 mm) in typical width. Based on the observations in the fields, some of these cracks leaded to form potential punchouts. To evaluate both transverse and longitudinal cracks together, a distress factor was created by considering the number of transverse cracks in 100 ft. section and the total length of longitudinal cracks in 100 ft. section. The total length of longitudinal cracks was measured by taking in account of a cluster of transverse cracks in a site. This total length included the continued and discontinued longitudinal cracks in a cluster. The total length might be more than 100 ft. (3048 cm) if a cluster

has significantly large number of longitudinal cracks. Ultimately, a distress factor was formed by proportioning the number of transverse cracks to total length of longitudinal cracks in 100 ft. (3048 cm) section. Figure 6.66 indicates the comparison of the normalized ratio of the sites in terms of their distress factors. Based on the results, the distress factor is a good indicator showing the pavement performance relatively. For instance, the Site 3 and Site 5, in poor conditions, had more distress factor with 3.33 and 3.23, respectively, although the Site 1 and Site 2, in good conditions, had the less distress factor value with 0.05 and 0.03, respectively.

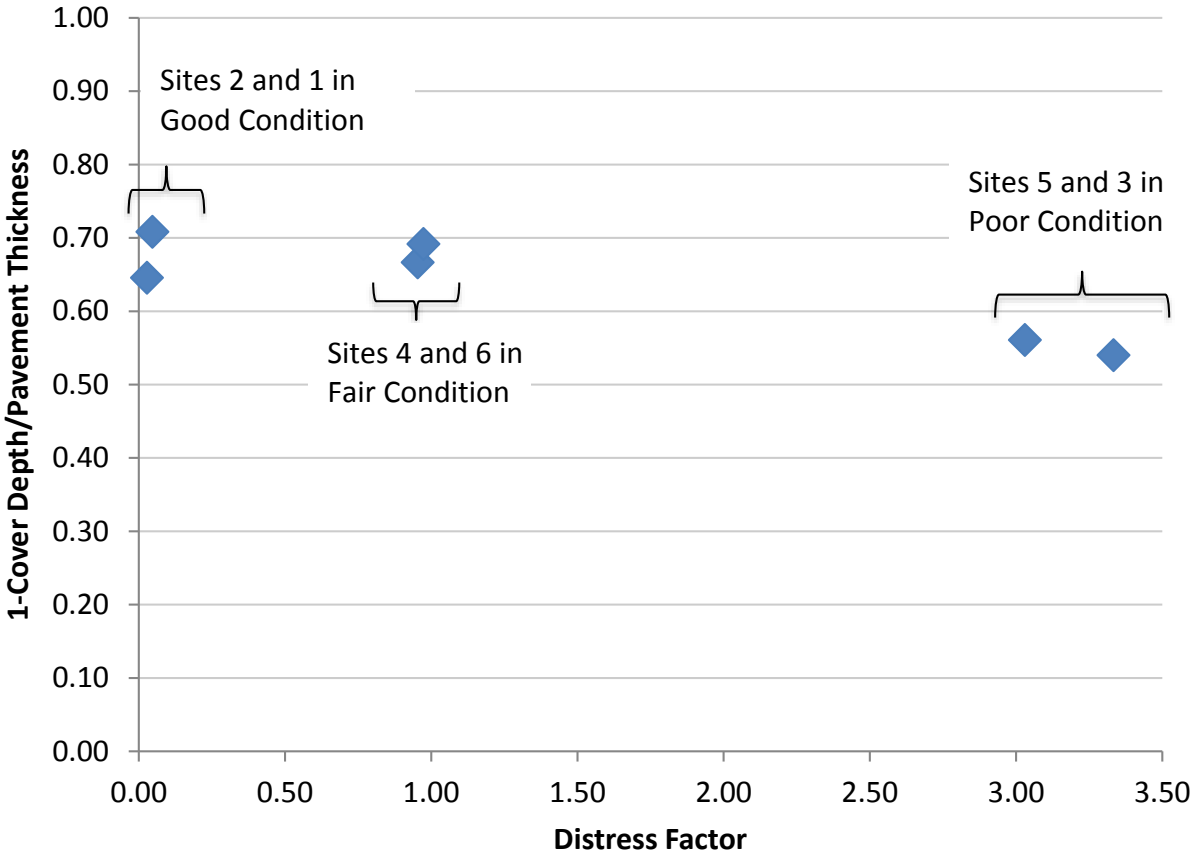


**Figure 6.66 – The Comparison of the Normalized Ratio and Distress Factors**

When considering the results obtained from the six sites, a question arises: why are the sites labeled as "in good, fair, and poor conditions" and how are they evaluated basically? In response to this question, many factors can be counted such as number of transverse cracks, total

length of longitudinal cracks, transverse crack widths, and, especially traffic loads. In this project, the evaluation began first by considering the normalized ratio of the sites. As seen in Table 6.9, the sites having close normalized ratio values were compared. It was shown, even if the design parameters are the same/similar, the pavement performance was different depending on the distress factor. Moreover, it was detected that there is a relationship between the distress factor and the Average Annual Daily Traffic (AADT). In other words, the most important causing factor for the evaluation of the site conditions as good, fair, and poor was the density of distresses and punchouts on the pavement in the sites, caused by AADT.

**Table 6.9 – The Comparison of the Site Conditions**

| | **Site 1 vs Site 6** | **Site 2 vs Site 4** | **Site 3 vs Site 5** |
|---|---|---|---|
| **Normalized Ratio** | 0.71 > 0.69 | 0.65 < 0.67 | 0.54 < 0.56 |
| **Transverse Crack Width (in)** | 0.075” > 0.06” | 0.080” > 0.04” | 0.1” < 0.15” |
| **Transverse Rebar Spacing (ft.)** | 3’ = 3’ | 3.25’ > 3’ | No > 3.25’ |
| **Cluster of Transverse Crack Spacing (ft.)** | 46’ > 6’ | 24’ > 12’ | 15’ > 1’ (no grouping) |
| **Number of Transverse Cracks in 100 ft. Section** | 22 < 75 | 35 < 61 | 30 < 31 |
| **Total Length of Longitudinal Cracks in 100 ft. Section** | 1 < 73 | 1 < 60 | 100 = 100 |
| **Distress Factor** | 0.05 < 0.97 | 0.03 < 0.98 | 3.33 > 3.23 |
| **AADT (2016)** | 37000 < 44600 | 36400 < 66300 | 67900 < 215000 |
| **Comparison of the Site Conditions** | **Site 1 ➔ Good**<br>**Site 6 ➔ Fair** | **Site 2 ➔ Good**<br>**Site 4 ➔ Fair** | **Site 3 ➔ Poor**<br>**Site 5 ➔ Poor** |

The summary of all pavement information and data collected from the GDOT inventory and the six site investigations are presented in Appendix G. Overall, the conditions and pavement performance levels of the six fields were evaluated relative to each other by being considered the mentioned all criteria. Thus, Sites 1 and 2 were described as being in good condition, Sites 3 and 5 as in poor condition, and Sites 4 and 6 as in fair condition.

# CHAPTER 7

# DEVELOPMENT of GDT-GPR for CRCPs

As it was discussed in the objectives in Chapter 1, this work is split into two distinct sections, one dealing with evaluating the performance of CRCP in Georgia using GPR technology together with eddy current technology, Profometer and one dealing with evaluating the utility of Profometer in the absence of a cored sample for the calibration process of GPR in the field. In addition, as a result of this entire research, a recommended GDT non-destructive test method for GPR has been created to be used in future research on evaluating the performance of CRCPs. This developed method describes the process applied during site investigations and post-processing.

GDT-GPR standard (Appendix H) has been defined under the eight subtitles including scope, apparatus, CRCP test section limits, equipment's installation, site investigation procedure, and post-processing procedures, calculations, and report. This test method is used to evaluate the performance of CRCP using GPR technique.

## 7.1. Scope and Apparatus

First section in GDT-GPR standard, scope, explains the content of this standard and what aim it shall be used for. In the second section, apparatus and equipment, which are needed to conduct a survey for evaluating data taken from pavement are listed. A site survey needs major components to be investigated, such as a GPR unit including antenna, survey wheel, and power supplies, a core equipment providing the accurate measurements for calibration of GPR, and

Manufacturer's Instruction Manuals. The GDT-GPR standard might be used as a guide before investigating a site.

### 7.2. CRCP Test Section Limits

CRCP test section limits state the practices planned to be performed during and before a site investigation. This part addresses the questions such as in which case the research is carried out and how the path shall be followed. Based on this research, the CRCP sections shall be tested in one-mile length and shall be divided in sub-segments by considering the density of the transverse and longitudinal cracks, punchouts, and existence of any distress types. Each sub-segment shall be surveyed by using GPR unit over damaged area and over non-damaged area in the transverse directions. In addition, the distance between sub-segments shall be tested using GPR in the longitudinal direction (traffic direction). The reason for this is to detect the location of longitudinal and transverse reinforcements and the concrete cover, and to designate whether there is a relationship between the locations of cracks and reinforcements in a way.

In addition, the standard mentions the limitations that allow for a survey to be conducted properly. One of these limitations is whether the site is wet or not. If the site is wet, the survey shall not be conducted because the dielectric constant values of material are affected, and the results might be affected from this condition. Additionally, the other requirement is to investigate site survey in the longitudinal direction of the GPR travel on the wheel-paths. The reason for this is that the locations of the wheel-path have more stress, resulting in more distress, because of the vehicle wheels.

### 7.3. Equipment Installation Procedure

Equipment installation procedure in the GDT-GPR standard details the experimental work for a site investigation. This section mentions the preliminary preparations including the required

equipment, adjustments made on settings of the equipment, and the survey wheel calibration of GPR. These preparations shall be fulfilled to collect more accurate results throughout field investigation before surveying site. For TerraSIRch SIR-System 3000, the following settings shall be set up if the concrete material is surveyed:

→ Frequency: 1.5 GHz (Model 5100)

→ Transmit Rate (T_RATE): 100 KHz

→ Samples per Scan: 512

→ Format (Resolution, bits): 16 bits

→ Range (nS): 12 nS

→ Scan per Unit: 5/inch

→ Number of Gain Points: 2

→ Vertical IIR High Pass (HP_IIR): 10 MHz

→ Vertical Low Pass Filter (LP_FIR): 3000 MHz

→ Vertical High Pass Filter (HP_FIR): 250 MHz

In addition, this section in standard provides a detailed procedure for the calibration process of GPR in the field through using operation of taking a core. To calibrate the GPR in the field is the most important part of the survey to get the accurate data from the sites as mentioned in Section 5.1 in Chapter 5. The procedure for calibration of GPR mentioned in the standard was derived from the manufacturer's manual (GSSI 2003) and the author's experiences at the sites.

**7.4. Site Investigation Procedure**

Site investigation procedure includes the general steps on how to survey a site for the aim mentioned in this project. This section takes the attention to a few subjects which shall be considered in order to evaluate the performance of a pavement in the field. Before a site

investigation, the equipment shall be prepared. Then, the GPR unit is calibrated based on provided information in the previous section in standard.

Each sub-segment in each site is surveyed to collect data using GPR in longitudinal and transverse direction. First, the locations of the longitudinal and transverse reinforcements are determined followed by the locations of transverse cracks are detected on whether they form at the location of transverse reinforcements or not. Finally, all data is recorded and taken by a compatible storage system to upload it to the software program for the post-processing.

### 7.5. Post-Processing Procedure

Post-processing covers the period after a site investigation and the procedure of post-processing states that a compatible software with GPR shall be used to accurately interpret the data taken from the site. For the TerraSIRch SIR System-3000, GPR model, the RadView software program is recommended because they are compatible to each other. If there is a need, the images might be calibrated or scaled in this software by considering the accurate measurements taken from the core specimens or profometer technology. After the adjusted and calibrated images, the depth and location of other reinforcements can be interpreted.

### 7.6. Calculations and Report

There is no need for calculations in this test. Finally, a report shall be prepared presenting all data and results obtained from a site.

This newly proposed approach and algorithm, GDT method, relied on a GPR system to be utilized during the proposed long-term monitoring plan of Georgia CRCP and development of a CPACES module for reliable CRCP condition assessment.

# CHAPTER 8

# CONCLUSIONS and RECOMMENDATIONS

## 8.1. Conclusions

In this project, the performance of CRCP sections was investigated using the non-destructive testing methods that included the GPR and eddy current technology, Profometer. The influence of reinforcement placement and concrete cover on distresses was evaluated. In addition, Profometer was utilized as a non-destructive cover meter technique for calibrating the GPR unit in the absence of a cored sample. Based on the results of the field tests, the following conclusions were made:

1- GPR is an effective technology to measure the concrete cover depth in the field. In addition, it has an option for being calibrated in the field if the actual cover depth is known. For the calibration process, the core specimens are necessary because the assumed dielectric value of concrete must be corrected during investigation.

2- As demonstrated by sites classified as being in poor condition during this project, if a pavement has inefficient concrete cover depth and pavement thickness, its performance might be reduced resulting in more clusters of single transverse cracks and/or punchouts.

3- The existence of single transverse cracks or cluster cracking is expected for CRC pavements. However, the spacing between the cracks has a key role in the formation of punchouts.

4- As the transverse and longitudinal reinforcements are placed lower within the pavement cross-section, the more transverse cracks occur. This results in wider crack widths and pose a fundamental problem, such as corrosion of steel within the pavement.

5- Eddy Current Technology, Profometer 600 in this research, is a practicable technique to make the calibration process fast during survey. It gives the estimated cover depth values which are close to GPR values. As the concrete cover depth increases, the accuracy of Profometer decreases. Due to having more sensitivity to external influence, Profometer gives the results that might be affected by many factors, such as bar diameter settings, existence of neighboring bars or probe settings for shallow or deep areas. Based on the field test results and the manufacturer's manual, the Profometer 600 is preferred when the concrete cover depth is not deep and the spacing between reinforcements is not small.

6- Based on the results, if the reinforcement is placed close to mid-depth of pavement thickness or deeper, the pavement performance might reduce. This design causes more distresses on the pavement. Therefore, it is recommended that the rebar shall be placed at the top-third of the total concrete thickness rather than within a specified cover range of 3.5 – 4.25in (89 – 108 mm). This places the cover depth at a ratio of the slab thickness than predetermined measurements.

7- It is assumed that as the transverse rebar spacing increases, the number of transverse cracks decrease under the same or similar design parameters of the pavement. For instance, while the transverse rebar spacing was 3 ft. (91 cm), the transverse cracks were formed between transverse rebars. However, while the transverse rebar spacing was 3.5 ft. (107 cm), the transverse cracks were formed at the location of the transverse rebars and there were no any cracks between the reinforcements.

## 8.2. Recommendations

The following are recommendations for future studies:

1- Monitoring of the pavement performance is recommended to be continued for better understanding of the causes of distresses and crack development on the CRCP.

2- To increase the accuracy of the Profometer, a recent version of the instrument having more options in probe settings that might be used for CRCP sections which have the increased depths of concrete cover.

3- The utility of Profometer might be evaluated once again for the calibration of GPR in the absence of cored samples by taking more than one core specimen and using the recent version instrument for future research. To calibrate GPR accurately, more core specimens might be taken from each site which separately has damaged and undamaged areas.

4- It is recommended the use of updated GPR model instead of TerraSIRch SIR 3000 model for the future research needed to be used 1.5 GHz antenna. In addition, depending on the GPR model, the updated software might be used to collect the detailed data and reliably calibrate the results in the software.

## REFERENCES


1. AASHTO (1986, 1993). AASHTO Guide for the Design of Pavement Structures, American Association of State Highway and Transportation Officials, Washington, DC.

2. AASHTO, T 336 (2011). Coefficient of Thermal Expansion of Hydraulic Cement Concrete. Standard Specifications for Transportation Materials and Methods of Sampling and Testing.

3. ACPA (2016). Continuously Reinforced Concrete Pavement (CRCP). http://wikipave.org/index.php?title=Continuously_Reinforced_Concrete_Pavement_(CRCP). Accessed December, 2016.

4. American Iron and Steel institute (2014). Steel Works. https://www.steel.org/~/media/Files/SMDI/Construction/CRCP%20-%20Marketing%20-%20CRCP%20Brochure.pdf?la=en. Accessed December, 2016.

5. Annan, A. P. (2004). Ground Penetrating Radar Principles, Procedures and Applications. Mississauga, Canada: Sensors & Software

6. ARA, Inc. (2003). Guide for Mechanistic-Empirical Design of New and Rehabilitated Pavement Structures, Appendix LL: Punchouts in Continuously Reinforced Concrete Pavements. Champaign, Illinois.

7. ARA, Inc. (2004). Guide for Mechanistic-Empirical Design of New and Rehabilitated Pavement Structures Part 3. Design Analysis Chapter 4. Design of New and Reconstructed Rigid Pavements: National Cooperative Highway Research Program, Transportation Research Board, National Research Council.

8. ASTM-D6432 (2011). Standard Guide for Using the Surface Ground Penetrating Radar Method for Subsurface Investigation, ASTM International, West Conshohocken, PA. www.astm.org.

9. ASTM, C1202-12 (2012).. "Standard Test Method for Electrical Indication of Concrete's Ability to Resist Chloride Ion Penetration." ASTM International, PA, USA.

10. ASTM C469 / C469M (2014). Standard Test Method for Static Modulus of Elasticity and Poisson's Ratio of Concrete in Compression, ASTM International, West Conshohocken, PA.

11. Caltrans (2015). Concrete Pavement Guide. State of California Department of Transportation.

12. Chen, D. H., & Scullion, T. (2008). Forensic investigations of roadway pavement failures. Journal of Performance of Constructed Facilities, 22(1), 35-44.

13. CMC (2007). Georgia-A Testament of CRCP Progress. Rebar Case Study, No. 02.

14. Conyers, L. B. (1995). The use of ground- penetrating radar to map the buried structures and landscape of the ceren site, el salvador. Geoarchaeology, 10(4), 275-299.

15. Conyers, L.B. (1998). Ground-Penetrating Radar. http://mysite.du.edu/~lconyer/Johnson_book_gpr.pdf. Accessed December, 2016.

16. CRSI (Concrete Reinforcing Steel Institute) (2003). CRCP in Georgia- Durable Pavement on Their Mind. Case History Report, No: 61.

17. Darter, M.I., S.A. LaCourseiere, and S.A. Smiley, (1979). Performance of Continuously Reinforced Concrete Pavement in Illinois. Transportation Research Record No. 715, Transportation Research Board, Washington, DC.

18. Delatte N. (2008). Concrete Pavement Design, Construction, and Performance. Taylor & Francis Group, London and New York.

19. Diamanti, N., & Redman, D. (2012). Field observations and numerical models of GPR response from vertical pavement cracks. Journal of Applied Geophysics, 81, 106-116.

20. FHWA Tech Brief (2003). Distress Identification Manual for the LTPP (Fourth Revised Edition). Chapter 3 Distress for Pavements With Continuously Reinforced Concrete Surfaces. Report No. FHWA-RD-03-031.

21. FHWA Tech Brief (2012). Continuously Reinforced Concrete Pavement Performance and Best Practices. Report No. FHWA-HIF-12-039.

22. FHWA Tech Brief (2013). Continuously Reinforced Concrete Pavement : Extending Service Life of Existing Pavements. Report No. FHWA-HIF-13-024

23. Folliard, K. J., & Prozzi, J. A. (2005). Early-age behavior of CRCP and its implications for long-term performance.

24. GDOT. (2013) "Standard Specifications for the Construction of Transportation Systems" <http://www.dot.ga.gov/PartnerSmart/Business/Source/specs/DOT2013.pdf> (Accessed December, 2016)

25. Gharaibeh, N., Darter, M., & Heckel, L. (1999). Field performance of continuously reinforced concrete pavement in Illinois. Transportation Research Record: Journal of the Transportation Research Board, (1684), 44-50.

26. Gulden, W. (1980). Evaluation of the Condition of the Continuous Reinforced Concrete Pavement Section on 1-95. Office of Materials and Research Pavement and Physical Research Branch.

27. GSSI (2003). TerraSIRch SIR System-3000 User's Manual.

28. GSSI (2006). GSSI Handbook For RADAR Inspection of Concrete.

29. GSSI (2016). Ground Penetrating Radar Explained. http://www.geophysical.com/whatisgpr.htm. Accessed January, 2017.

30. Ha, S., Yeon, J., & Won, M. C. (2012). CRCP ME Design Guide (No. Product 0-5832-P1).

31. Highway Research Board, (1973). Continuously Reinforced Concrete Pavement. National Cooperative Highway Research Program Synthesis of Highway Practice 16. Washington D.C.

32. IDOT (2005). Pavement Technology Advisory, Testing Pavement Friction, PTA-T3.

33. Impact Test Equipment (2017). Concrete Covermeter-Profometer Model 600. http://www.impact-test.co.uk/products/5496-concrete-covermeter-profometer-model-600/. Accessed October 2017.

34. Johnson C.E. (2016). An Investigation of Distress Found in Concrete and Asphalt Pavements for Georgia Forensic Guide Recommendation.

35. Kim, S. H. (2012). "Determination of Coefficient of Thermal Expansion for Portland Cement Concrete Pavements for MEPDG Implementation" GDOT No. 10-04.

36. Kohler, E., & Roesler, J. (2004). Active crack control for continuously reinforced concrete pavements. Transportation Research Record: Journal of the Transportation Research Board, (1900), 19-29.

37. Kohler, E. R., & Roesler, J. R. (2005). Crack width measurements in continuously reinforced concrete pavements. Journal of transportation engineering, 131(9), 645-652.

38. Kohler, E. R., & Roesler, J. R. (2006) Crack spacing and crack width investigation from experimental CRCP sections, International Journal of Pavement Engineering, 7:4, 331-340.

39. LaCourseiere, S.A., M.I. Darter, and S.A. Smiley, (1978). Structural Distress Mechanisms in Continuously Reinforced Concrete Pavement. Transportation Engineering Series No. 20, University of Illinois at Urbana-Champaign.

40. Lohonyai, A.J. (2015). To Engineer is Human. A Brief History of Ground Penetrating Radar. http://alohonyai.blogspot.com/2015/01/a-brief-history-of-ground-penetrating.html. Accessed January, 2017.

41. Lokesh, V., Swamy, B. S., & Vijaya, S. (2014). Study on Soundness of Reinforced Concrete Structures by NDT Approach. International Journal & Research in Engineering and Technology. eISSN, 2319-1163.

42. McGhee, K. H. (1998). A Guide to Evaluating Pavement Distress Through the Use of Video Images. Virginia Department of Transportation, Maintenance Division.

43. Mihai, P., Gosav, I., & Rosca, B. (2010). Study on the Earthquake Action of Old Masonry Structures. Journal of Applied Sciences, 10(3), 157-165.

44. NCHRP Web Document 35 (2001). Rehabilitation Strategies for Highway Pavements, Appendix A Pavement Distress Types and Causes. http://onlinepubs.trb.org/Onlinepubs/nchrp/nchrp_w35-b.pdf. Accessed December, 2016.

45. Penhall Technologies. Concrete Scanning and X-ray Using GPR. https://www.penhall.com/concrete-scanning-gpr/. Accessed January,2017.

46. Proceq. Profometer and Profoscope Concrete Cover Meter and Rebar Locators. https://www.proceq.com/compare/rebar-detection-and-cover-measurement/. Accessed July, 2017.

47. Rada, G. R., Jones D.J., Harvey J.T., Senn K.A., & Thomas M. (2013). "Guide for Conducting Forensic Investigations of Highway Pavements." Transportation Research Board, Vol. 747.

48. Ren, D. (2015). Optimisation of the Crack Pattern in Continuously Reinforced Concrete Pavements. doi:10.4233/uuid:599e8346-27d7-43e8-a67c-54f46ef03f76.

49. Roesler, J. R., Popovics, J. S., Ranchero, J. L., Mueller, M., & Lippert, D. (2005). Longitudinal cracking distress on continuously reinforced concrete pavements in Illinois. Journal of performance of Constructed Facilities, 19(4), 331-338.

50. Selezneva O.I., D. Zollinger, M.Darter, (2001). Mechanistic Analysis of Factors Leading to Punchout Development for Improved CRCP design Procedures. Proceedings of the 7th International conference on Concrete Pavements, p. 731-745.

51. Selezneva, O.I., (2002). Development of Mechanistic-Empirical Damage Assessment Procedures for CRC Pavements with Emphasis on Traffic Loading Characteristics. Ph.D. Dissertation, West Virginia University.

52. Sharma, S., & Das, A. (2008). Backcalculation of pavement layer moduli from falling weight deflectometer data using an artificial neural network. Canadian Journal of Civil Engineering, 35(1), 57-66.

53. Sivasubramanian, K., Jaya, K. P., & Neelemegam, M. (2013). Covermeter for identifying cover depth and rebar diameter in high strength concrete. International Journal of Civil and Structural Engineering, 3(3), 557.

54. Sub, Y. C., & McCullough, B. F. (1992). Early-Age Behavior of Continuously Reinforced Concrete Pavement and Calibration of the Failure Prediction Model in the CRCP-7 Program. Research Report 1244-3, Center for Transportation Research, The University of Texas at Austin.

55. Szymanik, B., Frankowski, P. K., Chady, T., & John Chelliah, C. R. A. (2016). Detection and Inspection of Steel Bars in Reinforced Concrete Structures Using Active Infrared Thermography with Microwave Excitation and Eddy Current Sensors. Sensors (Basel, Switzerland), 16(2), 234. http://doi.org/10.3390/s16020234.

56. Tsai, Y. J., & Wang, Z. (2014). Critical Assessment of I-85 CRCP Crack Spacing Patterns and Their Implications for Long-term Performance (No. FHWA-GA-14-1239).

57. Yoder, E. J., & Witczak, M. W. (1975). Principles of pavement design. John Wiley & Sons.

APPENDIX A

SR6NBCMP0-1:

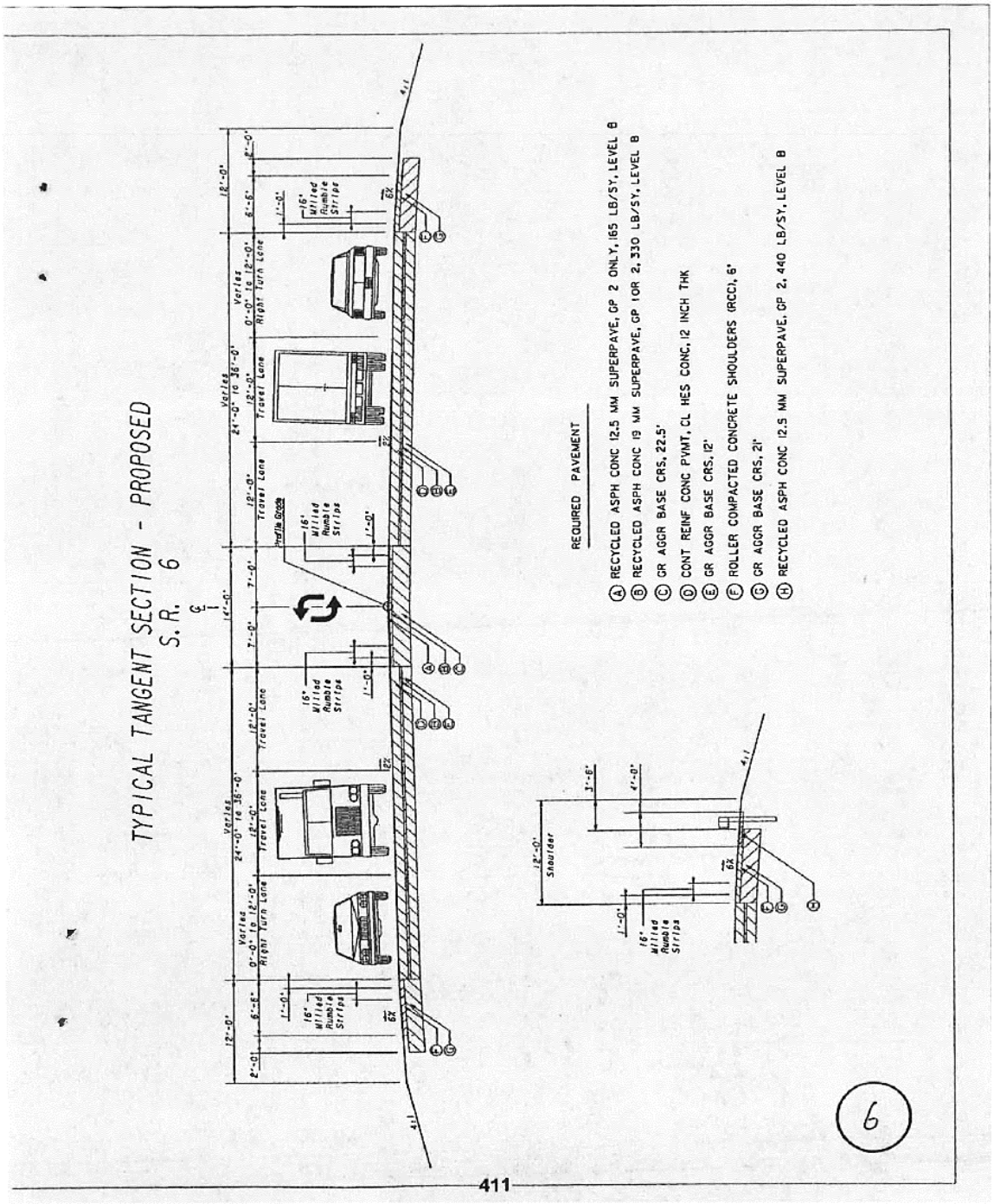

APPENDIX B

I20EBHMP4-5:

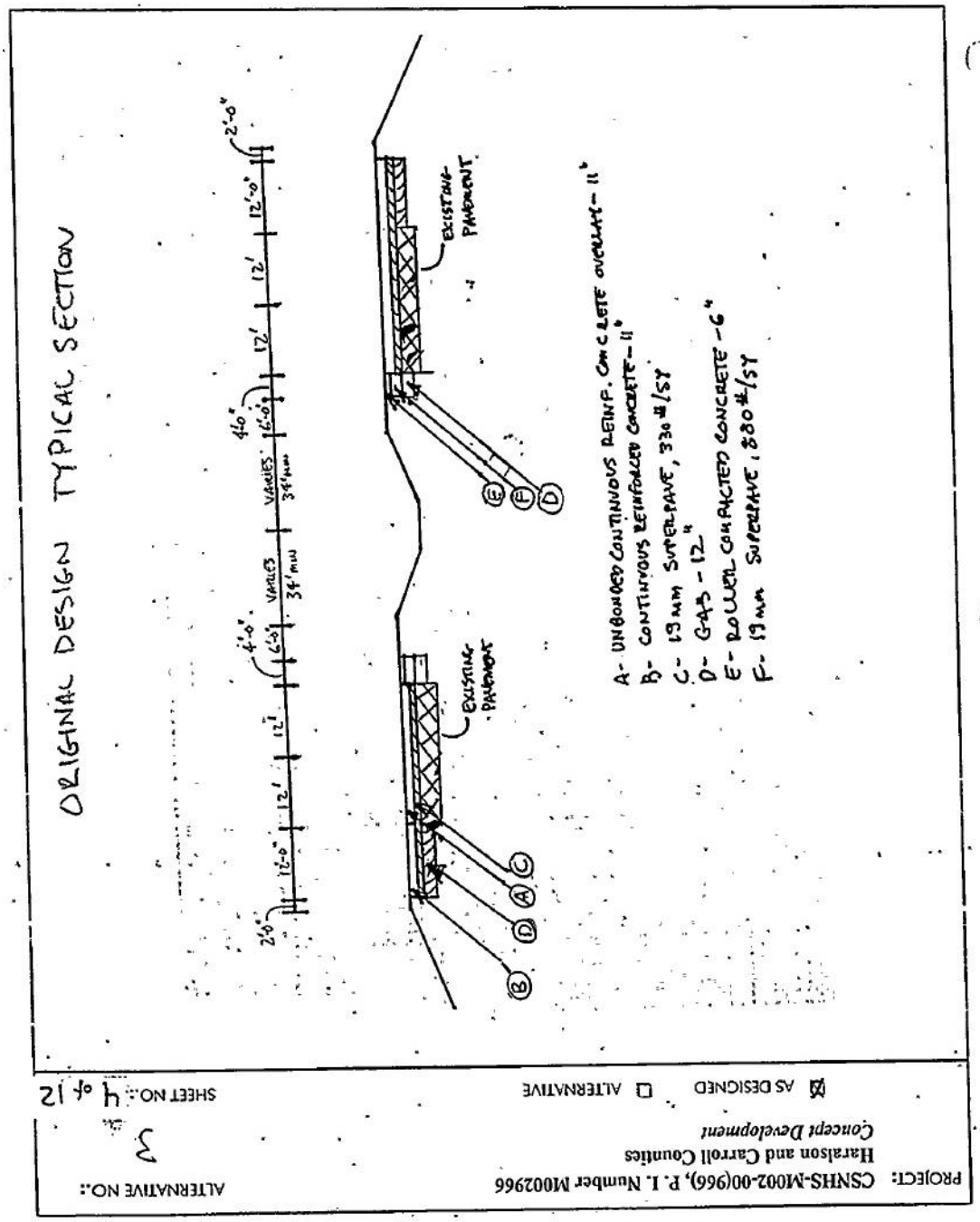

# APPENDIX C

I20WBCMP24-25:

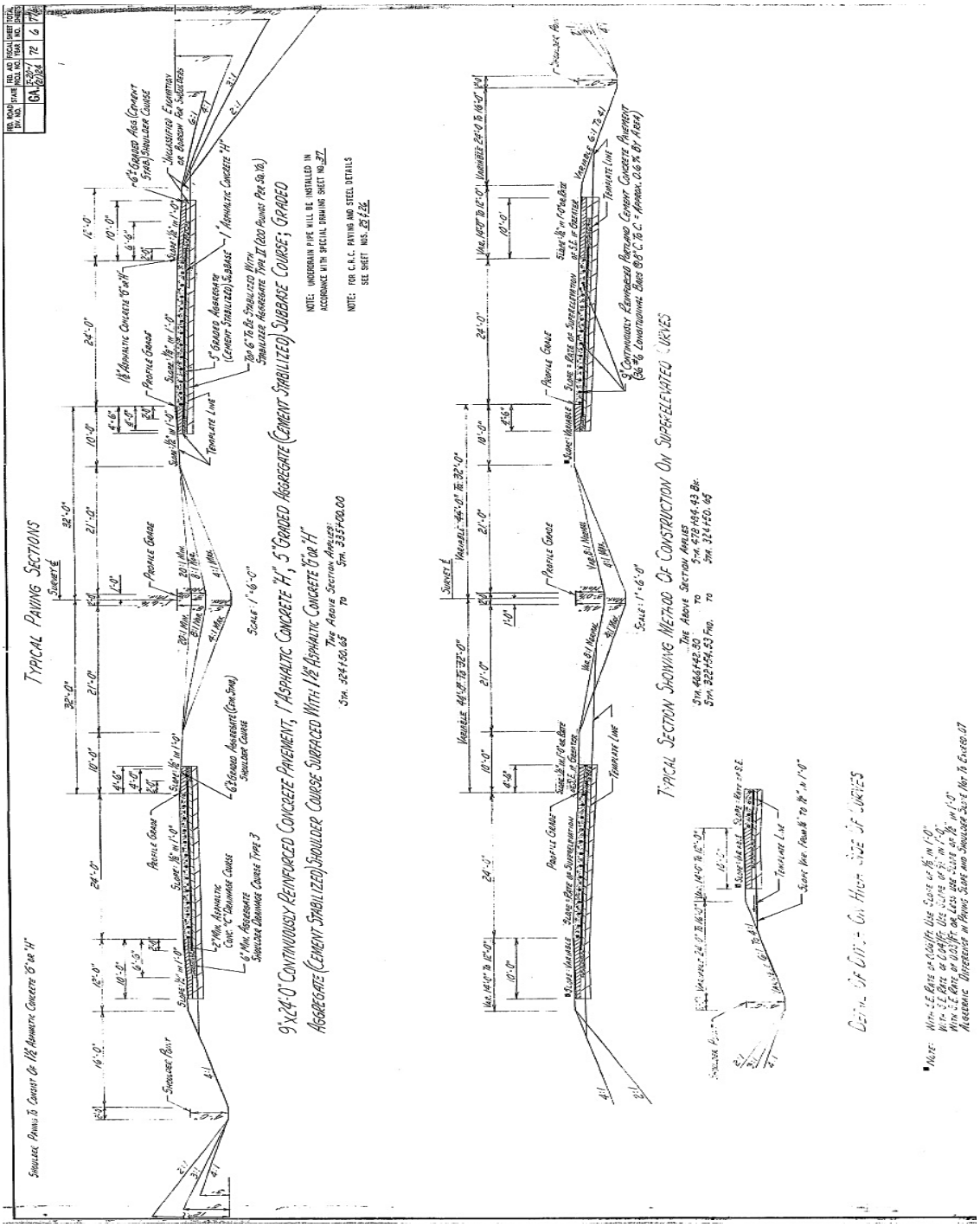

# APPENDIX D

I20EBNMP92-93:

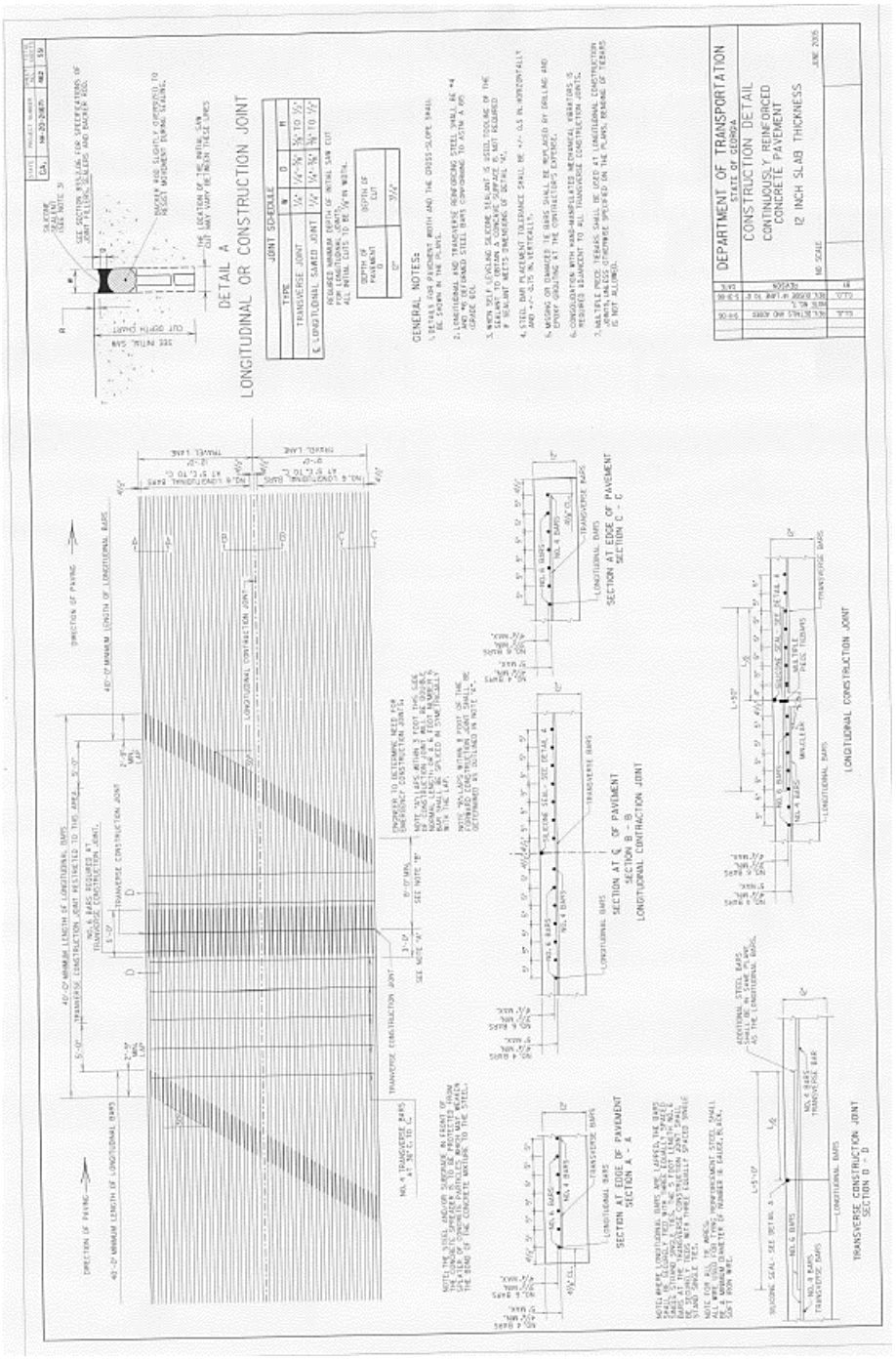

APPENDIX E

I75NBCMP267-268:

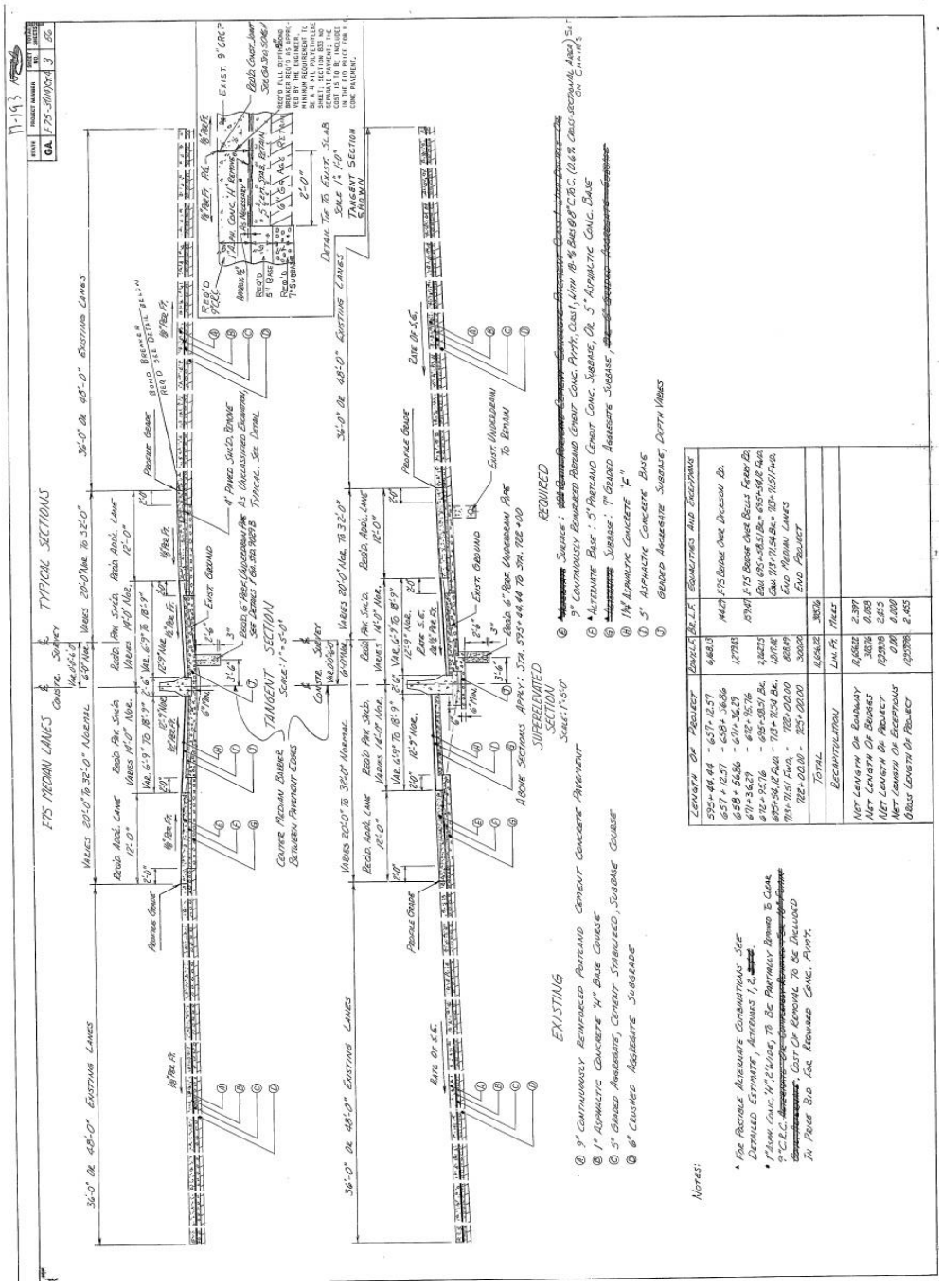

APPENDIX F

I75NBTMP57-58:

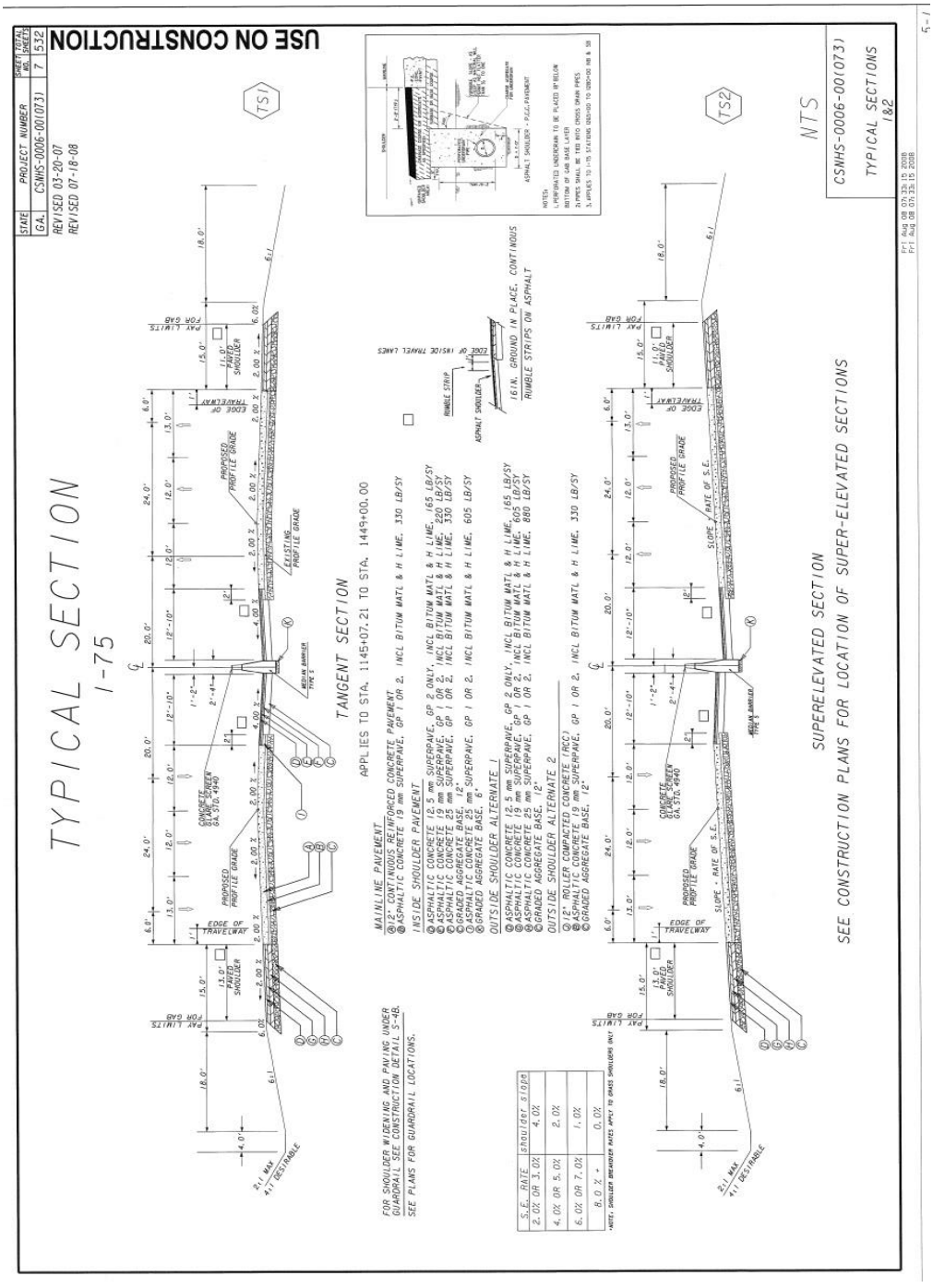

APPENDIX G: The Summary of All Pavement Information and Data

| | NDT Results \ Selected Sites | *Site 1 SR6NBCMP0-1* | *Site 2 I20EBHMP4-5* | *Site 3 I20WBCMP24-25* | *Site 4 I20EBNMP92-93* | *Site 5 I75NBC MP267-268* | *Site 6 I75NBTMP57-58* |
|---|---|---|---|---|---|---|---|
| | | SR-6 Cobb County | I-20Haralson County | I-20 Carroll County | I-20 Newton County | I-75 Cobb County | I-75 Tift County |
| **Design Parameters** | Site Condition | **Good** | **Good** | **Poor** | **Fair** | **Poor** | **Fair** |
| | Lane | Outside | Outside | Outside | Outside | Outside | Outside |
| | Age | 12 (2005) | 37 (1980) | 45 (1972) | 12 (2005) | 32 (1985) | 9 (2008) |
| | CRC Thck.(in) | 12” | 12” | 8.70” | 12” | 10.25” | 12” |
| | Longitudinal Rebar Size | #6 | #6 | #6 | #6 | #6 | #6 |
| | Spacing btw. Longt. Rebars (in) | 5” | 4” ~ 8” | 8” | 5” | 5” ~ 9.5” | 5” |
| | Transverse Rebar Size | #4 | #6 | - | #4 | #4 | #4 |
| | Spacing between Trns. Rebars (in) | 36” | 23” ~ 46” (typical 39”) | - | 36” | 25” ~ 40” (typical 39”) | 36” ~ 40” (typical 36”) |
| | Longitudinal Rebar Depth (in) | 3.50” | 4.25” | 4.00” | 4.00” | 4.50 | 3.75” |
| | Transverse Rebar Depth (in) | 4.50” | 5.00” | - | 4.75” | 5.25 | 4.50” |
| **Distress Assessment** | Spacing btw. Single Transverse Cracks (ft.) | 1’- 4’ (typical 1’) | 1.6’~ 4.0 ‘ (typical 1.63’) | 1’ | 1’- 10’ (typical 1’) | 1.5’- 4.25’ (typical 3.25’) | 1’~ 3’ (typical 1’) |
| | Spacing btw. Clusters of Cracks (ft.) | 46’ | 24’ | 10’~ 20’ | 12’~ 60’ (typical 12’) | No Grouping (typical 1’) | 6’~ 12’ (typical 6’) |
| | Transverse Crack width (in) | 0.04” ~ 0.14” (typical 0.075”) | 0.03” ~ 0.1” (typical 0.08”) | 0.06” ~ 0.12” (typical 0.1”) | 0.03” ~ 0.12” (typical 0.04”) | 0.10” ~ 0.15” (typical 0.15”) | 0.01” ~ 0.08” (typical 0.06”) |
| | Longitudinal Crack width (in) | - | - | - | 0.01” ~ 0.08” | 0.05” | 0.06” |
| | Number of Punchouts / mile | 0 | 0 | 10 | 0 | 0 | 0 |
| | **ADT (2016)** | 37000 | 36400 | 67900 | 66300 | 21500 | 44600 |

# APPENDIX H

# GDT-GPR

# TEST METHOD FOR EVALUATING THE PERFORMANCE OF CONTINUOUSLY REINFORCED CONCRETE PAVEMENTS (CRCPs) USING GROUND PENETRATION RADAR (GPR)

## A. SCOPE

This test method describes the proper procedures for evaluating the performance of Continuously Reinforced Concrete Pavements (CRCPs) using the non-destructive method Ground Penetration Radar (GPR).

This document, together with the manual and recommendations of the equipment manufacturers delineate the procedures for the installation and calibration of equipment and the guidelines for the proper survey.

## B. APPARATUS

The GPR technology is a non-destructive method used for a structural assessment to be performed correlating the pavement distresses at certain locations with known pavement conditions. The GPR unit shall have hardware and software to create and store pavement information from each site. The methodology for collecting the required data from a site includes the following major components:

- An antenna having a capability of working with 1.5 GHz frequency for CRCP sections (TerraSIRch SIR System-3000)
- Core equipment

- A metal plate
- The measurements and the required markers
- Manufacturer's Instruction Manuals

## C. CRCP TEST SECTION LIMITS

- CRCP sections shall be tested in one-mile (1.61 km) length for survey distance.
- At least one core bit shall be taken from the beginning of the site section.
- The survey distance shall be divided in sub-segments by designating in terms of density of crack types and existence of any distress types.
- The sub-segments shall be tested as separate sections, using GPR, over damaged area and non-damaged area in the transverse directions. In addition, the section from one sub-segment to the next sub-segment shall be tested using GPR in the longitudinal direction (traffic direction).
- The survey in the longitudinal direction of the GPR travel shall be performed on the wheel paths.
- The survey conducted in both longitudinal and transverse directions shall have the same alignment from the beginning to ending points.
- Pavement profile shall not be surveyed when it is wet due to the fact that equipment might not give the accurate data in this condition.

## D. EQUIPMENT INSTALLATION PROCEDURE

1. Preliminary Preparations

   a) Prior to testing, all tires pressures, charge of equipment's batteries, and connection of antenna and control unit of GPR shall be checked.

b) Remove all unwanted items and the pieces of metal from the pavement surface (if there is).

c) Establish all required preloaded setups including data collection parameters and filters for the SIR-3000 model of GPR unit. The steps for settings are as following:

- Select the TerraSIRch Mode for the site investigation.
- Select the frequency as 1.5/1.6 GHz antenna for concrete. Typical maximum depth scanned by GPR will be 1.5 ft. (50 cm).
- Select the transmit rate (T_RATE) as 100 KHz.
- Select the mode of distance based data collection. This mode requires a survey wheel calibration which will be described in the next bullet.
- Select 512 samples per scan for the use of 1.5 GHz frequency.
- Select 16- bits data format.
- Select 12-nS range for the recording of reflections from a single pulse.
- Select first the dielectric constant value as being between 5 and 8 for concrete materials. However, after calibration process of GPR, this value might change.
- Select the scan rate as 100 scans per second if the transmit rate is set to 100 KHz.
- Select the scan per unit of horizontal distance as 60 scans/foot or 5 scans/inch.
- Set the 2 gain points to neutralize effects of attenuation and to make subtle sections more visible.
- Set the following filters to remove noise in the ground:
    - → HP_IIR is set to 10 MHz.
    - → LP_FIR is set to 3000 MHz.
    - → HP_FIR is set to 250 MHz.

d) The survey wheel shall be calibrated to local conditions at every different site when the distance based data collection is selected in GPR. Here are the steps:

- A measured line shall be prepared on the survey surface. The longer the measured line, the more accurate the survey wheel calibration.
- The calibration distance, taken from the measured line, is entered and the position of the antenna is set for the beginning of the line as front, center, or rear of the antenna.
- The antenna is moved the survey distance.
- If this process is done several times and the average of the results is taken, the calibration of the survey wheel will be more accurate.

2. Calibration Testing

a) Move GPR unit on the wheel path in the longitudinal direction to detect the location of transverse reinforcements.

b) Select one of the scanned transverse reinforcements on the GPR screen, drive GPR back positioning on the selected reinforcement, and mark the location of transverse reinforcement on the pavement.

c) Place the metal plate on the marked location of transverse reinforced.

d) Drive GPR again on the area to confirm accuracy of the location of transverse reinforcement.

e) Scan the marked location in the transverse direction to detect the location of the longitudinal reinforcements.

f) Select one of the scanned longitudinal reinforcements close to the centerline of lane and mark the location (distance from the shoulder) on the pavement. Be sure that the

depth value of the selected reinforcement shall be equal or close to the one taken from the construction drawings or shall be close to the average of the scanned depth values.

g) Take a core from the marked location.

h) Measure the depth and size of longitudinal and transverse reinforcements and the layer thickness. Save these data in your file.

i) Drive GPR unit on the line, which the core is taken from, in the transverse direction.

j) Calibrate the scanned depth value to the measured depth value on the GPR screen when you are on the selected location.

k) Save the new depth value and the dielectric value might change by depending on the concrete cover.

l) Save the new dielectric value and start the site investigation.

## E. SITE INVESTIGATION PROCEDURE

1. Prepare the equipment and required items needed to be used in the site.
2. Calibrate equipment based on the information taken from a core.
3. Collect data using GPR in longitudinal and transverse directions from each sub-segment.
4. Determine the location of transverse cracks on whether they form at the location of the transverse reinforcements or not.
5. Examine pavement condition throughout one-mile (1.61 km) site survey in terms of cracks, punchouts, patched areas, material problems, etc.
6. Perform a minimum of four sub-segments to investigate the site in detail.
7. Record the data and take them by using a compatible storage system (i.e., portable storage media, memory card, etc.)

## F. POST-PROCESSING PROCEDURE

For post-processing, select the proper software which is compatible with GPR model. For the TerraSIRch SIR System-3000, GPR model, the RadView software program is selected. If required, the data taken by GPR might be calibrated in the software using the location of the core secured from the site. After calibrating the data on the basis of the known cover depth value, other reinforcements' depths shall be analyzed and interpreted.

## G. CALCULATIONS

No calculations are required for this test.

## H. REPORT

Report the summarized data and results obtained from a site investigation.